# HIV-INDUCED REDOX CHANGES AND INFLAMMATION IN THE CENTRAL NERVOUS SYSTEM AND MODULATORY FACTORS

A DISSERTATION SUBMITTED TO THE GRADUATE DIVISION OF THE UNIVERSITY OF HAWAIʻI AT MĀNOA IN PARTIAL FULFILLMENT OF THE REQUIREMENTS FOR THE DEGREE OF

DOCTOR OF PHILOSOPHY
IN
CELL AND MOLECULAR BIOLOGY

AUGUST 2013

BY
XIAOSHA PANG

Dissertation Committee:

Dr. Jun Paneʻe, Chairperson
Dr. Marla Berry
Dr. Robert Nichols
Dr. Frederick Bellinger
Dr. Cecilia Shikuma

*For my beloved parents, sister and Chris*

*特别感谢父母的支持*

**Acknowledgments**

Special thanks to Dr. Jun Paneʻe who provided guidance of the whole project and the dissertation. Thank you for your kindness and patience, and for giving me a second chance to pursue Ph.D.

Many thanks to my committee for their valuable suggestions to improve this work.

Many thanks to Dr. Linda Chang and colleagues in her lab who shared the clinical samples with us.

Thanks to Department of Cell and Molecular Biology of the John A. Burns School of Medicine, University of Hawaiʻi at Mānoa, for all the useful courses and training.

And a big mahalo to all the people in Dr. Marla Berry's group and CMB. It was great to have them around.

Thanks to INBREII, SNRP, and RCMI/BRIDGES research programs for the financial and technical supports.

**Abstract**

Currently 34 million people live with human immunodeficiency virus (HIV) infection. Although the lifespan of HIV patients has been prolonged by highly active antiretroviral treatment, the prevalence of HIV-associated neurocognitive disorders (HANDs) is increasing. Oxidative stress and inflammation in the central nervous system (CNS) are major causes of HANDs, and concurrent drug abuse may accelerate the progression of symptoms. This dissertation aims to study HIV-induced changes in antioxidants, oxidative stress, and inflammation in the CNS, assess the effects of concurrent methamphetamine (Meth) exposure, and evaluate the protective effect of dietary supplementation of bamboo *Phyllostachys edulis* extract (BEX). This study centered on the most abundant antioxidant in the brain - glutathione (GSH). The changes of GSH metabolism and GSH-dependent antioxidant enzymes were measured in cerebrospinal fluid (CSF) of human cohorts with HIV infection and/or uses of Meth, and in the brain tissues of HIV-1 model transgenic rats (HIV-1Tg expressing 7 HIV viral proteins) with or without Meth exposure. HIV infection resulted in elevated gamma-glutamyl transpeptidase (GGT) activity, GSH depletion and a several-fold increase in lipid peroxidation in human CSF. Compared to HIV infection, use of Meth resulted in less severe oxidative stress, which may be partially explained by the upregulation of glutathione peroxidase (GPx) and GSH in the CSF. Meth did not interact with HIV in modulating the redox changes in the CSF. In HIV-1Tg rats, redox and inflammatory changes were observed in the brain in a region-specific manner, with little synergy from Meth exposure. The thalamus was highlighted by its high GSH content and systematic upregulation of GSH biosynthesis and GSH-dependent antioxidant enzymes in the HIV-

1Tg rats. On the other hand, neuroinflammation markers, such as glial fibrillary acidic protein (GFAP) and p65, were increased in the hippocampus of the transgenic rats, and such changes were effectively normalized by dietary supplementation of BEX. In summary, this dissertation documents the significance of GSH and GSH-dependent antioxidant enzymes in regulating the redox status of CNS, and the potential anti-neuroinflammatory effects of BEX in the context of HIV infection.

**Table of Contents**

**List of Tables**

**List of Figures**

**List of Abbreviations**

| | |
|---|---|
| ABTS | 2,2'-azino-bis(3-ethylbenzothiazoline-6-sulphonic acid) |
| AIDS | Acquired immunodeficiency syndrome |
| ATF | Activation transcription factor |
| AZT | Zidovudine |
| BBB | Blood-brain-barrier |
| BEX | Bamboo extract |
| Bip | Binding immunoglobulin protein |
| B2M | Beta-2-microglobulin |
| CCL5 | Chemokine c-c motif ligand 5 |
| CCR5 | C-C chemokine receptor 5 |
| CD | Cluster of differentiation |
| CNS | Central nervous system |
| Ct | Cycle thresholds |
| CSF | Cerebrospinal fluid |
| CysGly | Cysteinylglycine |
| CX3CL1 | Fractalkine |
| CXCR4 | C-X-C chemokine receptor 4 |
| DA | Dopamine |
| EAAC1 | Excitatory amino acid carrier 1 |
| EAAT | Excitatory amino acid transporter |
| eIF2α | Eukaryotic initiation factor 2α |
| env | Envelope proteins |
| ER | Endoplamic reticulum |
| FLC | F344 rats fed low fat diet |
| FRAP | ferric reducing antioxidant power |
| gag | Group-specific antigen |
| GCS | γ-glutamylcysteine synthetase |
| GCS-HC | γ-glutamylcysteine synthetase heavy chain |
| GCS-LC | γ-glutamylcysteine synthetase heavy chain |
| GFAP | Glia fibrillary acid protein |
| GGT | γ-glutamyl transferase |
| Glrx | Glutaredoxin |
| gp120 | Envelope glycoprotein 120 |
| gp41 | Envelope glycoprotein 41 |
| GPx | Glutathione peroxidase |
| GR | Glutathione reductase |
| GS | Glutathione synthetase |
| GSH | Glutathione |

| | |
|---|---|
| GSSG | Oxidized glutathione |
| GST | Glutathione-S-transferase |
| GUSB | Glucuronidase beta |
| G6PH | Glucose-6-phosphate dyhydrogenase |
| HAART | Highly active antiretroviral therapy |
| HAD | HIV-associated dementia |
| HAND | HIV-associated neurocognitive disorders |
| HIV | Human immunodeficiency virus |
| HLC | HIV-1 transgensis rats fed low fat diet |
| HLB | HIV-1 transgenesis rats fed low fat diet with bamboo extract supplement |
| HNE | 4-hydroxynonenal |
| HNE-His | HNE histidine conjugation |
| HPRT | Hypoxanthine guanine phosphoribosyl transferase |
| IACUC | Institutional Animal Care and Use Committee |
| IL1β | Interleukin 1β |
| IL12 | Interleukin 12 |
| IL6 | Interleukin 6 |
| IκB | Inhibitor of κB |
| IP-10 | Interferon gamma-induced protein 10 |
| kDa | Kilodalton |
| MAP2 | Microtubule-associated protein 2 |
| MCP-1 | Monocyte chemoattractant protein 1 |
| MDA | Malondialdehyde |
| MDM | Monocytes-derived macrophages |
| Meth | Methamphetamine |
| MRP | Multidrug resistance-associated protein |
| nef | Negative factor |
| NeuN | Neuronal nuclei |
| NFκB | Nuclear factor kappa-light-chain-enhancer of activated B cells |
| NO | Nitric oxide |
| NOD | Non-obese diabetic |
| NOS | Nitric oxide synthetase |
| Nrf2 | Nuclear factor-erythoid 2 related factor 2 |
| NVP | Nevirapine |
| PBL | Peripheral blood lymphocytes |
| Perk | Protein kinase R-like endoplasmic reticulum kinase |
| pol | Polymerase |
| qPCR | Quantitative real-time PCR |
| Redox | Reduction-oxidation |

| | |
|---|---|
| rev | Regulator of virion expression |
| rGSH | Reduced glutathione |
| ROS | Reactive oxygen species |
| *Scid* | Severe combined immunodeficiency |
| SOD | Superoxide dismutase |
| tat | Trans-activator of transcription |
| TBP | TATA box binding protein |
| TGFβ | Transforming growth factor β |
| TNFα | Tumor necrosis factors α |
| UPR | Unfold protein response |
| vif | Viral infectivity factor |
| vpr | Viral protein R |
| vpu | Viral protein unique |
| xCT | System $x_c$- light catalytic chain |
| XBP | X-box binding protein |
| 5HT | Serotonin |

# Chapter 1

# Introduction

## 1.1 Overview of HIV

### 1.1.1 Prevalence of HIV

According to world health organization (WHO), currently 34 million people are living with human immunodeficiency virus (HIV) infection in the world, and over 1.1 million of them are in the United States (US). Since the first case of acquired immunodeficiency syndrome (AIDS) caused by HIV was reported in the US in June 1981, a significant amount of investigation has been carried out on HIV pathogenesis, medication, prevention, care, and education. Due to improved treatment in the US, the death caused by AIDS has dropped from over 50,000 in 1995 to about 15,000 in 2010, and the median age at death has increased from 36 years in 1987 to 48 years in 2009 [1]. However, even with improved prevention strategies, there are still approximately 50,000 people newly infected with HIV each year in the US.

### 1.1.2 Biological facts of HIV infection

HIV is a lentivirus of the *Retroviridae* family with single-strand RNA and a long incubation period. It usually takes several years to develop AIDS after HIV infection. There are two types of HIV, HIV-1 and HIV-2. The HIV-1 infection is common, and HIV-2 infection is mainly found in West Africa. Several clades of HIV-1 with different geographic distributions have been identified. The dominant subtype of HIV-1 in America is clade B.

HIV virus can live in blood, semen, vaginal secretions, and breast milk of infected individuals, and it can be spread through sexual contact, blood contamination, maternal-fetal transmission, and breastfeeding [2]. In the early stage of HIV infection, patients experience flu-like symptoms, and more severe symptoms, such as rapid weight loss, recurring fever, pneumonia, and memory loss can develop at later stage.

HIV has 9 genes. Three are structural and play roles in building new viral particles:

group-specific antigen (gag), polymerase (pol), and envelope protein (env). The other six genes regulate viral infection and replication, and they are viral infectivity factor (vif), viral protein R (vpr), trans-activator of transcription (tat), regulator of virion expression (rev), viral protein unique (vpu), and negative factor (nef). Once a virus enters the host cell, the viral surface protein glycoprotein 120 (gp120, surface subunit of Env) binds to cluster of differentiation 4 (CD4) and undergoes a conformational transition that expose binding sites for the co-receptor C-C chemokine receptor 5 (CCR5) or C-X-C chemokine receptor 4 (CXCR4). This triggers conformation rearrangement of glycoprotein 41 (gp41, subunit of Env) which inserts its fusion peptide into the plasma membrane of target cell and initiates fusion. When the viral core is released into the host cell, its genomic RNA is reverse transcribed by viral reverse transcriptase and generates a preintegration complex which is compromised of viral DNA and integrase. Then, the preintegration complex is transported into nucleus and integrates into the DNA of host cell. Using integrated proviral DNA as template and host Pol II RNA polymerase, viral mRNA is replicated during host DNA transcription. The viral mRNA is then translated to Gag and Gag-Pol polyproteins, which initiate viral assembly at host cell membrane. Assembly continues with the recruitment of newly synthesized Gag and Gap-Pol polyproteins to the membrane. Eventually, the membrane around the nascent particle fuses and releases non-infectious virus particle. The virus matures by cleavage of Gag and Gag-Pol by viral protease, generating the conical capsid, and activating HIV-1 enzymes [2].

Frequent mutations occurring in viral replication genes can result in antibody-resistant variants, which are either more difficult to kill or replicate faster. Besides mutation, HIV accessory proteins also help HIV evade the host immune system through interfering with cell surface protein expression (such as MHC, CD4, Fas) or cell cycles of host cells. The increase of viral number eventually causes the death of the host cell, through direct disruption of cell survival, inducing apoptosis, and signaling to CD8 killer cells.

The major target of HIV is CD4+ T cells. Monocytes also host HIV, and are believed to be the reservoir for long-term HIV persistence and, importantly, carry the virus to the

brain.

### 1.1.3 Current treatment and limitation

Due to the lack of an effective vaccine, antiviral drugs are currently the most common treatment for HIV infection. There are 7 classes of antiretroviral agents: 1) entry inhibitors, which impede the membrane fusion of virus and cells by impairing the HR1-HR2 interaction of Env proteins, such as enfuvirtide (ENF); 2) chemokine receptor antagonists, which block the interaction of gp120 and CCR5, such as maraviroc (MVC); 3) non-nucleoside reverse transcriptase inhibitors, which noncompetitively bind to reverse transcriptase, such as nevirapine (NVP); 4) integrase inhibitors, which have high affinity for the viral integrase, such as raltegravir (RAL); 5) nucleoside reverse transcriptase inhibitors, which inhibit the viral DNA elongation, such as zidovudine (AZT); 6) protease inhibitors, which bind to the active site of HIV protease and therefore block the processing of gag and pol precursor polyproteins, such as tipranavir (TPV); and 7) maturation inhibitors, which interrupt viral assembly, such as bevirimat (BVM) [3,4,5]. As a consequence of development of mutation-induced drug resistance, single drug administration can become less effective over time, and therefore the highly active antiretroviral therapy (HAART) combines three or four antiretroviral drugs. However, the blood-brain-barrier (BBB) has poor permeability to the antiviral drugs, and HIV replication in the brain is not effectively suppressed. Therefore, HIV-related neurological disorders remain as a major clinical challenge.

### 1.1.4 Entry of HIV to the brain

HIV can be transported to the brain by monocytes within a few days after the initial infection [6]. After infiltrating the BBB and entering the brain, the monocytes differentiate into brain resident macrophages [7] and spread virus to neighboring glial cells and neurons. HIV may also enter the brain as cell-free viral particle that can cross the BBB, through infected endothelial cells that release the virus into the brain, or through infected CD4+ T cells that transport the virus to astrocytes through the

virological synapse [6,8]. The pathways for entry of HIV to the brain are summarized in Figure 1.1. In the brain, viral replication mainly occurs in infected macrophages and microglia. The activated microglia/macrophages and brain microvascular endothelial cells release chemokines that recruit more lymphocytes and monocytes to the brain. The chronic release of HIV proteins and cytokines can impair the function of neurons and astrocytes and induce apoptosis.

### 1.1.5 HIV-associated neurocognitive disorders

Viral toxicity in the brain can cause HIV-associated neurocognitive diseases (HANDs), which are associated with shrinkage of white matter, break down of the BBB, astrocyte apoptosis, neuronal loss [9] and synaptodendritic simplification (such as significant loss of synapses, decreased numbers of dendritic branches, and retraction of dendritic spines) [10]. Based on the severity of symptoms, HANDs can be categorized into three classes by standardized measures of dysfunction: (1) asymptomatic neurocognitive impairment (ANI), where mild cognitive impairment is present but does not interfere with daily function, occurs in about 30% of HIV-infected individuals; (2) mild neurocognitive disorder (MND), in which mild cognitive impairment causes some interference in daily activities, occurs in 20-30% of HIV-infected individuals; and (3) HIV-1 associated dementia (HAD), characterized by severe neurocognitive impairment, emotional disturbance and motor abnormalities causing marked interference in daily function, occurs in 2-8% of HIV-infected individuals [4,11,12]. The severity of HANDs correlates with CD4+ T cell count and age [13], and the progression of HAD correlates with the densities of pyramidal neurons [14] and microglial, and apoptosis of astrocytes [9,15].

Before application of HAART, the HIV replication in the brain was mainly found within the basal ganglia, brain stem, and deep white matter [16,17]. The active viral replication is shifted to the hippocampus and the adjacent parts of entorhinal and temporal cortex after HAART treatment [18]. HAART has decreased the incidence of HAD from 6.6% in 1989 to 1% in 2001 [18], and decreased the total incidence of HANDs by about 75%

[4]. Due, in part, to the inefficient penetration of the antiretroviral drugs through the BBB [19,20,21], the reversal of HANDs by HAART is slow [22] and incomplete [23], and the overall prevalence of HANDs remains 15%-50% in the HIV patients [4].

### 1.1.6 HIV-induced inflammation in the center nervous system (CNS)

Neuroinflammation is one of the major causes of HANDs. Once HIV-infected CD14+/CD16+ monocytes migrate to the brain, they can release viral proteins, which activate glial cells and induce the release of chemokines. Tat and gp120 can both induce the release of tumor necrosis factor α (TNFα), interleukin 1β (IL1β), interleukin 6 (IL6), monocyte chemoattractant protein 1 (MCP-1), macrophage inflammatory protein 1α (MIP-1α), MIP-1β, and Tat can also induce the release of transforming growth factor β (TGFβ), IL-8, interferon gamma-induced protein 10 (IP-10), and chemokine c-c motif ligand 5 (CCL5) [18]. Some of the chemokines, such as MCP-1 and fractalkine (CX3CL1), can further recruit HIV-infected or non-infected monocytes into the brain, and the recruited monocytes or macrophages can, in turn, release more chemokines, forming a vicious circle. In fact, accumulation of monocytes and macrophages is one of the hallmarks of HANDs. Increased MCP-1 levels have been detected in both macrophages and astrocytes under HIV infection [24]. In the cerebrospinal fluid (CSF), the level of MCP-1 is related to viral load and the severity of neurocognitive impairment [18]. CX3CL1 is constitutively expressed in neurons and is upregulated by inflammatory stimuli in the CNS. CX3CL1 receptor is expressed on many types of cells, including T cell, neurons and astrocytes.

Increased inflammation in the basal ganglia and mid-frontal cortex in the brain of HIV-infected individuals has been detected by magnetic resonance spectroscopy (MRS) using choline/ creatine and myoinositol/ creatine as biomarkers. However, no further progress of inflammation has been observed in more severe cases of HANDs, implicating that the inflammation may have reached a plateau in the brain in the early stages of the infection. On the other hand, a marker of neuronal damage has been found to increase significantly

in the basal ganglia and front white matter in severe HANDs subjects [25], suggesting that there are other factors contributing to the severity of HANDs, such as oxidative stress.

### 1.1.7 HIV-induced oxidative stress in the CNS

HIV induces oxidative stress through activation of macrophage, microglia and astrocytes [26]. HIV proteins that are released from infected glia also induce oxidative stress in neurons [27,28]. In CSF or some brain regions of HIV-infected patients, levels of antioxidants such as glutathione (GSH) [29], glutathione peroxidase (GPx), Cu/Zn superoxide dismutase (SOD) [30], ascorbic acid [31] and vitamin E [32] have been found reduced, while oxidants or oxidative stress markers such as 4-hydroxynonenal (HNE) [32,33], ceramide [32,33], sphingomyelin [32,33], and protein carbonyls [34] are elevated. Similarly, in the animals challenged by HIV viral proteins, lower levels of GSH and total SOD, but higher levels of hydroxyl radical and malondialdehyde (MDA), were found in the brain [35].

Viral proteins induce oxidative stress through different mechanisms in different types of cells. In microglia, HIV-1 entry has been linked to the binding of gp120 to chemokine receptors and subsequent increase in intracellular calcium concentration, which further upregulates the release of chemokines. On the other hand, Tat can elevate the expression of TNF$\alpha$, which increases inducible nitric oxide synthetase (iNOS) expression and subsequently nitric oxide (NO) accumulation. In astrocytes, Tat can induce NO generation, and gp120 can inhibit glutamate re-uptake and cause glutamate accumulation in the extracellular environment. The increased concentration of extracellular glutamate inhibits cysteine uptake by neurons, leading to impeded generation of GSH and, eventually, GSH depletion. Extracellular glutamate can also over-stimulate glutamate receptors on neurons, leading to increase of intracellular calcium that impairs mitochondria function through depolarization of mitochondrial membrane potential and generation of free radicals, such as superoxide. Although HIV does not infect neurons,

the HIV proteins and cytokines released from infected glia can damage the neurons by increasing intracellular calcium concentration, causing oxidative stress and initiating apoptosis [6]. An example of HIV-induced oxidative stress in the neuron is graphed in Figure 1.2.

### 1.1.8 Rodent models for HAND studies

The infection of HIV is species-specific. It is therefore a challenge to establish an ideal animal model to mimic the HIV infection in human. HIV is genetically close to simian immunodeficiency virus (SIV). Many African monkeys and apes are natural hosts for SIV, and they generally do not develop the disease as a consequence of infection [36]. In contrast, SIV-infected Asian macaques closely resemble the HIV infection in human [37]. However, the cost of this model is high and the end-organ damage is different from that observed in the HIV-infected humans [38]. Although HIV does not infect rodents, various techniques have been applied to establish HIV rodent models due to the low cost and easy management of rodents, and well-established methods for manipulating the rodent genome. Transgenic and humanized rodents are the major models used in current HIV studies.

Humanized mouse models have reconstituted human immune system by engrafting human tissue to severe combined immunodeficiency (*scid*) mice which do not have functional T cells and B cells due to a mutation in the protein kinase catalytic subunit (PRKDC) [37]. Injection of HIV-1 or HIV-infected human cells can infect implanted human tissue in the animals. However, the success rate of engraftment in *scid* mice is low. To overcome this, NOD/scid mice were developed. These mice were generated by crossing *scid* mice and non-obese diabetic (NOD) mice, and they have low host natural killer cells and improved efficiency of engraftment. To study the HIV infection in the brain, huPBL-HIVE mouse model was developed. In this model, the reconstituted human immune system is achieved by transplanting human peripheral blood lymphocytes (PBLs) to NOD/scid mice, and HIV-1 infected human monocytes-derived macrophages (MDMs)

are injected into the basal ganglia of the brain. This model is useful for studying innate and adaptive immunity in HANDs progression and resolution [39], but not for long-term study due to the short lifespan caused by the high rate of thymic lymphomas in these mice [37,38]. Another limitation of using humanized mice is that the mice cannot be bred and each humanized mouse need to be generated by surgical engraftment of human tissue, which increases technical challenge and cost [37]. In contrast, transgenic rodents can be bred and maintained at low cost.

The transgenic mouse models established to date express individual HIV-1 subgenomic fragments including gp120, Tat, Vpr, Nef, and LTR. Viral protein-induced toxicities in the brain have been reported in HIV-1gp120, HIV-1Tat, and HIV-1Vpr transgenic mice [38]. Rodents expressing full-length HIV-1 proviral DNA with or without modification have also been established. Viral proteins were detectable in the brain and these animals showed impaired brain function [38]. Each of these models can replicate some aspects of the pathogeneses of human HIV infection, but the viral proteins are expressed in atypical tissues due to the promoter regulation of the viral genes [40].

In 2001, the HIV-1 transgenic (HIV-1Tg) rat model was established in the Bryant lab at the University of Maryland. The genome of the HIV-1Tg rats carries HIV-1 pNL4-3 provirus DNA with functional deletion of Gag and Pol (Figure 1.3). The rest of the viral proteins are expressed in the HIV-1 Tg rats, and they are: Vpr, Env, Nef, Vif, Vpu, Rev and Tat. These rats have circulating gp120 in the blood and efficient viral mRNA expression in many tissues, including lymph nodes, spleen, thymus, and brain [40]. This model recapitulates many key features of human AIDS, such as muscle wasting, cataracts, immune deficiencies, respiratory difficulty and HIV-associated neurological abnormalities [40,41,42,43,44]. Neuronal loss, reactive gliosis [40], and impaired spatial learning ability [45] were also reported. Due to the low level of viral protein expression in the brain, this is a useful model for studying the pathogenesis of HANDs in patients with controlled viral replication as a result of HAART. However, this model lacks human

immune system, and therefore cannot be used for studying viral replication and spread, nor testing antiretroviral drugs.

## 1.2 Glutathione as a key redox regulator

### 1.2.1 Reactive oxygen species and antioxidants

Molecules with ability to gain electrons from other reactants are oxidants and the substrates donate electrons are reductants. The reactions of electrons transfer between oxidants and reductants are called redox (reduction-oxidation reaction). Reactive oxygen species (ROS) are oxidants contain oxygen and have high reactive activity. There are radical ROS, such as superoxide anion ($O_2^{\bullet -}$), hydroxyl ($HO^{\bullet}$), peroxyl ($RO_2^{\bullet}$), alkoxyl ($RO^{\bullet}$), and nonradical ROS, such as hydrogen peroxide ($H_2O_2$). At physiological level, ROS function as signaling molecules regulating cell proliferation, differentiation, host defenses, apoptosis, blood clotting, and gene expression. However, over-production of ROS can damage cells and induce cell death. The major source of ROS is the electron transport chain in the mitochondria. Other sources include dehydrogenation in peroxisomes and a variety of cytosolic enzyme systems, such as monooxygenase and NADPH oxidase (NOX) [46]. A number of external stimuli, such as UV light and radiation, can also trigger ROS production in the cells.

Antioxidants are reductants with protective functions of cellular impairment induced by oxidation. Antioxidants can be small molecules, such as glutathione (GSH), ascorbic acid, α-tocopherol and flavonoids; or they can be enzymes, such as glutathione peroxidase (GPx), thioredoxin, catalase, and SOD. Both ROS and antioxidants are important for cell survival. Under normal physiological conditions, the generation of ROS and antioxidants is balanced to maintain cell function. When ROS accumulate and cannot be efficiently reduced by antioxidants, they can damage DNA, proteins, and lipids and cause oxidative stress, which is involved in many diseases, such as cancer, cardiovascular disease and neurodegenerative disorders.

### 1.2.2 Glutathione-centered antioxidant system

Glutathione (L-γ-glutamyl-L-cysteinylglycine) is the most abundant nonprotein thiol in eukaryotic cells. It plays important roles in antioxidant defense, DNA synthesis, apoptosis and cell proliferation. It can function as a reducing substrate for antioxidant enzymes or it can directly conjugate oxidants [47]. There are two forms of GSH, reduced GSH (rGSH) and oxidized GSH (GSSG). When functioning as an antioxidant, rGSH is oxidized to GSSG. GSSG can be reduced to rGSH by glutathione reductase (GR) (Figure 1.4). The ratio of rGSH/GSSG is a commonly used redox marker.

Glutamylcysteine synthetase (GCS) is the rate-limiting factor for GSH biosynthesis. This enzyme catalyzes the ligation of glutamate and cysteine, the first and rate-limiting step in the *de novo* synthesis of GSH [48]. GSH synthesis is completed by glutathione synthetase (GS), which catalyzes ligation of glycine to gamma-glutamylcysteine. GSH is synthesized in the cells and can be transported by multidrug resistance proteins (MRP) to the extracellular space, where gamma-glutamyltransferase (GGT) catalyzes the rate-limiting step of GSH catabolism. Degraded GSH releases cysteine which can be transported back to the cells by the excitatory amino acid carrier 1 (EAAC1), or oxidized to cystine and then transported into the cells through the membrane protein cystine/glutamate antiporter system $x_c$- [49]. In cells, cystine can be reduced to cysteine for next cycle of GSH synthesis [50]. As a cofactor for enzymes, GSH is used for glutathione peroxidase (GPx) to reduce lipid peroxides and hydrogen peroxide; for glutaredoxin to reduce protein disulfide bonds; and for glutathione-S-transferase to conjugate oxidized molecules, such as 4-hydroxynonenal (HNE). The summary of GSH metabolism pathways is shown in Figure 1.5.

GCS is a holoenzyme consisting of a catalytic heavy chain (GCS-HC) and a modulatory light chain (GCS-LC). GCS-HC possesses the catalytic activity and is also the site of GSH feedback inhibition. When bound with GCS-LC, GCS-HC has reduced feedback inhibition by GSH and an increase in the affinity for glutamate. Oxidant stimulation

increases gene and protein expressions of both subunits [51], and HNE-induced upregulation of GCS mRNAs through Nrf2 and JNK pathways [52]. Oxidative stress can also post-translationally regulate GCS activity [53].

GGT is the only enzyme known that can break the γ-glutamyl bond in GSH, GSH conjugates, and GSSG. Inhibition of GGT activity results in increased extracellular GSH and decreased intracellular GSH, suggesting its importance for thiol metabolism. In response to oxidative stress, GGT mRNA is upregulated [54]. However, GGT can become a pro-oxidant as well, as accumulation of its product cysteinylglycine can generate hydroxyl radical from superoxide through the Fenton reaction [55]. In humans, there are at least seven GGT genes or pseudogenes [56]. In rodents, GGT is a single copy gene with multiple promoters, which control GGT expression in different tissues and developmental stages. HNE has been reported to upregulate gene expression of some GGT isoforms through ERK1/2, Nrf2 and c-JUN pathways [57,58].

HNE is a byproduct of lipid peroxidation, and is relatively stable *in vivo*. At low relative concentrations (1μM or lower), HNE regulates cell proliferation and differentiation, but at high concentrations it is toxic to the cell. HNE is considered a key mediator of oxidative stress damage [54]. HNE can be removed from cells through reduction by aldehyde reductase, oxidation by adehyde dehydrogenase, or conjugation by GSH [54]. Depending upon cell types, up to 70% of HNE can be removed by GSH [59]. GSH conjugates HNE spontaneously or through GST.

### 1.2.3 Glutathione metabolism in the brain

GSH is the most abundant endogenous antioxidant in the brain. The concentration of GSH in the brain is in a range of 1 to 3 mM, depending on cell type, age, and brain region [60]. Lower GSH concentrations areobserved in neurons and younger animals, and higher concentrations in astrocytes and older animals [61]. The intracellular GSH concentration is much higher than the extracellular concentration (e.g. in the CSF), partially due to rapid GSH degradation by GGT outside of the cells. In the brain, mRNAs of GGT1,

GGT5, GGT6 and GGT7 have been detected. Among them, GGT7 had the highest expression level and was only found in the nervous system [62]. The GGT activity is concentrated in the choroid plexus and the expression of GGT is high in glia cells but low in neurons [56].

MRPs transport GSH, GSSG, and GSH conjugates from inside to outside of the cells. There are at least 9 isoforms of MRPs, and their exact locations and functions are yet to be determined. mRNAs of MRP1, 2, 3, 4, and 5 have been found in rat brain [63]. However, only MRP1 and MRP2 showed GSH-related transport function[63]. MRP1 was found to be expressed in neurons, astrocytes and microglia, and MRP2 expression was not detectable in microglia nor astrocytes, and its expression in neurons is not clear [63]

Both neurons and astrocytes can take up cysteine and cystine for GSH synthesis. Cysteine uptake is mediated by EAAC1, a member of the EAAT family. Although EAAT1, EAAT2 and EAAC1 can all transport cysteine, only EAAC1 transports cysteine with high affinity [64]. EAAT1 and 2 are primarily located on astrocytes, while EAAC1 is located on neurons. EAAC1 can take up nearly 90% of free extracellular cysteine. Knockout of EAAC1 results in a 30-40% decrease of GSH content in mouse brain. Use of cystine for GSH synthesis is much higher in the astrocytes than in the neurons [65]. Cysteinylglycine is also used for GSH synthesis, but the transporter of this dipeptide is not clear [60]. The availability of cysteine is limited in neurons, and co-culture of neurons with astrocytes enhances GSH synthesis in the neurons. Therefore astrocytes seem to supply cysteine for neuronal GSH synthesis [60].

### 1.2.4 HIV-induced changes in GSH metabolism

In the 1980's, HIV-associated GSH depletion was found for plasma, lung epithelial lining fluid and peripheral blood mononuclear cells [66,67]. Decreases in GSH content in CD4+ and CD8+ T cells in HIV patients were reported shortly thereafter [68]. A change in GSH levels in the CNS of HIV patients was not documented until 1995 [29]. Using cell culture

and animal models, HIV viral proteins have been found to induce changes of GSH and GSH-related enzymes [35,69,70,71].

## 1.3 Modulatory factors of neurological outcomes of HIV infection

### 1.3.1 Methamphetamine

#### *1.3.1.1 Methamphetamine and HIV infection*

Methamphetamine (Meth) is a CNS stimulant with a high potential for addiction. More than 26 million people worldwide use Meth, a population larger than users of heroin and cocaine combined, mainly due to the relatively low cost and long-lasting stimulatory effects of this substance [72,73]. In 2005, an estimated 10.4 million persons aged 12 and older in the U.S. had used Meth at least once in their lifetime [74]. In 2011, more than 400,000 (0.2% of US population) people were current Meth users which is much lower than the peak year 2007 (731,000 persons) [75].

Injection drug use (including Meth) contributes 7.4% of new HIV infection in the US in 2011 [76]. Multiple studies have demonstrated the contribution of drug abuse to the risk of HIV infection [77,78,79,80,81,82,83]. These studies also showed an association between Meth abuse and the spread of HIV through both shared use of contaminated needles and a culture of risky sexual behavior. On the other hand, people with HIV infection tend to use Meth for stimulation and "self-medication" of negative feelings [84]. The convergence of HIV infection and Meth abuse has thus unfortunately exposed a seemingly increasing segment of population to the additive symptoms of the two diseases, especially their synergistic deleterious impacts on the CNS.

#### *1.3.1.2 Impacts of Methamphetamine on the CNS*

Regardless of the route of Meth exposure, this drug can cross the BBB and increase the release of neurotransmitter dopamine (DA) in the striatum, resulting in euphoria [85]. Long-term Meth use can result in decreases of DA and serotonin (5HT) neurons, tyrosine

hydroxylase activity, and DA uptake sites [86], which cause mental symptoms such as paranoia, hallucinations, anxiety, and irritability [87,88]. DA is synthesized in the cytoplasm and transported into the synaptic vesicle at the expense of a proton gradient in this compartment. As a highly lipophilic drug, Meth rapidly enters the terminal through the dopamine transporter (DAT) on dopaminergic neurons or through diffusion. It then enters the vesicle collapsing the proton gradient and redistributing DA into the cytoplasm [89,90]. Excess DA in the cytoplasm is then shuttled out into the synapse by reverse transport through the DAT [91].

When released from the synaptic vesicles into the cytoplasm, DA is subjected to auto-oxidation and enzymatic degradation, which result in the formation of hydrogen peroxide ($H_2O_2$) and superoxide [92,93,94,95]. Via the Fenton reaction, $H_2O_2$ can form hydroxyl radicals ($HO^{\cdot -}$), the most reactive free radical currently known [96]. Meth also increases the extracellular concentration of glutamate [97], which activates nitric oxide synthase (NOS) and increases the production of nitric oxide [98] and subsequently peroxynitrite, resulting in the inhibition of the mitochondrial electron transport chain (ETC) [99,100] at the site of complex II [101], which in turn increases the production of superoxide. The co-incident release of superoxide and nitric oxide results in a vicious circle of peroxynitrite formation. Consequently, increased oxidative stress within the dopaminergic terminal has been reported on exposure to Meth [102,103,104]. Rodent models have demonstrated that Meth administration increased lipid peroxidation, 3-nitrotyrosine formation, and the production of hydroxyl radicals in the striatum [87,105]. Increased activities of antioxidant enzymes such as GPx and SOD, are also reported in the brain of animals treated with Meth [106,107]. Meth-induced changes on GSH are region- and time-dependent [106,108]. Several studies have shown that administration of antioxidants protects against dopaminergic toxicity following Meth exposure [87,109,110,111,112,113].

#### *1.3.1.3 Synergistic effects of Meth abuse and HIV infection on the CNS*

HIV-infected individuals using drugs suffer from more severe encephalitis and rapid neurological progression of the disease compared to those who do not abuse drugs [114,115,116]. Use of Meth not only can increase HIV viral load *in vitro* and *in vivo* [117], but also increase inflammation and oxidative stress in the brain [85,118]. In Meth users, HIV caused greater neuronal injury and cognitive impairment compared with nondrug abusers [119]. Proton magnetic resonance spectroscopy (MRS) showed additive effects of Meth on glial activation and neuronal injury in HIV-infected/Meth using patients compared to non-Meth using patients [120]. Post-mortem analysis of brains from HIV-infected/Meth using patients also showed increased neuronal injury and dendritic loss in the frontal cortex compared to the non-Meth using patients [121]. Animal studies demonstrated that Tat and Meth interact in the rat striatum, causing a synergistic neurotoxicity to the dopaminergic system [122,123]. *In vitro* studies on neurons and hippocampal cell lines revealed Tat and Meth synergistically increase mitochondrial dysfunction and oxidative stress, which can be attenuated by antioxidants [123,124]. The mechanism of the synergistic effects between Meth and HIV is not fully revealed, but have been partially attributed to the synergistic damage of DA terminals, increase of extracellular glutamate [119], and the fact that Meth promotes retroviral replication [125,126].

### 1.3.2 Complementary and alternative medicine (CAM) in HIV treatment

#### *1.3.2.1 Use of CAM in the United States*

CAM employs practices and products not generally used in conventional medicine (western or allopathic medicine) to prevent and treat diseases and to improve health. A National Health Interview Survey (NHIS) carried out in 2007 reported that ~38% of adults in the United States used CAM, and $14.9 billion was spent on nonvitamin, nonmineral natural products (the most used CAM therapy), which is equivalent to ~1/3 of total out-of-pocket spending on prescription drugs ($47.6 billion) [127]. People choose

CAM because they prefer holistic treatment, want to avoid side effects associated with prescription drugs, are dissatisfied with conventional medicine, due to cultural beliefs, ease of access, convenience, or for financial reasons [128].

*1.3.2.2 Dietary supplement and natural products in HIV treatment*

Although HAART can effectively suppress HIV replication, the prevalence of drug-resistant viral variants is increasing [129,130,131]. Most of the drugs also have side effects and associate with relatively high costs. Therefore, in addition to the development of new antiretroviral drugs, some scientists also direct their efforts to explore alternative treatments of HIV.

HIV infection is associated with low food intake and high energy expenditure, which results in nutrient imbalance, further compromised immune system, and increased risk of death [132]. Supplementation of micronutrients such as selenium [133], vitamins A [134], E, and C [135] have been found beneficial to HIV patients.

Potential applications of compounds isolated from natural products have also been tested for HIV treatment. For example, it has been reported that palmitic acid extracted from brown algae (*Sargassum fusiforme*) can inhibit HIV fusion [136], guanidine alkaloids isolated from sea sponge (*Crambe crambe)* can inhibit Nef activity [137], and epicatechins isolated from green tea can protect neurons from HIV viral protein-induced toxicity [138]. Use of CAM in HIV treatment is a relatively new research field, and the possibilities are yet to be fully explored.

## 1.4 Aims of this study

The aims of this study were to investigate the redox and inflammatory changes induced by HIV infection in the CNS, and to test whether these changes can be aggravated by concurrent use of Meth, or ameliorated by natural product application. To achieve these purposes, we have used cerebrospinal fluids collected from human cohorts to evaluate the

redox changes caused by HIV infection and use of Meth in the extracellular environment of the CNS. We have also employed HIV-1 transgenic rats with Meth exposure to simulate the pathogenic factors in the human subjects and to analyze the redox and inflammatory changes in different regions of the brain. As GSH is the most abundant antioxidant in the brain and is highly responsive to oxidative challenges, the GSH-centered metabolic and antioxidant systems have been used in our study as redox indicators. The thalamus has caught our special attention due to its high content of GSH. At the end of the study, we supplemented the diet of the HIV-1 transgenic rats with an extract from bamboo *Phyllostachys edulis*, and evaluated the anti-neuroinflammatory effects of this natural product.

**Figure 1.1. HIV invasion in the brain.** ① HIV enters the brain through infected monocytes. The infected monocytes infiltrate the blood-brain-barrier (BBB) and differentiate to macrophages. ② Cell-free HIV particles cross the BBB. ③ Infected brain microvascular endothelial cells release HIV particles in the brain. ④ Astrocytes take up HIV particles from infected CD4+ T cells and release them to the brain parenchyma. The activated glia cells release chemokines and reactive oxygen species (ROS) that cause damages to the neurons.

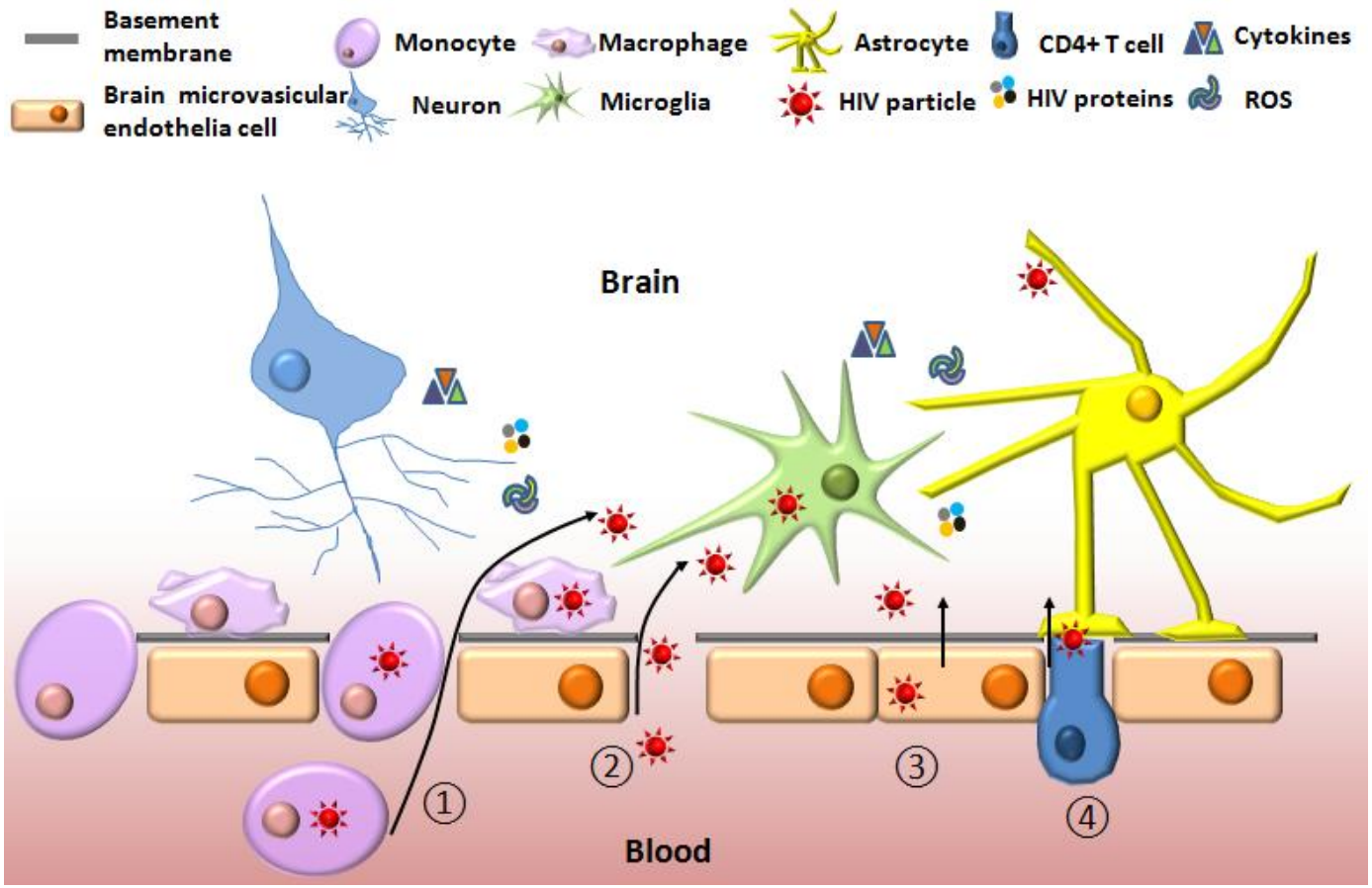

**Figure 1.2. An example of HIV-induced oxidative stress in the brain.** HIV-infected macrophages release tumor necrosis factor α (TNFα) which can induce glutamate (Glu) release from astrocytes and inhibit Glu uptake by astrocytes. Increased extracellular Glu over stimulates N-methyl- D-aspartate (NMDA) receptor and induced calcium ($Ca^{2+}$) influx to the neuron. Increased intracellular $Ca^{2+}$ damages mitochondrial function through $Ca^{2+}$ overtake and induces generation of superoxide ($O_2^{\bullet-}$). Increased intracellular $Ca^{2+}$ also increases expression of nitric oxide synthase (NOS) which leads to increase level of nitric oxide (NO). The reaction of NO and $O_2^{\bullet-}$ generates even more toxic reactive oxygen species (ROS) peroxynitrite ($ONOO^-$).

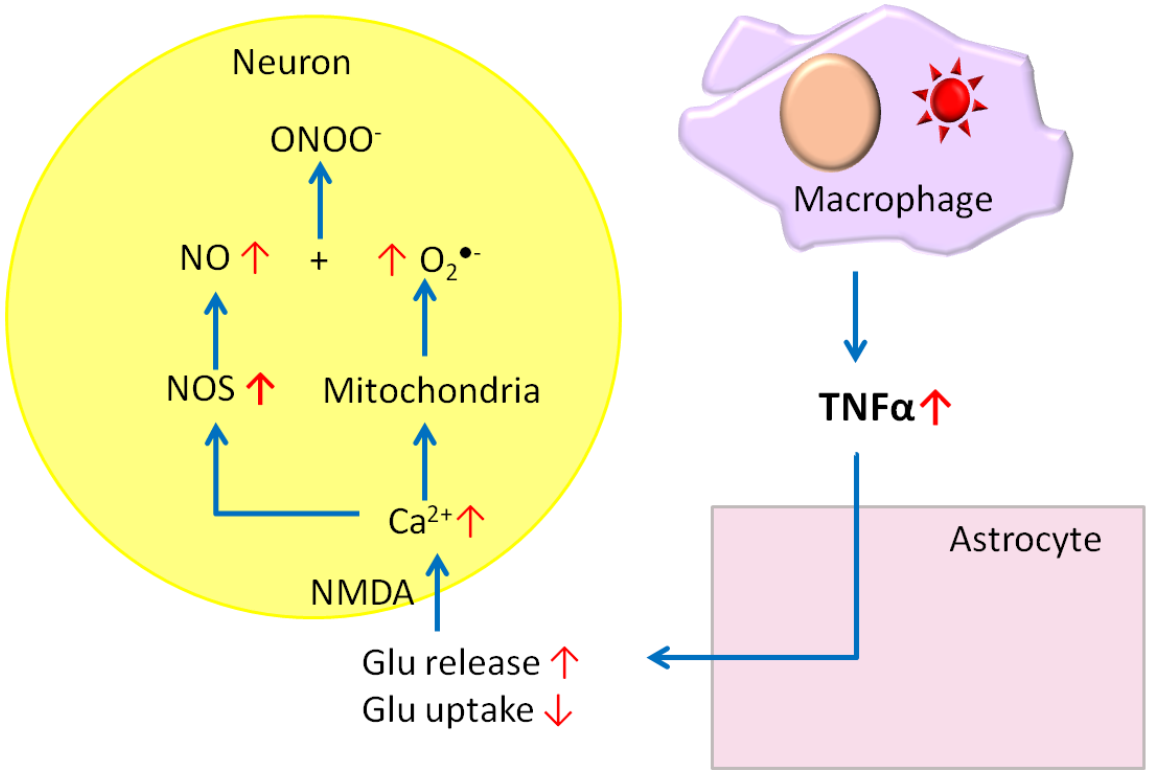

**Figure 1.3. The HIV provirus DNA structure inserted in the genome of the HIV-1 transgenic rats.** gag, group-specific antigen; pol, polymerase; env, envelope proteins; vif, viral infectivity factor; vpr, viral protein R; tat, trans-activator of transcription; rev, regulator of virion expression; vpu, viral protein unique; nef, negative factor.

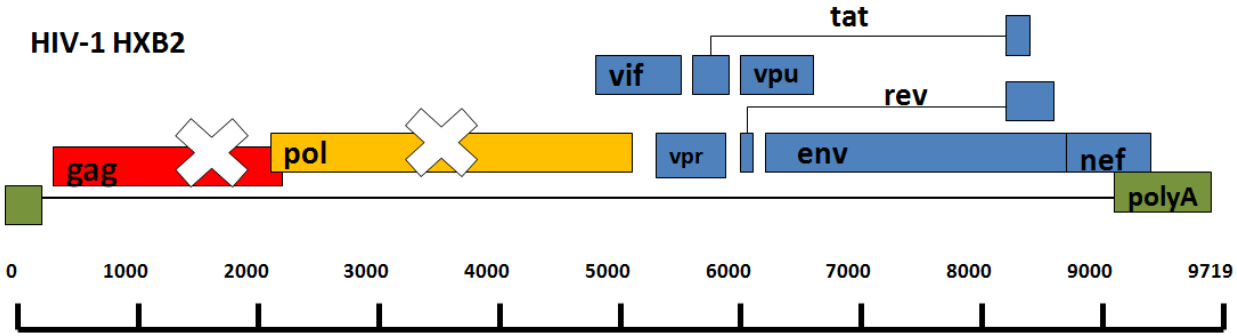


Modified from HIV molecular immunology 2009

**Figure 1.4. Structures of reduced and oxidized glutathione and the redox reactions converting the two forms**. Glutathione (GSH) is constituted by glutamate (Glu), cysteine (Cys) and glycine (Gly). Two molecules of reduced GSH are used for hydrogen peroxide ($H_2O_2$) reduction catalyzed by glutathione peroxidase (GPx), and generate one molecule of oxidized GSH (GSSG). GSSG can be reduced by glutathione reductase (GR) with hydrogen donated from NADPH.

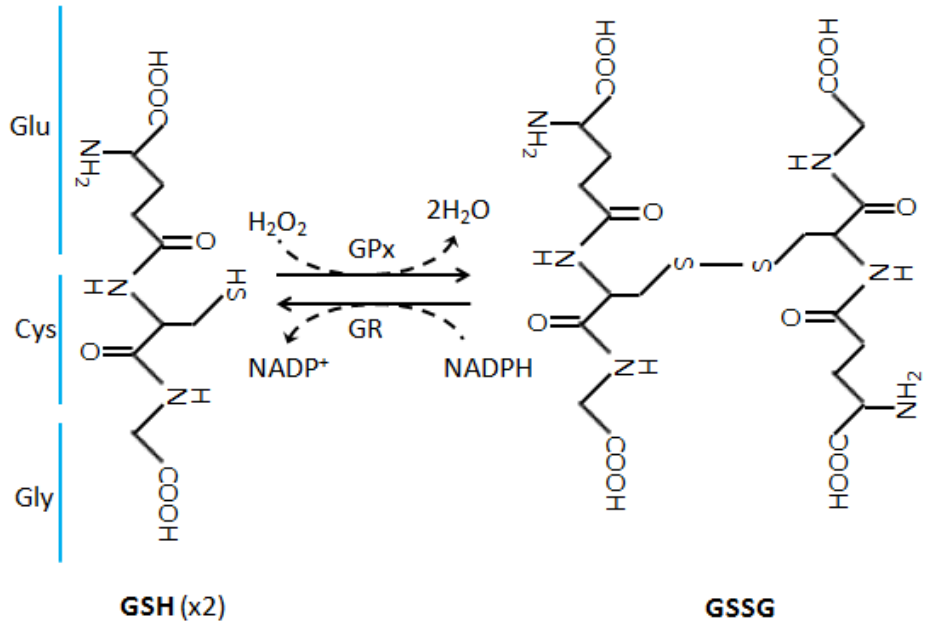

**Figure 1.5. The pathway of glutathione metabolism.** GSH, glutathione; GSSG, oxidized GSH; MRP, multidrug resistance proteins; GGT, gamma-glutamyl transferase; Glu, glutamate; CysGly, cysteinylglycine; Cys, cysteine; Gly, glycine; GCS, glutamylcysteine synthetase; GS, glutathione synthetase; GR, glutathione reductase; GPx, glutathione peroxidase; Glrx, glutaredoxin; GST, glutathione-S-transferase; HNE, 4-hydroxynonenal.

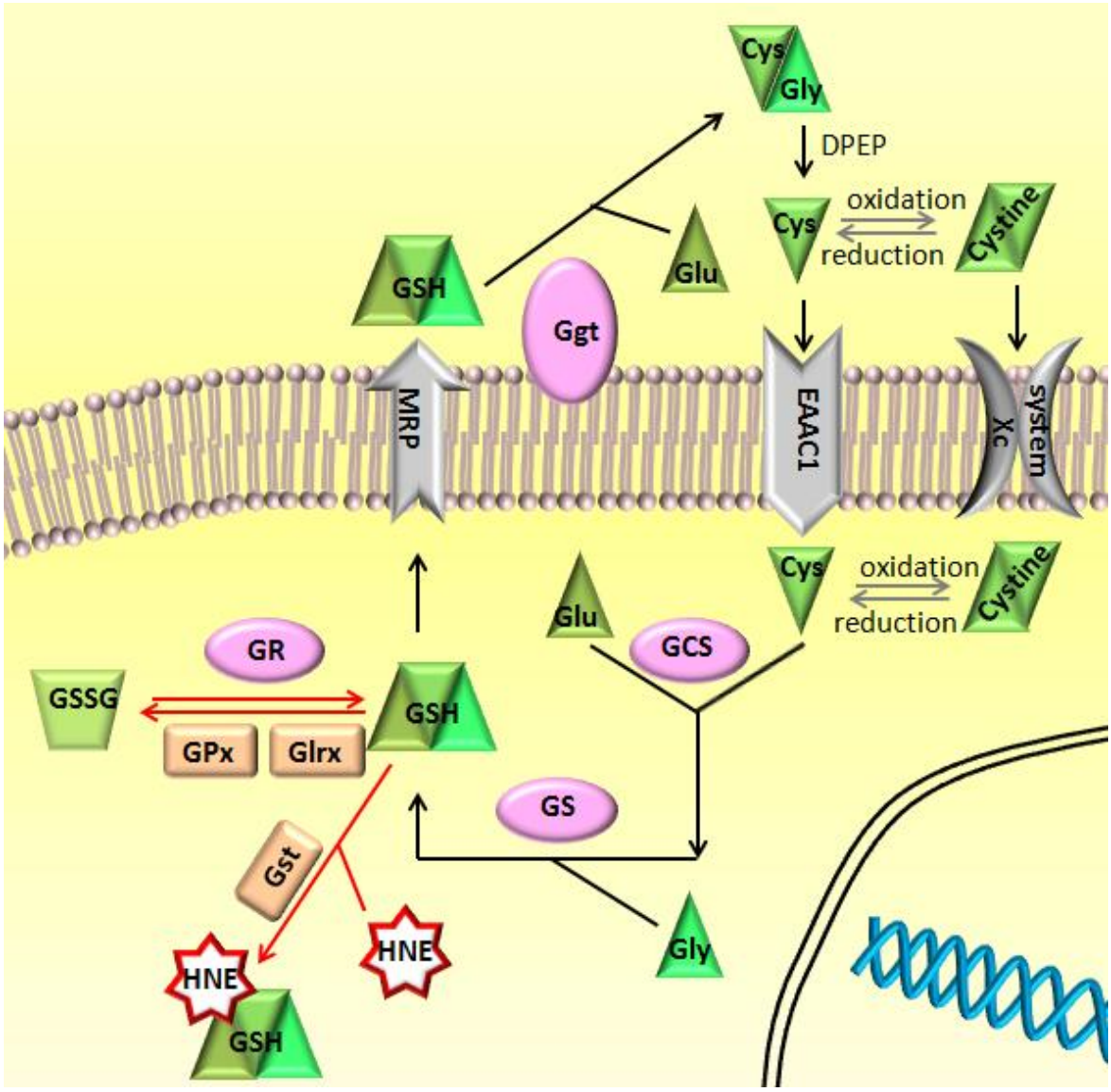

# Chapter 2

## Differential Effects of HIV Infection and Methamphetamine Abuse on Glutathione Metabolism and Oxidative Stress in Human Cerebrospinal Fluid

## 2.1 Background

Despite the application of HAART, the incidence of HANDs in HIV-infected population in the United States remains up to 50% [4,139], suggesting the CNS is under significant stress, including oxidative stress, even with antiviral drug treatment. Meth exposure has been reported to increase HIV replication both *in vitro* and *in vivo* [117]. For example, Meth can increase HIV Long terminal repeat (LTR) activity and nuclear factor kappa-light-chain-enhancer of activated B cells (NFκB) expression, with the later regulates TNFα expression. Both HIV LTR and TNFα can enhance HIV replication in macrophage [117]. Meth also induces oxidative stress in the brain [140,141]. The concurrence of HIV infection and abuse of Meth may facilitate the development of neurocognitive disorders through increased oxidative stress, as shown in cultured neurons [123,124] and in mouse brain [142].

GSH was found decreased in the plasma and T cells of HIV-infected HAART-naïve patients [67,68]. Although HAART improved the rGSH/GSSG ratio [143], lower GSH levels in plasma and lymphocyte cells were consistently observed in HIV patients with antiretroviral treatments [66,67,68,143,144]. Furthermore, antiretroviral drugs such as zidovudine (AZT) and indinavir (IDV) have been reported to cause GSH depletion at high concentrations [145,146,147]. Although GSH is the most abundant antioxidant in the brain, HIV-induced changes of GSH and GSH-dependent antioxidant enzymes in the CNS have not been fully studied.

Meth exposure also affects GSH status in the brain, and these effects are dose-, time- and cell type-dependent [106,108]. Whether the concurrence of HIV and Meth can interactively regulate the GSH system in the CNS has not been investigated.

The aim of this study was to delineate both separate and combined influences of HIV infection and Meth abuse on GSH metabolism, GSH-centered antioxidant enzyme activity, and oxidative stress in the cerebrospinal fluid (CSF).

## 2.2 Materials and Methods

### 2.2.1 Research participants

The study protocol was approved by the Institutional Review Board (IRB) of the University of Hawai‘i. One hundred and twenty-three participants were carefully evaluated to ensure they fulfilled the study criteria prior to subject enrollment. The participants were separated into 4 groups: (1) HIV group, HIV-infected individuals who have not used Meth in their life time, n=34; (2) HIV+Meth group, HIV seropositive individuals who used Meth, N=23; (3) Meth group, HIV seronegative individuals who used Meth, N=25; and (4) Control group, HIV seronegative individuals who have not used Meth in their life time, N=41. For Meth users, their last use of Meth was to be within 6 months prior to the lumbar puncture for CSF sample collection. The demographics and clinical evaluations of the study subjects are listed in Table 2.1.

### 2.2.2 Specimen Collection and Processing

CSF was collected from research subjects via lumbar puncture using a 22-gauge sprotte needle. A 20µL aliquot was used for cell counting in a hemocytometer. The samples were kept on ice and quickly centrifuged at 400 x g for 10 minutes at 4°C to remove any contaminating cells. The CSF supernatant was transferred into fresh Eppendorf tubes and further centrifuged at 1000 x g for 10 minutes at 4°C to remove any cellular debris. The CSF samples were aliquoted and then stored at -80°C untill the assays were conducted.

### 2.2.3 Chemicals and instruments

All chemicals used in this study were purchased from Sigma (St. Louis, MO) unless otherwise noted. The concentration tubes (cut-off size = 3kDa) were purchased from Millipore (Amicon Ultra-0.5, Billerica, MA). The spectrophotometers used in the colorimetric and fluorescent assays were SpectraMax 340 (for GSH and HNE-His assays) and SpectraMax M3 (for GGT and GPx assays) from Molecular Devices (Sunnyvale, CA).

### 2.2.4 GSH assay

This assay is based on the colorigenic reaction between GSH and 5,5'-dithiobis-2-nitrobenzoic acid (DTNB) [148]. The pH of CSF samples was adjusted to 7.6 using 1N HCl and stored at -80°C until use. To measure GSH, 30 μl of sample was added into a final mix (50 μl) containing: 0.5 mM DTNB, 5 U/ml GR, and 125 μM NADPH in 50 mM phosphate buffer with 5 mM EDTA (pH 7.4). Absorbance at 412 nm was recorded using a spectrophotometer for 5 min, and the reaction rates were compared to a standard curve obtained from GSSG. The assay was carried out in triplicate.

### 2.2.5 GGT activity assay

The GGT activity assay was based on a published method [149] with modification. Briefly, CSF samples were centrifuged in concentration tubes until the volume decreased by 7 times. For each reaction, 8 μl concentrated CSF sample was added to 36 μl reagent solution which consisted of five volumes of L-gamma-glutamyl-p-nitroanilide (GPNA) (6.8 mM, pH 8.2) and one volume of Gly-Gly (344.5 mM pH 8.2). The absorbance at 410 nm was measured for 1 h at 37°C. One unit of activity was defined as a consumption of 1 μmol of GPNA per minute calculated from the expression $(Vmax * V_t/V_s)/ (0.0088* D)$, where $V_t$ is the total volume of reaction solution in microliters, $V_s$ is the sample volume in microliters, 0.0088 $\mu M^{-1}cm^{-1}$ is the extinction coefficient for GPNA at 410 nm, and D is the reaction solution depth in wells in centimeters. Each sample was measured in triplicate.

### 2.2.6 GPx activity assay

The GPx activity assay was modified from a previous publication [150]. CSF samples were concentrated as described above. Six μl concentrated sample and 4 μl buffer were added to a mixture (18μl) containing 5mM GSH, 5μg/ml GR, and 0.26mM NADPH in 50 mM potassium phosphate buffer with 5 mM EDTA (pH 7.4), followed by incubation at 37°C for 3 min. The reaction was initiated by adding 2 μl of 6 mM tert-butylhydroperoxide. The absorbance at 340 nm was recorded for 10 min at 37°C. One

unit of enzyme activity was defined as a consumption of 1 μmol of NADPH per minute calculated from the expression (Vmax * $V_t/V_s$)/ (0.0062* D), where 0.0062 $\mu M^{-1}cm^{-1}$ is the extinction coefficient for NADPH at 340 nm. Each sample was measured in triplicate.

2.2.7 Lipid peroxidation assay

The concentration of histidine-conjugated HNE (HNE-His) in the CSF samples was measured using ELISA kits from Cell Biolabs (San Diego, CA).

2.2.8 Statistical analysis

Statistical analysis was performed using SAS Enterprise 4.3 (SAS Institute Inc, Cary, NC, USA). Concentration of GSH, HNE, and activity of GGT were log-transformed to yield normally distributed data for further analyses. T-test was performed to compare the difference of means between the groups. A one-way ANCOVA was performed with age as a co-variable to compare the results of GPx and log transformed HNE, GSH and GGT among the control, HIV, Meth and HIV+Meth groups. Covarying for age, post hoc Bonferroni multiple comparisons were performed on results showing significance in ANCOVA ($p<0.05$). A two-way ANCOVA was also performed, with HIV and Meth status as independent variables and age as a co-variable. Relationships between continuous variables were examined using Pearson correlations. The significance difference between the slopes was performed by ANCOVA.

**2.3 Results**

2.3.1 Study subject characterization

As shown in Table 2.1, the range of age and distribution of gender were comparable among the 4 groups, but the ethnicity and race distributions were significantly different. In addition, Meth group showed the least educational attainment, and HIV+Meth group showed the lowest estimated verbal IQ. All the groups with HIV infection and/or Meth use had higher symptoms of depression than Control group. The severity of HIV infection was similar in the 2 HIV seropositive groups, as accessed by duration of HIV

infection, CD4 cells, viral load and demential scale. However, HIV+Meth group had lower Nadir CD4 cells than HIV group. The portion of subjects received antiretroviral medication in the 2 HIV seropositive groups was similar. The amount and duration of Meth use were similar in the 2 Meth-use groups. Since nicotine and alcohol use can induce oxidative stress, we also compared use of them among the four groups and no differences were found.

### 2.3.2 GSH, GSH-related enzymes and HNE levels in the CSF

#### *2.3.2.1 HNE Concentration*

Table 2.2 lists both original and log-transformed HNE measurements in the CSF. Figure 2.1A shows that HIV infection, not Meth use, is associated with significant elevation of HNE concentration ($p<0.0001$, two-way ANCOVA). Compared with the control group, the value of $\log_{10}$HNE was 45% higher in the HIV group ($p<0.0001$, Bonferroni post hoc) and 39% higher in the HIV+Meth group ($p<0.0001$, Bonferroni post hoc). These correspond to 3.5-fold and 2.25-fold increases from the control group, respectively, when the original data in Table 2.2 are compared. Likewise, the value of $\log_{10}$HNE was 41% higher in HIV group ($p<0.0001$, Bonferroni post hoc) and 34% higher in HIV+Meth group ($p=0.0004$, Bonferroni post hoc) when compared with Meth group. These translate to 3-fold and 1.9-fold increases compared to the Meth group, respectively, when the original data in Table 2.2 are used in the calculation. In contrast, the HNE level in the Meth group was similar to that in the control group.

#### *2.3.2.2 GSH Concentration*

Figure 2.1B shows HIV infection was significantly associated with lower GSH concentrations in CSF ($p=0.0021$, two-way ANCOVA). The value of $\log_{10}$GSH in the HIV group was 6.7% lower than control group ($p=0.04$, t-test) and 12% lower than Meth group ($p=0.004$, Bonferroni post hoc). $\text{Log}_{10}$GSH level was 10% lower in the HIV+Meth group compared to Meth group ($p=0.01$, t-test). These translate to -34%, -49%, and -40%, respectively, when the original measurements in Table 2.2 are used for the comparisons.

The original data also showed 30% increase of GSH in Meth group compared with control group (P=0.16, t-test).

*2.3.2.3 GGT activity*

As shown in Figure 2.1C, GGT activity in the CSF was also significantly affected by HIV infection (p=0.0018, two-way ANCOVA). Compared to control group, $Log_{10}$GGT value was 8.5% higher in HIV group (p=0.02, t-test) and 11% higher in HIV+Meth group (p=0.01, Bonferroni post hoc). HIV+Meth also showed 9% higher $Log_{10}$GGT value compared with Meth group (p=0.01, t-test). These equal to +32%, +37%, and +27%, respectively, when the original data in Table 2.2 are used for the comparisons.

*2.3.2.4 GPx activity*

Figure 2.1D shows that Meth use had significant effect on GPx activity in the CSF (p=0.001, two-way ANCOVA). GPx activity in the Meth and HIV+Meth groups is 23% higher than control group (p=0.009 and p=0.04, respectively, Bonferroni post hoc) and 12% higher than HIV group (p=0.08 and p=0.1, respectively, t-test).

2.3.3 Correlations between age and CSF GGT activity

Figure 2.2 shows correlations between age and CSF GGT activity in the 4 study groups. Both control group and HIV group showed significant correlation with age (p=0.0015 and p=0.01, respectively, Pearson correlation) and Meth group showed a trend of correlation with p=0.06. No correlation between age and GGT activity was found in the HIV+Meth group. When all the subjects were combined, age and GGT activity showed a strong correlation with p<0.0001 (Pearson correlation).

2.3.4 Correlations among GSH, GSH-related enzymes and HNE in the CSF

*2.3.4.1 Correlations between HNE and GSH*

An increase in HNE concentration can upregulate the gene expression of GCS [51], which can potentially enhance GSH *de novo* biosynthesis. To test if this transcriptional

regulation affects GSH metabolism in the CSF, the concentrations of HNE and GSH were plotted (Figure 2.3A). Level of HNE was found positively correlated with GSH concentration in the control group (p=0.03, Pearson correlation) and Meth group (p=0.05, Pearson correlation) but not in the 2 HIV seropositive groups. The slopes of the regression lines in the HIV group and HIV+Meth group were significantly different from that of control group (p=0.04 and p=0.02, respectively, ANCOVA). Likewise, the slope of the regression line in the Meth group was significantly different from those in HIV group (p=0.04, ANCOVA) and HIV+Meth group (p=0.03, ANCOVA).

*2.3.4.2 Correlations between GPx and HNE*

GPx reduces lipid peroxidation and therefore can decrease the generation of HNE. To test the relationship between GPx activity and level of HNE in the CSF, these two parameters were plotted (Figure 2.3B). HIV+Meth group showed a significantly negative correlation between GPx activity and HNE level (p=0.01, Pearson correlation) and HIV group showed a trend of correlation (p=0.06, Pearson correlation). The slope of the regression line in control group was significantly different from those in HIV+Meth group (p=0.0045, ANCOVA) and HIV group (p=0.02, ANCOVA).

*2.3.4.3 Correlations between GGT and GSH*

GGT catabolizes GSH for amino acid recycle. The correlations between CSF GGT activity and GSH concentration are shown in Figure 2.3C. Meth group showed a negative correlation between GGT activity and GSH concentration (p=0.02, Pearson correlation). With the four groups combined, GGT and GSH showed a significant negative correlation (p=0.05, Pearson correlation).

*2.3.4.4 Correlations between GGT and GPx*

As shown in Figure 2.3D, all four groups showed significant positive correlations between CSF GGT activity and GPx activity (p=0.02 for control group, p=0.0001 for HIV group, p=0.004 for Meth group and p=0.02 for HIV+Meth group, Pearson correlation). No differences were found among the slopes of the regression lines in the

four groups. A stronger positive correlation between GGT and GPx was found when all four groups were combined ($p<0.0001$, Pearson correlation).

## 2.4 Discussion

This study, with a two-by-two design, demonstrated differential effects of HIV infection and use of Meth on GSH metabolism and oxidative stress in the CSF. Higher levels of GGT activity and lipid peroxidation, and lower GSH concentration were found in the CSF of the HIV and HIV+Meth groups, with HIV as the causative factor. Decreased GSH content and elevated lipid peroxidation have been reported in the CNS of HIV patients [29,32,33,34], and our results confirmed these findings. Meanwhile higher GPx activity was found in the Meth and HIV+Meth groups, with Meth as the causative factor. GGT activity was found positively correlated with age in three groups but the HIV+Meth group; negatively correlated with GSH content in the Meth group, and positively correlated with GPx activity in all four groups. GPx activity tended to negatively correlate with HNE under HIV seropositive conditions (HIV and HIV+Meth), while HNE positively correlated with GSH under HIV seronegative conditions (Control and Meth). No significant interactive effects between HIV and Meth were observed in this study.

### 2.4.1 Changes of GGT activity and its effect on GSH

GGT plays an important role in sustaining GSH homeostasis [151,152]. It breaks down GSH and GSH conjugates and then recycles cysteine for intracellular GSH *de novo* synthesis. Increased GGT activities were found in the plasma under many diseased conditions, including liver diseases, cardiovascular disease, cancer, and type 2 diabetes [153,154,155,156]. In the CSF, higher GGT activity also related with certain brain diseases [157,158]. In patients with HIV infection with and without antiretroviral therapy, higher GGT activity was found in the periphery [159,160]. Antiretroviral drug Nevirapine (NVP), a non-nucleoside reverse transcriptase inhibitor drug, was reported to induce GGT activity elevation in the blood [161]. As NVP can penetrate the blood-brain-barrier, it may upregulate GGT activity in the CNS [161]. The influences of Meth use on GGT activity in both CNS and the periphery have not been sufficiently studied.

Alterations of GGT activity are associated with oxidative stress. GGT deficiency can decrease intracellular GSH *de novo* synthesis by limiting cysteine/cystine supply to the cells, which can eventually lead to oxidative stress [162,163]. Whereas elevated GGT activity can increase the catabolism of extracellular GSH, produce a surplus of cysteinylglycine and generate hydroxyl radical (·OH) through Fenton reaction, which can also result in oxidative stress [55]. Increase of HNE through lipid peroxidation can further upregulate GGT expression forming a vicious circle [58,164]. Consistent with the aforementioned relationships, higher GGT and HNE, along with lower GSH levels were found in the CSF of the HIV seropositive subjects (HIV and HIV+Meth) in this study. The hypothetical links among these changes are illustrated in Figure 2.4A. It is noticeable that no significant correlations were found between GGT/GSH and GSH/HNE in these patients, which contrasts with the correlations found in Meth groups (Figure 2.3, A and C). This implies that in the presence of HIV infection, (1) elevated GGT activity may not be the only factor causing GSH depletion in the CSF; and (2) due to certain mechanistic defect(s), the extracellular environment of the CNS may not be able to upregulate GSH in response to increased lipid peroxidation, which contributes to the resultant oxidative stress.

### 2.4.2 HIV infection and GSH metabolism

The GSH concentration in the CSF can also be affected by the rates of intracellular GSH synthesis and GSH efflux. However, these two aspects of GSH metabolism have not been fully studied in the context of HIV infection and the available reports are controversial. For example, one study reported decreased peripheral release and clearance of GSH in HIV patients [165]; but another study documented increased GSH efflux from cultured rat primary astrocytes through multidrug resistant protein 1 (MRP1) upregulation when exposed to gp120 [166]. Furthermore, when the activity of GCS, the rate-limiting enzyme in GSH synthesis, was measured in the livers of SIV infected macaques [167] and Tat transgenic mice [168], controversial results were obtained. The controversies in these reports may be caused by (1) different regulations of GSH metabolism in the periphery and in the CNS, and (2) different levels of stress from systemic viral infection verse single viral protein expression. Antiviral drugs may also affect GSH metabolism in the

CNS. AZT, a nucleoside reverse transcriptase inhibitor drug has been documented to damage mitochondria and induce oxidative stress [145], and *in vitro* studies showed high doses of AZT resulted in GSH depletion [146,147]. Notably, the concentration used in these studies were 50 to 200 times higher than that of clinical use (1μM), and the authors claimed that high dose/short time AZT experimental exposure was comparable to low dose/long time AZT clinical treatment.

### 2.4.3 Changes of GPx activity

GPx reduces hydrogen peroxide and lipid peroxides, while using GSH as a cofactor. GPx3 is the major isoform in the CSF. Decreased GPx activity in the CSF has been found in HIV patients with neurocognitive symptoms but not in asymptomatic patients [30]. In our study, the average GPx activity in the CSF of the HIV group was slightly (+10%) but not significantly increased compared with the control group, and GPx activity negatively correlated with HNE in both HIV and HIV+Meth groups, implicating GPx has a significant role in preventing HNE formation under HIV seropositive conditions, most likely through reducing lipid peroxides. However, the function of GPx may be compromised in these patients by the concurrent GSH depletion.

Acute Meth exposure has been reported to affect GSH concentration in the brain tissues in a time-dependent manner. For example, in mouse brain, GSH was upregulated 2-6 hours after Meth injection [106,108], but normalized after 24 hours [108]. Both increases and decreases in GPx activity in the brain tissues upon Meth exposure have been reported [106,169,170]. However, Meth-induced increases of HNE in the brain tissues were consistent among the reports [106,169,170]. In our study, use of Meth increased GPx activity in the CSF in both Meth and HIV+Meth groups. GSH and HNE were found moderately increased in the CSF of the Meth group compared to the control (+30% for GSH and +12.5% for HNE), and positive correlations between GSH and HNE were found in both Meth and control groups. These changes implicate that (1) use of Meth alone did not compromise the GSH upregulation in response to HNE formation, which can facilitate the conjugation of excessive HNE either directly by GSH or through GST catalysis; and (2) higher GPx activity supported by elevated GSH concentration (albeit

moderate) can effectively reduce lipid peroxides. Collectively, the GSH-centered antioxidant system has a significant role in ameliorating oxidative stress in the CSF upon Meth exposure, and the hypothetical pathway is outlined in Figure 2.4B.

### 2.4.4 Correlations between GGT/GPx and GGT/age

In our study, strong positive correlations between GGT and GPx activities in the CSF were observed in all groups, and GGT activity was found to increase with age in all but the HIV+Meth group. Such correlations have not been reported before. The underlying mechanism of the simultaneous changes of GGT and GPx is not clear and warrants further investigation.

## 2.5 Conclusion

In summary, this study documented differential effects of HIV infection and use of Meth on GSH metabolism and oxidative stress in the CSF in humans, analyzed intrinsic links among the changes of the measured parameters, and implicated the significance of the GSH-centered antioxidant system in relieving oxidative stress in the extracellular environment of the CNS during HIV infection and Meth exposure.

**Table 2.1 Demographic and clinical characteristics of the study subjects.**

| Group/Variable | Control (n=41) | Meth (n=25) | HIV (n=34) | HIV+Meth (n=23) | p value ANOVA, T and $X^2$ |
|---|---|---|---|---|---|
| Age | 39.7 ± 2.0 | 39.1 ± 2.0 | 41.8 ± 1.9 | 43.0 ± 1.6 | 0.54 |
| Sex (Male/Female) | 37 (90%)/ 4 (10%) | 22 (88%)/ 3 (12%) | 32 (94%)/ 2 (6%) | 22 (96%)/ 1 (4%) | 0.73 |
| Ethnicity (Hispanic/Non-Hispanic) | 1 (2%) / 40 (98%) | 4 (16%) / 21 (84%) | 5 (15%) / 29 (85%) | 7 (30%) / 16 (70%) | 0.019 |
| Race:<br>American Indian/Native Alaskan<br>Asian<br>African American/Black<br>Native Hawaiian/Pacific Islander<br>White<br>Mixed | <br>1 (2%)<br>8 (20%)<br>1 (2%)<br>3 (7%)<br>22 (54%)<br>6 (15%) | <br>0 (0%)<br>6 (24%)<br>0 (0%)<br>5 (20%)<br>5 (20%)<br>9 (36%) | <br>1 (3%)<br>4 (12%)<br>2 (6%)<br>0 (0%)<br>18 (53%)<br>9 (26%) | <br>0 (0%)<br>7 (30%)<br>3 (13%)<br>2 (9%)<br>5 (22%)<br>6 (26%) | 0.032 |
| Education | 14.3 ± 0.3 | 12.2 ± 0.2 | 13.8 ± 0.4 | 13.4 ± 0.5 | 0.002 |
| Estimated Verbal IQ (WTAR) | 105.8 ± 2.8 | 100.1 ± 2.7 | 107.0 ± 2.4 | 94.8 ± 3.3 | 0.026 |
| CES-Depression Scale | 6.2 ± 1.0 | 15.2 ± 2.0 | 17.8 ± 1.7 | 17.7 ± 2.9 | <0.0001 |
| **Clinical Variables** | | | | | |
| HIV Duration (months) | | | 199.1 ± 16.8 | 177.1 ± 18.9 | 0.40 |
| CD4 (cells/mL) | | | 433.1 ± 38.1 | 367.0 ± 46.7 | 0.28 |
| Nadir CD4 (cells/mL) | | | 212.9 ± 29.0 | 109.4 ± 23.8 | 0.015 |
| HIV Viral Load (log cp/mL) | | | 2.8 ± 0.3 | 2.6 ± 0.3 | 0.64 |
| HIV Dementia Scale (0-16) | | | 14.4 ± 0.3 | 13.4 ± 0.7 | 0.15 |
| Karnofsky Scale (0-100) | | | 92.1 ± 1.5 | 90.9 ± 1.4 | 0.59 |
| CSF WBCs (cells/$mm^3$) | 4.6 ± 2.4 | 13.3 ± 10.4 | 1.8 ± 0.6 | 31.5 ± 25.6 | 0.24 |
| CSF Glucose (mg/dL) | 60.9 ±1.0 | 60.9 ± 1.2 | 61.2 ± 3.3 | 62.0 ± 1.9 | 0.99 |
| HIV Medication (yes/no) | | | 28 (82%)/ 6 (18%) | 21 (91%)/ 2 (9%) | 0.57 |
| **Methamphetamine use** | | | | | |
| Daily average Meth use (g) | | 1.0 ± 0.21 | | 1.0 ± 0.15 | 0.91 |
| Total lifetime Meth use (g) | | 3751 ± 892 | | 2877 ± 595 | 0.42 |
| Duration of Meth use (months) | | 188 ± 20 | | 196 ± 26 | 0.81 |
| Total days of abstinence | | 107 ± 19 | | 71 ± 12 | 0.13 |
| **Other Drug use** | | | | | |
| Nicotine (yes/no) | 30 (73%)/ 11 (27%) | 19 (76%)/ 6 (24%) | 24 (71%)/ 10 (29%) | 12 (52%)/ 11 (48%) | 0.26 |
| Alcohol (yes/no) | 37 (90%)/ 4 (10%) | 23 (92%)/ 2 (8%) | 28 (82%)/ 6 (18%) | 18 (78%)/ 5 (22%) | 0.41 |

**Table 2.2. Concentrations of 4-hydroxynonenal (HNE), glutathione (GSH), and activities of gamma-glutamyltransferase (GGT) and glutathione peroxidase (GPx) in the cerebral spinal fluid (CSF) samples.**

| | Mean(±SEM) | | | | One-way ANCOVA* | | Two-way ANCOVA * | | | |
|---|---|---|---|---|---|---|---|---|---|---|
| | Control (n=41) | HIV (n=34) | Meth (n=25) | HIV+Meth (n=23) | Groups | Age | HIV | Meth | HIVxMeth | Age |
| | | | | Original data | | | | | | |
| HNE (f.i.) | 0.08(±0.01) | 0.36(±0.06) | 0.09(±0.01) | 0.26(±0.05) | <0.0001 | 0.78 | <0.0001 | 0.32 | 0.16 | 0.71 |
| GSH (nM) | 161.96(±20.08) | 106.57(±11.01) | 210.10(±27.69) | 126.63(±17.70) | 0.0054 | 0.41 | 0.0015 | 0.09 | 0.50 | 0.41 |
| GGT (U/ul) | 15.30(±0.73) | 20.24(±1.70) | 16.44(±1.12) | 20.89(±1.27) | 0.0033 | <0.0001 | 0.0006 | 0.53 | 0.64 | <0.0001 |
| GPx (U/ul) | 0.43(±0.02) | 0.47(±0.03) | 0.53(±0.02) | 0.53(±0.03) | 0.0044 | 0.10 | 0.66 | 0.001 | 0.28 | 0.1 |
| | | | | Log transformed data | | | | | | |
| $Log_{10}$HNE | -1.17(±0.04) | -0.64(±0.08) | -1.08(±0.04) | -0.71(±0.07) | <0.0001 | 0.54 | <0.0001 | 0.82 | 0.17 | 0.54 |
| $Log_{10}$GSH | 2.1 (±0.05) | 1.96(±0.05) | 2.23(±0.06) | 2.02(±0.06) | 0.0056 | 0.41 | 0.0021 | 0.06 | 0.55 | 0.41 |
| $Log_{10}$GGT | 1.17(±0.02) | 1.27(±0.04) | 1.19(±0.03) | 1.3(±0.03) | 0.0083 | <0.0001 | 0.0018 | 0.31 | 0.94 | <0.0001 |

*Covarying for age; f.i., fluorescence intensity.

**Figure 2.1. A graphical presentation of Table 2.2.** This figure shows HNE concentration (A), GSH concentration (B), GGT activity (C), and GPx activity (D) in the CSF of control (n=41), HIV (n=34), Meth (n=25) and HIV+Meth (n=23) groups. Values of $P_{HIV}$ and $P_{Meth}$ were calculated from two-way ANOVA. * p<0.05; ** p<0.01; *** p<0.0001, Bonferroni multiple comparison test. Both two-way ANOVA and Bonferroni post-hoc tests covaried for age.

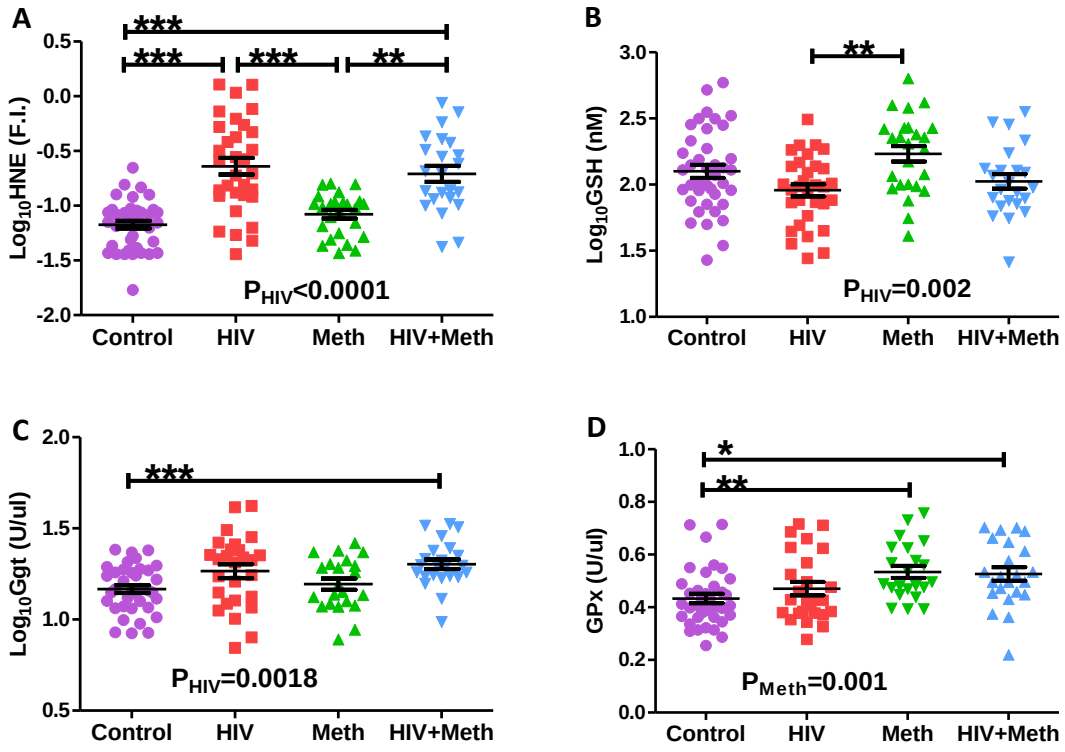

**Figure 2.2. Correlations between age and GGT activity in the CSF.** Pearson correlation was used to test the correlation and ANCOVA was used to test difference between slopes of the regression lines (i.e. interaction-p). Age was covaried in all the tests. n.s., non-significant.

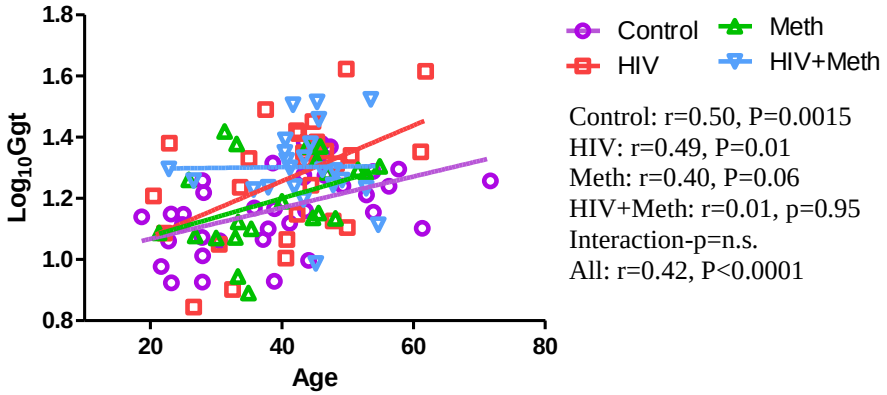

**Figure 2.3. Correlations among GSH concentration, HNE concentration, GGT activity, and GPx activity in the CSF samples.** (A) Correlations between HNE and GSH; (B) correlations between GPx and HNE; (C) correlations between GGT and GSH, and (D) correlations between GGT and GPx. Pearson correlation was used to test the correlation and ANCOVA was used to test difference between slopes of the regression lines (i.e. interaction-p). Age was covaried in all the tests.

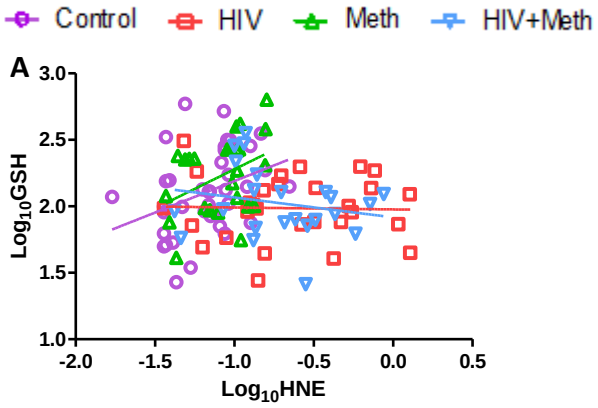


Control: r=0.34, p=0.03; HIV: r=-0.03, p=0.89
Meth: r=0.39, p=0.05; HIV+Meth: r=-0.20, p=0.36
Interaction-p=0.02

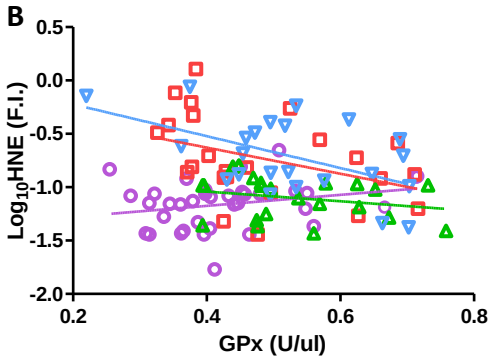


Control: r=0.26, p=0.13; HIV: r=-0.39, p=0.06
Meth: r=-0.25, p=0.26; HIV+Meth: r=-0.52, p=0.01
Interaction-p=0.008

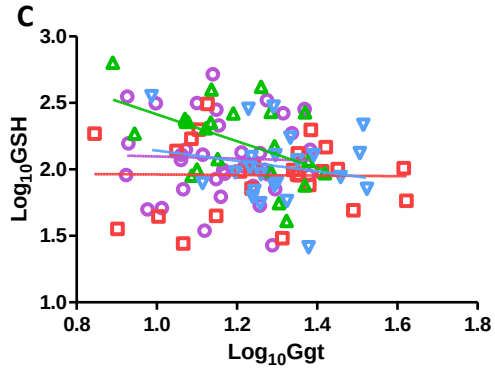


Control: r=-0.03, p=0.84; HIV: r=--0.02, p=0.94
Meth: r=-0.49, p=0.02; HIV+Meth: r=-0.19, p=0.39
Interaction-p=n.s.; All: r=-0.19, p=0.05

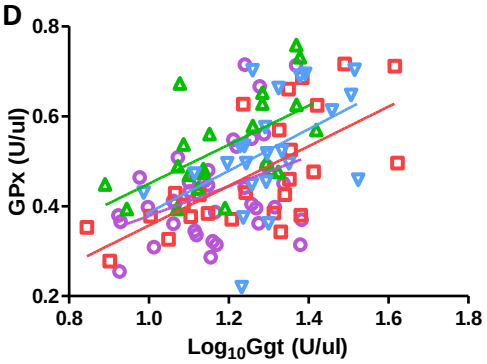


Control: r=0.39, p=0.02; HIV: r=0.68, p=0.0001
Meth: r=0.59, p=0.004; HIV+Meth: r=0.47, p=0.02
Interaction-p=n.s.; All: r=0.54, p<0.0001

**Figure 2.4. Hypothetical links between GSH metabolism and oxidative stress in the CSF under the conditions of HIV infection and Meth exposure.** (A) Links between increased GSH catabolism and increased oxidative stress in the CSF of patients with HIV infection. (B) Contributions of increased GSH and GPx to the amelioration of oxidative stress in the CSF upon Meth exposure. Red arrows indicate changes observed in this study.

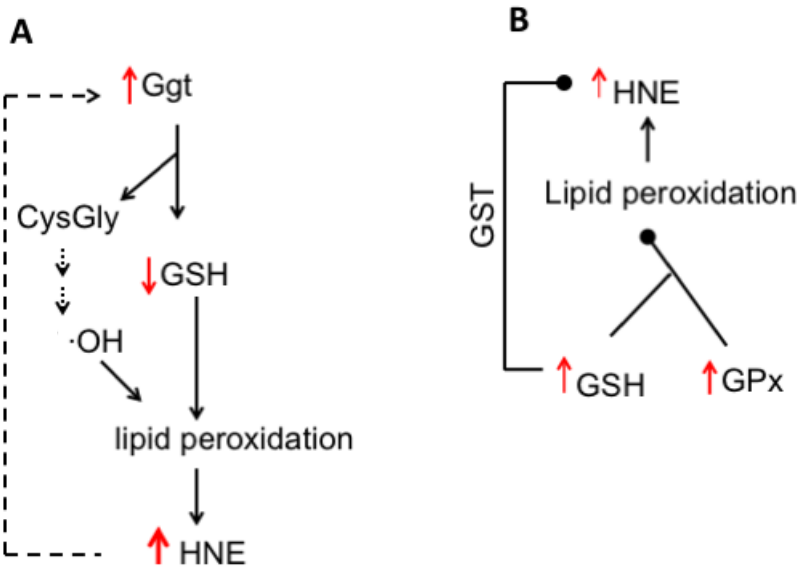

# Chapter 3

## Regional Variations of Glutathione Metabolism and Oxidative Stress in the Brain of HIV-1 Transgenic Rats With and Without Methamphetamine Administration

## 3.1 Background

In Chapter 2, we have studied the changes of GSH metabolism and oxidative stress in the CSF of human cohorts with HIV infection, Meth use, or the concurrence of both conditions, and demonstrated HIV- and Meth-induced changes in the extracellular environment in the CNS. In this chapter, we employ the HIV-1 Tg rat model to investigate how HIV viral protein expression and Meth exposure affect the GSH-centered antioxidant system and oxidative stress in different brain regions, and if these two factors have interactive effects. This study was carried out in collaboration with Dr. Linda Chang at the Department of Medicine, JABSOM, UH, and with Dr. Sulie Chang at Seton Hall University, NJ. Rats at a relatively young age (3 months, in contrast to the older rats used in the studies reported in Chapter 4) were used in the experiment, and the brain regions studied included thalamus, striatum, hippocampus, cortex (frontal and other), and cerebellum.

## 3.2 Animal and Methods

### 3.2.1 Animals

Eight (8) HIV-1 NL4-3 gag/pol transgenic rats (HIV-1Tg) and 8 genetic background control Fisher 344 (F344) rats were purchased from Harlan Inc. (Indianapolis, IN) at the age of 4 weeks. The animals were housed at the Laboratory Animal Services facility of Seton Hall University, NJ. The rats were maintained on a 12-h light/dark schedule. Food and water were accessible *ad libitum* throughout the experiment. All procedures were carried out in accordance with the guidance of the Seton Hall University Institutional Animal Care and Use Committee. At age 13 weeks, the rats were separated into 4 groups with 4 rats in each group based on their genotypes and received injections: (i) Control group, F344 rats received a single intraperitoneal (i.p.) saline injection (2 ml saline per kg body weight) per day for 6 consecutive days; (ii) Meth group, F344 rats received a single Meth i.p. injection (2.5 mg Meth in 2 ml/kg body weight saline) per day for 6 consecutive days; (iii) HIV group, HIV-1Tg rats with saline i.p. injection, same dose and schedule as the Control group; (iv) HIV+Meth group, HIV-1Tg rats with Meth i.p. injection, same dose and schedule as the Meth group. The dose of Meth was used to obtain behavior

sensitization [171]. The rats were sacrificed by decapitation approximately 24 h following the last Meth administration.

### 3.2.2 Sample preparation

The brains were excised and immediately stored at -80°C. Prior to the assays, the brain samples were further dissected into 6 regions: cortex ("frontal" and the remainder which we called "other"), striatum, thalamus, hippocampus, and cerebellum. Soluble proteins/peptides were extracted by sonicating a suitable amount of tissue in cold PBS on ice. The samples were then centrifuged at 18,000 x g for 10 min at 4°C. The supernatants were collected, and the protein concentrations were measured using Bradford assay (BioRad, Hercules, CA). The processed samples were stored at -80°C.

### 3.2.3 Chemicals and instruments

All chemicals used in this study were purchased from Sigma (St. Louis, MO) unless otherwise noted. The spectrophotometers used in the colorimetric and fluorescent assays were SpectraMax 340 (for GSH, ABTS, FRAP, GCS, and HNE-His assays) or SpectraMax M3 (for GGT, GPx, Glrx, and GST assays) from Molecular Devices (Sunnyvale, CA). Protein electrophoresis system was from BioRad (Hercules, CA), and the western blot imaging was carried out using an Odyssey Infrared Imaging System, and Odyssey Application Software Version 3.0 (Li-Cor Biosciences, Lincoln, NE). Real-time PCR was carried out using a Lightcycler 480 II (Roche Applied Science, Indianapolis, IN).

### 3.2.4 Total GSH assay

This measurement quantitated a colorigenic reaction between GSH and 5,5'-dithiobis-2-nitrobenzoic acid (DTNB) [148]. Oxidized GSH (GSSG) was used to establish a standard curve, and the result was further normalized against sample protein concentration.

All assays in this study were carried out in triplicate unless noted otherwise.

### 3.2.5 ABTS assay

This assay measured the ability of the samples to scavenge the 2,2'-azino-bis (3-ethylbenzthiazoline- 6-sulfonic acid) (ABTS) radical as previously described [150]. 6-hydroxy- 2,5,7,8-tetramethylchroman-2-carboxylic acid (Trolox) was used as a standard and the results were expressed as Trolox equivalent antioxidant capacity (TEAC). The result was further normalized against protein concentration.

### 3.2.6 FRAP assay

Ferric reducing antioxidant power (FRAP) assay measured the reducing ability of the samples to ferric ion at pH 3.6 [172]. Trolox was used as a standard. The result was further normalized against protein concentration.

### 3.2.7 Real-time PCR

Total RNA was extracted using RNeasy Mini Kit (Qiagen, Valencia, CA). cDNA was synthesized using the SuperScript III First-Strand Synthesis System (Invitrogen, Carlsbad, CA). The quantitative real-time PCR (qPCR) primers were designed using an online tool provided by Roche Applied Science. The qPCR was performed in quadruplicate using Platinum SYBR Green qPCR SuperMix-UDG kit (Invitrogen). The primer sequences of the housekeeping genes were: GAPDH forward: tgggaagctggtcatcaac, reverse: gcatcaccccatttgatgtt; 28S forward: tgcagatcatgctgtttaagaac, reverse: ggacctgctccccagatt; HPRT forward: ctcctcagaccgcttttcc, reverse: tcataacctggttcatcatcactaa. The primer sequences of the target genes were: GCS-HC forward: cgatgttcttgaaactctgcaa, reverse: ctggtctccagagggttgg; GCS-LC forward: ctgactcacaatgacccaaaag, reverse: gatgctttcttgaagagcttcct; GS forward: gctggacaacgagcgagt, reverse: gctgcttctcatcctgcaa; GGT7 forward: tggcccaataggactgctaa, reverse: tccctggctgtaccgagtt; GR forward: ttcctcatgagaaccagatcc, reverse: tgaaagaacccatcactggtta; GPx1 forward: acagtccaccgtgtatgcctt, reverse: ctcttcattcttgccattctcctg; GPx4 forward: tctgtgtaaatggggacgatgc, reverse: tctctatcacctggggctcctc; Glrx3 forward: ccacagtgtgtacagatgaacg, reverse: agcttcggcttccagctt. The relative abundance of a target

gene was normalized to a housekeeping gene using the ratio of $2^{\text{Cp housekeeping}} / 2^{\text{Cp target}}$, where Cp is the value of crossing point.

### 3.2.8 GCS activity assay

This assay measured the amount of gamma-glutamylcysteine (GC) synthesized from L-glutamate and cysteine during a fix period of time, as indicated by a fluorescent signal derived from 2,3-naphthalenedicarboxaldehyde (NDA) and serine in the presence of thiols [173]. The fluorescence intensities were measured at 472 ex/ 528 em.

### 3.2.9 GGT activity assay

This assay measured the rate of transferring the glutamyl residue from L-gamma-glutamyl-p-nitroanilide (GPNA) to glycine-glycine [149]. One unit of activity was defined as consumption of 1 μmol of GPNA per minute calculated from the expression $(Vmax * V_t/V_s)/ (0.0088* D)$, where $V_t$ is the total volume of reaction solution in microliters, $V_s$ is the sample volume in microliters, 0.0088 $\mu M^{-1}cm^{-1}$ is the extinction coefficient for GPNA at 410 nm, and D is the reaction solution depth in wells in centimeters.

### 3.2.10 GR activity assay

GR was measured using a commercial kit from Cayman Chemical (Ann Arbor, MI, Catalog number 703202). The rate of absorbance decrease of NADPH at 340 nm was used as an indicator for GR activity.

### 3.2.11 Glrx activity assay

This assay measured the disulfide reduction in *bis*(2-hydroxyethyl) disulfide (HED) catalyzed by the samples in the presence of GSH and NADPH [174]. One unit of activity was defined as a consumption of 1 μmol of NADPH per minute calculated from the expression $(Vmax * V_t/V_s)/(0.0062* D)$, where 0.0062 $\mu M^{-1}cm^{-1}$ is the extinction coefficient for NADPH at 340 nm.

### 3.2.12 GST activity assay

This assay measured the conjugation rate of GSH to 1-chloro-2,4-dinitrobenzene (CDNB) [175]. One unit of activity was defined as a consumption of 1 μmol of CDNB per minute calculated from the expression (Vmax * $V_t/V_s$)/(0.0096* D), where 0.0096 $\mu M^{-1}cm^{-1}$ is the extinction coefficient for glutathione-dinitrobenzene conjugate (GS-DNB) at 340 nm.

### 3.2.13 GPx activity assay

This assay measured the reduction rate of tert-butyl hydroperoxide catalyzed by the samples upon the oxidation of GSH and NADPH [150]. One unit of enzyme activity was defined as a consumption of 1 μmol of NADPH per minute calculated from the expression (Vmax * $V_t/V_s$)/ (0.0062* D), where 0.0062 $\mu M^{-1}cm^{-1}$ is the extinction coefficient for NADPH at 340 nm.

### 3.2.14 xCT Western Blot

Proteins in the tissue lysates were separated electrophoretically in 4-20% SDS-PAGE gels (Bio-Rad, 567-1094), and transferred overnight to Immobilon PVDF transfer membranes (Millipore, Billerica, MA, IPFL00010). The membranes were blocked with blocking buffer (Li-Cor, 927-40000) for at least 1 hour before incubated in primary antibody solutions (0.3% PBST and blocking buffer, 1:1). After washing 3 times with 0.3% 1x PBST (10 min each wash), the membranes were incubated in secondary antibody solutions and washed 3 times with PBST before scanning. The primary antibodies were rabbit anti-xCT (1:500 dilution, Abcam ab93030) and mouse anti-beta-actin (1:20,000 dilution, Li-Cor, 926-42212), and the secondary antibodies were anti-rabbit secondary antibody (1:10,000 dilution, Li-Cor, 926-32211) and anti-mouse secondary antibody (1:20,000 dilution, Li-Cor 926-68020). The membranes were scanned using an Odyssey Infrared Imaging System (Li-Cor, Lincoln, NE) and the densitometric analysis was performed using Odyssey Application Software Version 3.0.

3.2.15 Lipid peroxidation assay

Histidine-conjugated HNE (HNE-His) is a major HNE conjugates [176]. Its content was measured using an ELISA kit from Cell Biolabs (San Diego, CA).

3.2.16 Statistical analysis

Prism 5.0a (GraphPad Software Inc., La Jolla, CA) was used for statistical analyses. Two-way ANOVA was used to evaluate the effects of HIV transgenesis, Meth injection, and their possible interaction. Differences among the means were analyzed using (1) two-way ANOVA followed by Bonferroni post-test, or (2) one-way ANOVA followed by post-hoc Tukey's multiple comparison test or Student t-test. But non-parametric Mann Whitney test was used to compare the means of ratios in Table 3 and Figure 2. $P < 0.05$ was considered statistically significant in all tests.

**3.3 Results**

3.3.1 Regional variation of total antioxidant capacities in six brain regions

To assess antioxidant distribution throughout the brain, we measured total GSH content and total antioxidant capacity (TAC) in the six brain regions of the 4 groups of rats. TAC is a concept established about two decades ago to quantify the total amount of substances with free radical-scavenging or reducing abilities in biological samples without distinguishing the contributions from individual compounds. In this study, we employed two methods to measure antioxidant potential of different categories of molecules. The ABTS method measures the radical scavenging ability of proteins, peptides (including GSH), and other small molecules at a physiological pH value (7.4), while FRAP measures the reducing ability of non-protein small molecules (such as ascorbic acid) at pH 3.6, and this low pH inactivates the antioxidant function of thiols (such as GSH).

*3.3.1.1 ABTS assay for total antioxidant capacity*

As shown in Table 3.1, the baseline ABTS reading was 1-2 fold higher in the thalamus than in the other brain regions of the Control group ($p=0.0001$, one-way ANOVA,

Tukey's post hoc), and similar differences were observed in the other 3 groups of rats ($p<0.0001$ in HIV-1 Tg group, $p=0.0028$ in Meth group, and $p<0.0001$ in HIV-1+Meth group, one-way ANOVA). Two-way ANOVA shows HIV-1Tg decreased the ABTS reading in the hippocampus ($p=0.013$). A significant difference in the cerebellum between the Meth group and the HIV-1Tg+Meth group was also detected.

*3.3.1.2 FRAP assay for total antioxidant capacity*

Table 3.1 shows that the FRAP readings of the six brain regions in each group of rats were significantly different (One-way ANOVA). In the Control group, the FRAP readings were ~2 folds higher in the other cortex and the cerebellum than the rest of the brain regions ($p<0.0001$, one-way ANOVA, Tukey's post hoc). Meth seemed to affect the FRAP readings in several brain regions. For example, Meth injection in F344 rats increased FRAP in cerebellum (+106% Meth vs. Control, $p=0.055$, t-test) and frontal cortex (+29% Meth vs. Control, $p=0.04$; t-test), but decreased the reading in striatum (-37%, Meth vs. Control, $p=0.04$, t-test). The effect of Meth injection in F344 rats was different than that in the HIV-1Tg rats in frontal cortex (-26%, HIV+Meth vs. Meth, $p=0.05$, t-test) and in other cortex (+33%, HIV+Meth vs. Meth, $p=0.03$, t-test).

3.3.2 Changes of GSH-centered antioxidant defense

*3.3.2.1 Regional variations of total brain GSH in the 4 groups of rats*

Similar to the ABTS result in Table 3.1, the baseline concentration of total GSH was over 1-2 folds higher in the thalamus than in the other regions of the Control F344 rats ($p<0.0001$, one-way ANOVA, Table 3.2). The changes of GSH in the thalamus, striatum, and frontal cortex are listed in Table 3.2, and further illustrated in Figure 3.1 for convenient comparison. In the thalamus, HIV-1Tg rats had significantly lower GSH levels than the F344 rats ($p_{HIV}=0.0011$, two-way ANOVA), 31% lower in HIV-1Tg and 46% lower in HIV-1Tg+Meth than in their controls. Similarly, HIV-1Tg rats, regardless of Meth status, had lower GSH levels in the striatum ($p_{HIV}=0.045$, two-way ANOVA). Meth injection increased GSH content in the striatum ($p_{Meth}=0.019$, two-way ANOVA), particularly in F344 rats (+37%, Meth vs. Control, $p=0.05$, t-test). The GSH contents in

the cortex (frontal and other), hippocampus, and cerebellum did not show significant differences among the four groups.

*3.3.2.2 Transcriptional responses of GSH-related genes and viral protein genes in the thalamus and striatum*

To further evaluate the responses of enzymes to the changes of GSH contents in the thalamus and striatum, the mRNA levels of genes involved in GSH biosynthesis (GCS-HC, GCS-LC, GS), catabolism (GGT7), recycling (GR), and antioxidant function (GPx1, GPx4, Glrx3) were measured. Three housekeeping genes (HPRT, GAPDH, and 28S) were tested, and the expression levels of HPRT were found consistent among the four groups, and therefore it was used to normalize the relative expression levels of the target genes (Figure 3.2). The gene expression levels of multiple isoforms of GGT and Glrx have been screened in rat brain tissues in a pilot study, the mRNA levels of GGT7 and Glrx3 were found to be the highest in each family of the enzymes (data not shown), and therefore these two isoforms were selected in this part of the study. In order to assess the potential impact of Meth exposure on HIV-1 viral protein gene expression, the mRNA levels of Tat and gp120, the two viral proteins most commonly recognized as causative factors of oxidative stress, were measured in the thalamus and striatum.

As shown in Table 3.3, in the thalamus, HIV-1Tg significantly upregulated the expression of genes involved in GSH metabolism, such as GCS-HC, GS, and GGT7 (two-way ANOVA). Interestingly, Meth injection in F344 rats seemed to decrease the expression of the genes in this category, while Meth exposure of HIV-1Tg rats appeared to have the opposite effect (except for GGT7). Consequently, the mRNA levels of GCS-HC, GCS-LC and GS were 2-4 folds higher in the HIV-1Tg+Meth group compared with the Meth group. However, in the striatum, neither HIV-1Tg nor Meth injection caused any significant changes in the expression of these genes.

Quantification of the mRNA levels of Tat and gp120 in the HIV-1Tg and HIV-1Tg+Meth groups showed Meth had no significant regulatory effect of the expression of these 2 viral protein genes in both thalamus and striatum.

*3.3.2.3 Activities of GSH-related enzymes*

In addition to gene transcription, the activities of the aforementioned enzymes were also measured in thalamus and striatum. For comparison, we also included frontal cortex in this part of the study as a brain region in which the GSH content did not change in response to HIV-1Tg or Meth. As shown in Table 3.4, HIV-1Tg did not affect the activity of GCS and GGT in any of the 3 brain regions, which is in contrast to the upregulated gene expression of GCS-HC and GGT7 in the thalamus. Meth was associated with marked elevation of the GCS activity in the F344 rats (+88% Meth *vs.* Control, p=0.03, t-test) and even greater elevation in the HIV-1Tg rats (+224% HIV-1Tg+Meth *vs.* HIV-1Tg, p<0.0001, t-test), leading to an interactive effect between HIV-1Tg and Meth ($P_{meth}$<0.0001, $P_{interaction}$=0.02, two-way ANOVA). Conversely, Meth injections resulted in decreased GCS activities in both striatum ($P_{meth}$=0.0002, two-way ANOVA) and frontal cortex ($P_{meth}$<0.0001, two-way ANOVA). In the frontal cortex, Meth increased the activity of GGT ($P_{meth}$=0.044, two-way ANOVA), while in thalamus, an interactive effect was found for GGT activity, which was elevated in the HIV-1Tg rats (+36%, vs. Control) but normalized in the HIV-1Tg+Meth rats ($P_{Interaction}$=0.014, two-way ANOVA).

As a key enzyme catalyzing GSH recycling, the activity of GR was decreased by both HIV-1Tg and Meth in the thalamus ($P_{HIV}$=0.042, $P_{meth}$=0.011, two-way ANOVA), but was increased by Meth in the striatum ($P_{meth}$=0.0002, two-way ANOVA). No significant change of GR activity was found in the frontal cortex.

Among the GSH-dependent antioxidant enzymes, the activity of Glrx was found significantly influenced by HIV-1Tg, Meth, or both in the 3 brain regions. In the striatum, the Glrx activity was upregulated by Meth (+89%, Meth vs. Control, p=0.0001, t-test; +82% HIV-1Tg+Meth vs. HIV-1Tg, p<0.0001, t-test, $P_{Meth}$<0.0001, two-way ANOVA). In thalamus and frontal cortex, Meth and HIV-1Tg interactively regulated Glrx activities. In the frontal cortex, both HIV-1Tg and Meth rats had decreased Glrx activity (-24%, Meth vs. Control, p=0.002, t-test; -38%, HIV-1Tg vs. Control, p<0.0001, t-test), but converging of the 2 factors did not result in further activity reduction (-30%, HIV-1Tg+Meth vs. Control, p=0.002, t-test); in the thalamus, Meth increased the Glrx activity

(+44%, Meth vs. Control, p=0.001, t-test), but the concurrence of HIV-1Tg and Meth normalized the activity level. Changes in GPx and GST activities were only found in striatum: Meth decreased GPx activity ($P_{Meth}$=0.001, two-way ANOVA) and HIV-1Tg decreased GST activity ($P_{HIV\text{-}1Tg}$=0.016, two-way ANOVA).

*3.3.2.4 Protein expression of xCT*

Another rate-limiting factor in GSH *de novo* biosynthesis is the supply of cysteine, which can be derived from dipeptide cystine that is transported into the cells through system xc-. The activity of system xc- is determined by the catalytic chain xCT. Therefore the protein expression of xCT was measured using western blotting (Figure 3.3). In the thalamus, Meth-treated F344 rats showed significantly lower amount of xCT protein compared to the control group (-22%, p=0.01, t-test) and the HIV-1Tg+Meth group (-19%, p=0.03, t-test), and the difference almost reached significance compared to the HIV-1Tg group (-19%, P=0.057). In the frontal cortex, the amount of xCT protein decreased in all 3 experimental groups compared to the Control group, and two-way ANOVA showed that Meth exposure contributed to some of these decreases ($P_{Meth}$=0.0002). Interestingly, interactions between HIV-1Tg and Meth were found in both thalamus and frontal cortex (thalamus, $P_{interaction}$=0.0114; frontal cortex, $P_{interaction}$=0.018, two-way ANOVA). In the striatum, no significant difference was found between Control and HIV-1Tg+Meth rats; however, comparisons with the Meth and HIV-1Tg rats were not performed in this region due to the fewer sample sizes available.

3.3.3 Lipid peroxidation

HNE-His concentration was measured in the thalamus, striatum, and frontal cortex (Figure 3.4). In both thalamus and frontal cortex, HNE-His levels were higher in the Meth-treated rats than in the Control group (thalamus: +33%, p=0.005; frontal cortex: +52%, p=0.003; t-test) and in HIV-1Tg group (thalamus: +44%, p=0.016; frontal cortex: +60%, p=0.01, t-test). Since Meth exposure also led to higher HNE-His levels in the HIV-1Tg+Meth rats (+45% *vs.* HIV-1Tg, p=0.024, t-test) in the frontal cortex, a stronger Meth effect was observed in this brain region ($P_{meth}$=0.0002, two-way ANOVA) than in

thalamus ($P_{meth}$=0.0122, two-way ANOVA). No significant changes in the HNE-His level were found in the striatum.

### 3.4 Discussion

This study focused on the intrinsic changes of GSH-centered antioxidants and oxidative stress caused by Meth exposure and HIV-1Tg in rat brain. The main findings included: HIV-1Tg rats showed decreased GSH content in both thalamus and striatum suggesting decreased antioxidant defense. Their thalamus upregulated the expression of genes involved in GSH metabolism, but not the activity levels of these enzymes, indicating the lack of compensation at this time point. In contrast, Meth-exposed rats showed compensatory increase of GSH concentration and altered activities of GSH-centered enzymes only in the striatum. Meth exposure also regulated the activities of GSH-related enzymes, inhibited xCT protein expression, and increased lipid peroxidation in the thalamus and frontal cortex.

#### 3.4.1 GSH content in different brain regions

In this study, the highest GSH content and the ABTS radical scavenging ability were found in thalamus, which were 1-2 folds higher than the other five brain regions. Similarly, a HPLC study on human brain tissues also reported the highest GSH level in the thalamus among 7 brain regions [177], but the differences were marginal, which contrasts with the several-fold differences in our study. Contrary to our findings, a NMR study reported that GSH content in the thalamus of Sprague–Dawley rats (5-6 months) was comparable to the levels in 4 other brain regions [178]. These variable findings of GSH levels in the thalamus relative to the other brain regions may be due to differences in species, strain, age of the study subjects, or a combination of these factors.

#### 3.4.2 GSH and HIV

The lower GSH levels in both thalamus and striatum of the HIV-1Tg rats may be due to oxidative stress caused by the neurotoxic viral proteins. Similarly, intravenous injections of Tat and gp120 resulted in GSH depletion in the whole brain in mice [179]. In the

thalamus, this GSH depletion was associated with upregulation of the genes involved in GSH metabolism, such as GCS-HC, GS, and GGT7, which reflects an ongoing compensatory response to the depletion in this brain region. However, similar decrease of GSH in the striatum did not cause any transcriptional changes in these genes. This difference may implicate the relative importance of the GSH system in different regions of the brain. Additionally, in HIV-infected human macrophages, GSH along with the mRNA levels of GCS-HC, GCS-LC, GS, and GGT1 decreased [180], suggesting potentially different regulatory mechanisms in these peripheral cells than in the CNS in response to HIV-1 mediated GSH depletion.

A previous study measured the mRNA levels of Tat, gp120, nef, and vif in 6 brain regions (hypothalamus, striatum, hippocampus, cerebellum, prefrontal cortex, and the remainder parts of cortex) of 2-3-month old HIV-1Tg rats, and the gene expression levels were found varied across these regions [181]. Tat and gp120, the two most commonly known oxidative viral proteins, seemed to have the highest expression level in the cerebellum, but a moderate expression level in the striatum. Our study showed that in HIV-1Tg rats of a similar age, the GSH content did not change in the cerebellum, but significantly decreased in the striatum. This contrast implicates the regulation of GSH metabolism is region specific in the context of HIV-1Tg, but is not directly correlated with the gene expression levels of viral proteins. Although in cultured bone marrow microvascular endothelia cells (BMEC), Tat was reported to dose-dependently decrease GSH concentration [12485413]. The complicity of the study system and the correlation between gene and protein expressions of viral proteins may partially explain the varied findings in different studies.

### 3.4.3 HIV and oxidative stress

HIV-1Tg rats not only showed GSH depletion in the thalamus and striatum, but also showed decreased activities of GR (thalamus), GST (striatum), and Glrx (frontal cortex). However, no changes of lipid peroxidation were found in these samples. The apparent lack of oxidative stress in these brain regions of the HIV-1Tg rats contrasts with previous reports of oxidative stress caused by HIV infection or viral protein treatment

[32,33,34,179]. This discrepancy indicates that viral infection, endogenous viral protein expression, and exogenous viral protein injection may lead to different pathogeneses. Moreover, since the HIV-1Tg rats were born with viral protein expression, systemic adaptation to the long-term stress may have been developed. The consumption (therefore depletion) of GSH per se may have contributed to the removal of oxidants. Furthermore, the compromised GSH-centered antioxidant system may be compensated by the upregulation of other antioxidants, such as SOD, catalase, or non-protein small molecules.

### 3.4.4 GSH recycling in thalamus

In addition to the high GSH content, thalamus also showed high GGT and GR activities in comparison to striatum and frontal cortex (Table 3.4), which are essential in supporting GSH recycling through extracellular catabolism and intracellular reduction. Notably both HIV-1Tg and Meth caused decreases in GR activity in thalamus, suggesting that lowered rates of GSH recycling may limit the utilization of GSH in thalamus in the context of HIV-1Tg and Meth, and the two factors also seem to have an additive effect in inhibiting thalamus GR activity.

### 3.4.5 GSH and Meth

Although the low dose and repeated Meth administration in this study did not affect the gene expression of GCS-HC and GCS-LC, it significantly increased the activity of GCS in the thalamus, and decreased it in striatum and frontal cortex, suggesting that Meth regulates GCS activity at translational and/or post-translational levels. Meth also affected Glrx activities in these three brain regions. Elevated Glrx in thalamus and striatum of Meth rats suggests that this small redox enzyme may have an important role in neuroprotection during Meth exposure, potentially through maintaining mitochondrial integrity or activating NFkappaB survival pathway [182,183,184]. However, the activity of Glrx in the frontal cortex was decreased by both HIV-1Tg and Meth, which suggest that the frontal brain region may have less capacity to respond and therefore be more vulnerable to oxidative stress caused by both HIV and Meth.

### 3.4.6 Meth and striatum

Meth-mediated neurotoxicity [25] and oxidative stress [185] in striatum have been reported previously. In the present study, after the low dose and repetitive Meth administration, increased lipid peroxidation was found in the thalamus and frontal cortex but not in the striatum. Instead, the striatum of Meth rats showed compensatory increases of GSH concentration, and GR and Glrx activities, implicating the importance of the GSH-centered antioxidants in this brain region. Similarly, when male C57BL/6 mice were treated with a single intraperitoneal dose of Meth (10 mg/kg body weight), the GSH content in the striatum increased in 3 h, but normalized to baseline level in 24 h [106]. Furthermore, when the same dose of Meth was administered to adult male Sprague-Dawley rats over an 8 h period at 2-h intervals, the GSH content in the striatum increased in 2 h and normalized in 24 h [140]. The brain samples in the present study were harvested approximately 24 h after the last Meth injection, but the low dose chronic treatment (2.5 mg/kg body weight/day for 6 days) differs from the high dose acute treatment in previous reports. Multiple time point sampling will be needed to fully elucidate the temporal profile of Meth-induced GSH changes in the striatum, and to understand if the decreased GCS activity observed in our study reflects a negative feedback response to the elevated GSH concentration [53].

### 3.4.7. Transporters involved in GSH metabolism

Brain cells take up cystine through the membrane protein cystine/glutamate antiporter system $x_c$-, which consists of a light catalytic chain (xCT) and a heavy regulatory chain (4F2) [49]. In the CNS, xCT is considered as the determinant protein for the system $x_c$- activity [49]. Increased expression of xCT is considered as a response to oxidative stress [186]. However, in the present study, in spite of higher lipid peroxidation levels in thalamus and frontal cortex in the Meth-exposed rats, the xCT protein was downregulated in these two regions, suggesting a lack of compensatory regulation.

Although the expression of xCT subunit is critical to the system xc- activity [49], the cellular uptake of cystine is collectively determined by several factors. For example, as a

membrane protein, the trafficking of xCT to the cell membrane determines the efficiency of cystine transport [64]. Moreover, the gradient between the high intracellular and low extracellular glutamate concentrations is the driving force for cystine import [49]. Increased extracellular glutamate, such as that caused by HIV-mediated blockage of glutamate reuptake, can lead to system xc- dysfunction, deplete intracellular glutathione and result in nerve cell death [187]. The function of system xc- is also associated with the excitatory amino acid transporters (EAAT), which clean up extracellular glutamate and help maintain the intra- and extra-cellular glutamate gradient [49]. In fact, cysteine can be directly transported into neurons by excitatory amino acid carrier 1 (EAAC1, a member of the EAAT), and this process is competed by extracellular glutamate [188]. The function of EAAT may be inhibited by HIV or gp120 [189]. Meth-treatment also may increase extracellular glutamate concentration [106,108], and how this affects GSH metabolism has not been studied.

### 3.4.8 Limitations of the present study

Glutathione metabolism in the brain is a complex network involving interactions between astrocytes and neurons [61]. The investigation methods used in the present study did not distinguish cell types in the brain tissues. Future work employing immunohistochemical staining to localize and quantify target proteins may lead to a better understanding of the cellular mechanisms at play.

Since this study focused on the GSH-related antioxidant system, the changes of other antioxidants, such as SOD and catalase, were not investigated. In a nonhuman primate study, the combination of SIV and Meth was found to increase the protein concentrations of both GST and extracellular SOD in plasma compared to SIV treatment alone [190]. The alterations of the non-GSH-related enzymes may have significant roles in preventing HIV- and Meth-induced oxidative stress.

## 3.5 Conclusion

This study demonstrated region-specific responses of GSH-centered antioxidants and oxidative stress in rat brain to endogenous HIV viral protein expression and Meth

exposure. Among the brain regions studied, thalamus showed the highest baseline GSH concentration, potentially higher GSH recycling rates, and transcriptional responses to GSH depletion caused by HIV-1Tg. Both HIV-1Tg and Meth resulted in decreased GR activity in thalamus, and decreased Glrx activity in frontal cortex. Increased GR and Glrx activities synergized with increased GSH concentration might have partially prevented Meth-induced oxidative stress in striatum. Interactive effects between Meth and HIV-1Tg were observed in thalamus on the activities of GCS and GGT, and in thalamus and frontal cortex on Glrx activity and xCT protein expression.

**Table 3.1. Effects of HIV-1 transgenesis (HIV-1Tg) and methamphetamine (Meth) on total antioxidant capacities measured by the ABTS and FRAP methods in six brain regions.** Control, F344 rats with saline injection; Meth, F344 rats with Meth injection; HIV-1Tg, HIV-1Tg rats with saline injection; HIV-1Tg+Meth, HIV-1Tg rats with Meth infection. Four rats per group, mean (SD). Unit = μmol trolox equivalent antioxidant capacity per gram protein.

| ABTS | Mean (SD) | | | | Two-way ANOVA | | |
|---|---|---|---|---|---|---|---|
| | Control | Meth | HIV-1Tg | HIV-1Tg +Meth | HIV-1Tg | Meth | Interaction |
| **Thalamus** | 422.12 (145.23)* | 474.36 (248.22) | 494.03 (121.12) | 504.00 (174.09) | n.s. | n.s. | n.s. |
| **Striatum** | 133.09 (14.61) | 127.85 (35.82) | 126.61 (16.84) | 132.74 (33.44) | n.s. | n.s. | n.s. |
| **Cortex (frontal)** | 140.80 (12.55) | 155.76 (21.03) | 136.86 (2.80) | 133.71 (11.24) | n.s. | n.s. | n.s. |
| **Cortex (other)** | 225.95 (48.60) | 214.77 (62.04) | 193.01 (31.14) | 205.48 (51.83) | n.s. | n.s. | n.s. |
| **Hippocampus** | 151.43 (52.76) | 178.05 (29.23) | 112.10 (31.51)[b] | 114.48 (19.07)[b] | P=0.013 | n.s. | n.s. |
| **Cerebellum** | 217.01 (56.26) | 194.71 (20.65) | 238.14 (29.64) | 234.39 (22.41)[b] | n.s. | n.s. | n.s. |
| **One-way ANOVA** | P=0.0001 | P=0.0028 | P<0.0001 | P<0.0001 | | | |

| FRAP | Mean (SD) | | | | Two-way ANOVA | | |
|---|---|---|---|---|---|---|---|
| | Control | Meth | HIV-1Tg | HIV-1Tg +Meth | HIV-1Tg | Meth | Interaction |
| **Thalamus** | 13.84 (3.20) | 12.27 (3.70) | 16.45 (2.97) | 11.00 (4.58) | n.s. | n.s. | n.s. |
| **Striatum** | 16.18 (2.61) | 10.17 (3.40)[a] | 12.39 (2.63) | 13.28 (4.83) | n.s. | n.s. | n.s. |
| **Cortex (frontal)** | 17.52 (3.40) | 22.54 (1.92)[a] | 20.63 (2.36) | 16.80 (2.08)[b] | n.s. | n.s. | P=0.0041 |
| **Cortex (other)** | 31.50 (10.58)* | 24.07 (3.70) | 31.45 (3.71)[b] | 32.13 (4.11)[b] | n.s. | n.s. | n.s. |
| **Hippocampus** | 12.18 (2.49) | 16.99 (4.41) | 15.37 (3.73) | 13.93 (2.59) | n.s. | n.s. | n.s. |
| **Cerebellum** | 33.97 (4.40)* | 70.06 (30.03) | 30.67 (12.74) | 36.17 (21.05) | n.s. | n.s. | n.s. |
| **One-way ANOVA** | P<0.0001 | P<0.0001 | P=0.0006 | P=0.0033 | | | |

[a] compared to the same region of Control group; [b] compared to the same region of Meth group; [c] compared to the same region of HIV-1Tg group; * compared to all the other brain regions in the Control group; n.s., non-significant; P<0.05, one-way ANOVA post hoc or Student t-test.

.

**Table 3.2. Effects of HIV-1 transgenesis and methamphetamine on total glutathione content in six brain regions.** N=4 / group, mean (SD). Unit=μmol per g protein.

| | Mean (SD) | | | | Two-way ANOVA | | |
|---|---|---|---|---|---|---|---|
| | **Control** | **Meth** | **HIV-1Tg** | **HIV-1Tg +Meth** | **HIV-1Tg** | **Meth** | **Interaction** |
| **Thalamus** | 21.62 (5.40)[*] | 25.76 (4.58) | 14.92 (4.35)[b] | 14.01 (2.44)[b] | P=0.001 | n.s. | n.s. |
| **Striatum** | 8.65 (1.72) | 11.89 (2.03)[a] | 7.24 (1.75)[b] | 9.10 (1.97) | P=0.045 | P=0.019 | n.s. |
| **Cortex (frontal)** | 8.76 (1.64) | 10.07 (2.20) | 9.77 (2.36) | 8.37 (1.20) | n.s. | n.s. | n.s. |
| **Cortex (other)** | 6.82 (1.03) | 5.65 (1.36) | 6.36 (1.28) | 6.34 (1.39) | n.s. | n.s. | n.s. |
| **Hippocampus** | 6.20 (2.09) | 5.17 (1.16) | 4.81 (0.76) | 4.39 (0.79) | n.s. | n.s. | n.s. |
| **Cerebellum** | 5.89 (0.41) | 6.48 (0.70) | 6.15 (0.94) | 6.41 (0.43) | n.s. | n.s. | n.s. |
| **One-way ANOVA** | P<0.0001 | P<0.0001 | P<0.0001 | P<0.0001 | | | |

[a] compared to the same region of Control group; [b] compared to the same region of Meth group; [*] compared to all the other regions of the Control group; n.s., non-significant; P<0.05, one-way ANOVA post hoc or Student t-test.

**Table 3.3. Regulatory effects of HIV transgenesis and methamphetamine on gene expression of enzymes involved in GSH metabolism and function, and viral protein Tat and gp120 in the thalamus and the striatum.** The results were calculated using HPRT as a housekeeping gene. Mean (SD), n=4/group, unit = relative abundance compared to HPRT.

| | | Mean (SD) | | | | Two-way ANOVA | | |
|---|---|---|---|---|---|---|---|---|
| | | **Control** | **Meth** | **HIV-1Tg** | **HIV-1Tg +Meth** | **HIV-1Tg** | **Meth** | **Interaction** |
| **Thalamus** | | | | *Enzymes involved in GSH metabolism* | | | | |
| | **GCS-HC** | 0.22 (0.093) | 0.11 (0.052) | 0.32 (0.17) | 0.38 (0.13)[b] | P=0.014 | n.s | n.s |
| | **GCS-LC** | 0.24 (0.031) | 0.12 (0.041) | 0.19 (0.053) | 0.37 (0.25)[b] | n.s | n.s | n.s |
| | **GS** | 0.055 (0.045) | 0.034 (0.018) | 0.11 (0.039) | 0.17 (0.14)[b] | P=0.049 | n.s | n.s |
| | **GGT7** | 0.48 (0.31) | 0.20 (0.11) | 1.17 (0.66) | 0.88 (0.27) | P=0.0091 | n.s | n.s |
| | | | | *Enzymes that use or recycle GSH* | | | | |
| | **GR** | 0.036 (0.01) | 0.032 (0.006) | 0.030 (0.009) | 0.041(0.019) | n.s | n.s | n.s |
| | **GPx1** | 0.061 (0.015) | 0.047 (0.013) | 0.040 (0.02) | 0.042 (0.018) | n.s | n.s | n.s |
| | **GPx4** | 1.36 (0.18) | 1.09 (0.18) | 1.37 (0.57) | 1.06 (0.3) | n.s | n.s | n.s |
| | **Glrx3** | 0.88 (0.21) | 0.70 (0.39) | 1.0 (0.24) | 0.79 (0.54) | n.s | n.s | n.s |
| | | | | *HIV proteins* | | | | |
| | **Tat** | - | - | 0.032 (0.01) | 0.026 (0.017) | | | |
| | **gp120** | - | - | 0.051 (0.015) | 0.042 (0.033) | | | |
| **Striatum** | | | | *Enzymes involved in GSH metabolism* | | | | |
| | **GCS-HC** | 0.32 (0.06) | 0.29 (0.035) | 0.27 (0.035) | 0.35 (0.09) | n.s | n.s | n.s |
| | **GCS-LC** | 0.26 (0.07) | 0.24 (0.046) | 0.24 (0.019) | 0.25 (0.051) | n.s | n.s | n.s |
| | **GS** | 0.071 (0.016) | 0.07 (0.014) | 0.057 (0.011) | 0.063 (0.027) | n.s | n.s | n.s |
| | **GGT7** | 0.61 (0.10) | 0.50 (0.026) | 0.57 (0.01)[b] | 0.5 (0.22) | n.s | n.s | n.s |
| | | | | *Enzymes that use or recycle GSH* | | | | |
| | **GR** | 0.025 (0.015) | 0.047 (0.023) | 0.046 (0.029) | 0.041 (0.008) | n.s | n.s | n.s |
| | **GPx1** | 0.005 (0.002) | 0.011 (0.008) | 0.005 (0.002) | 0.006 (0.003) | n.s | n.s | n.s |
| | **GPx4** | 2.30 (0.92) | 2.10 (0.87) | 2.11 (0.52) | 2.51 (1.23) | n.s | n.s | n.s |
| | **Glrx3** | 0.92 (0.16) | 0.68 (0.19) | 0.88 (0.23) | 0.85 (0.37) | n.s | n.s | n.s |
| | | | | *HIV proteins* | | | | |
| | **Tat** | - | - | 0.028 (0.021) | 0.04 (0.026) | | | |
| | **gp120** | - | - | 0.044 (0.043) | 0.054 (0.03) | | | |

[a] compared to Control; [b] compared to Meth; P<0.05, one-way ANOVA post hoc or Mann Whitney Test. n.s., non-significant

**Table 3.4. Activities of enzymes involved in GSH metabolism, use, and recycling in the thalamus, striatum and frontal cortex of F344 and HIV-1Tg rats with and without methamphetamine.** Mean (SD), N=4/group. Units: GCS, fluorescent intensity; the others, U per g protein.

| | | Mean (SD) | | | | Two-way ANOVA | | |
|---|---|---|---|---|---|---|---|---|
| | | **Control** | **Meth** | **HIV-1Tg** | **HIV-1Tg +Meth** | **HIV-1Tg** | **Meth** | **Interaction** |
| **Thalamus** | | | | *Enzymes involved in GSH metabolism* | | | | |
| | **GCS** | 1.64 (0.66) | 3.09 (0.81)[a] | 1.37 (0.33)[b] | 4.44 (0.51)[a,b,c] | n.s. | P<0.0001 | P=0.020 |
| | **GGT** | 68.20 (9.68) | 75.40 (10.24) | 92.80 (14.12)[a] | 68.25 (9.16)[c] | n.s. | n.s. | P=0.014 |
| | | | | *Enzymes that use or recycle GSH* | | | | |
| | **GR** | 0.49 (0.10) | 0.39 (0.03) | 0.36 (0.06) | 0.30 (0.03)[a,c] | P=0.042 | P=0.011 | n.s. |
| | **GPx** | 3.48 (0.91) | 2.30 (1.23) | 2.92 (1.21) | 2.12 (0.60) | n.s. | n.s. | n.s. |
| | **Glrx** | 9.04 (1.29) | 12.98 (0.58)[a,] | 10.21 (1.53)[b] | 8.63 (1.16)[b] | P=0.020 | n.s. | P=0.0006 |
| | **GST** | 12.19 (1.82) | 9.98 (2.26) | 11.13 (1.51) | 11.13 (1.25) | n.s. | n.s. | n.s. |
| **Striatum** | | | | *Enzymes involved in GSH metabolism* | | | | |
| | **GCS** | 8.12 (0.63) | 5.14 (2.10) | 9.73 (0.61)[a,b] | 4.46 (1.09)[a,c] | n.s. | P=0.0002 | n.s. |
| | **GGT** | 30.14 (2.99) | 29.50 (2.75) | 29.28 (4.24) | 29.80 (10.48) | n.s. | n.s. | n.s. |
| | | | | *Enzymes that use or recycle GSH* | | | | |
| | **GR** | 0.066 (0.010) | 0.144 (0.019)[a] | 0.060 (0.031)[b] | 0.090 (0.045) | n.s. | P=0.009 | n.s. |
| | **GPx** | 2.31 (0.37) | 1.73 (0.22)[a] | 2.13 (0.23) | 1.44 (0.19)[a,c] | n.s. | P=0.001 | n.s. |
| | **Glrx** | 5.05 (0.14) | 9.54 (0.70)[a] | 5.28 (0.60)[b] | 9.61 (0.09)[a,c] | n.s. | P<0.0001 | n.s. |
| | **GST** | 5.47 (0.49) | 5.61 (0.65) | 4.56 (0.31) | 4.49 (0.90) | P=0.016 | n.s. | n.s. |
| **Frontal Cortex** | | | | *Enzymes involved in GSH metabolism* | | | | |
| | **GCS** | 1.83 (0.10) | 0.53 (0.50)[a] | 1.77 (0.19)[b] | 0.54 (0.16)[a,c] | n.s. | P<0.0001 | n.s. |
| | **GGT** | 26.16 (6.10) | 37.49 (10.75) | 22.93 (3.82)[b] | 28.16 (7.01) | n.s. | P=0.044 | n.s. |
| | | | | *Enzymes that use or recycle GSH* | | | | |
| | **GR** | 0.16 (0.016) | 0.20 (0.055) | 0.14 (0.023) | 0.17 (0.053) | n.s. | n.s. | n.s. |
| | **GPx** | 10.54 (1.08) | 10.02 (0.64) | 9.44 (0.68) | 9.81 (1.92) | n.s. | n.s. | n.s. |
| | **Glrx** | 10.79 (0.73) | 8.32 (0.60)[a] | 6.71 (0.33)[a,b] | 7.56 (0.07)[a,b,c] | P<0.0001 | P=0.007 | P<0.0001 |
| | **GST** | 8.10 (0.87) | 8.21 (0.90) | 8.03 (0.55) | 8.21 (0.54) | n.s. | n.s. | n.s. |

[a] compared to Control; [b] compared to Meth; [c] compared to HIV-1Tg; P<0.05, one-way ANOVA post hoc or Student t-test.

**Figure 3.1. Glutathione levels in the thalamus (A), striatum (B) and frontal cortex (C).** This is a graphic presentation of the selected data in Table 3.2. * $p<0.05$, t-test; $^{\#}p<0.05$, Bonferroni's post-hoc; values of $P_{HIV\text{-}1\ Tg}$ and $P_{Meth}$ were calculated using two-way ANOVA.

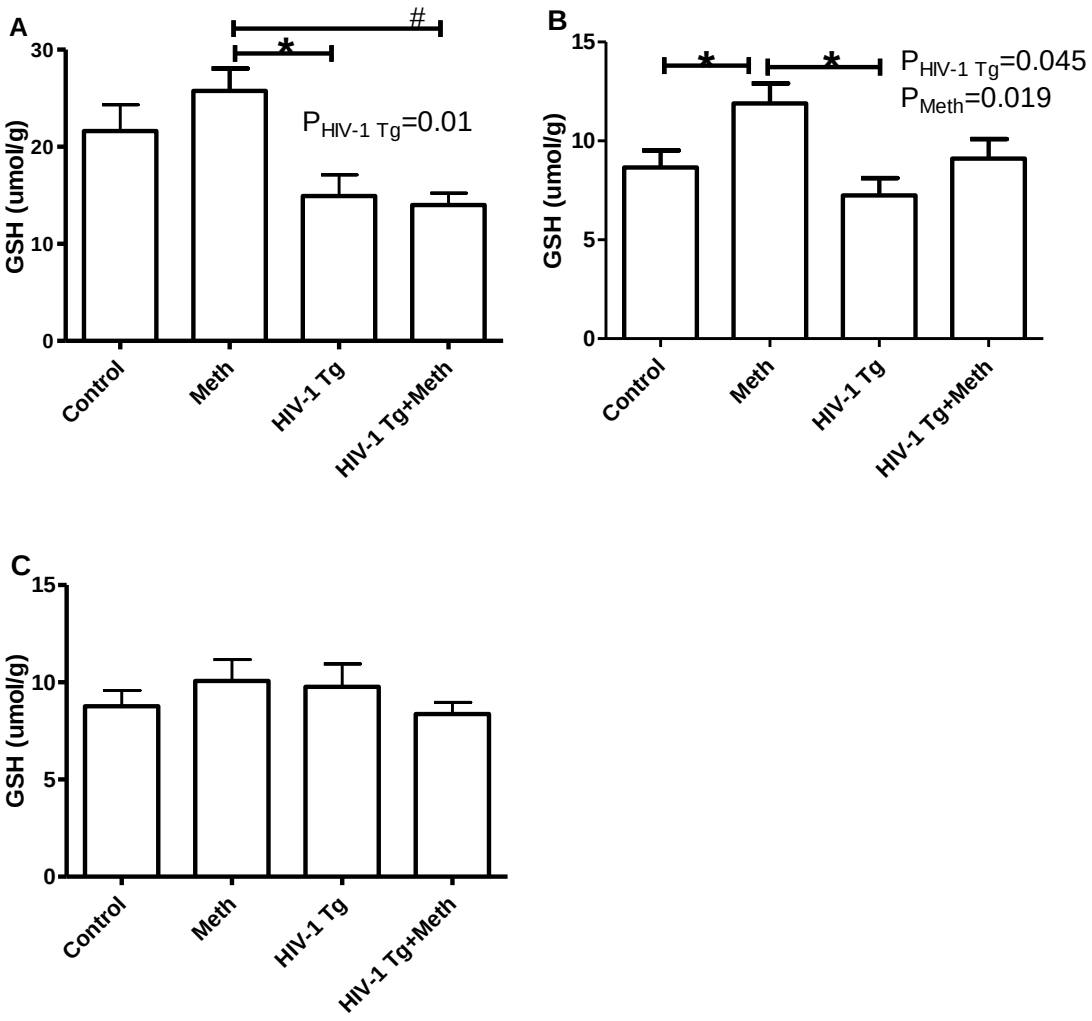

**Figure 3.2. The cross threshold (Ct) value in quantitative real-time PCR of housekeeping genes HPRT (A) and GAPDH (B) in thalamus, and 28S (C) in striatum.** * $p<0.05$, t-test.

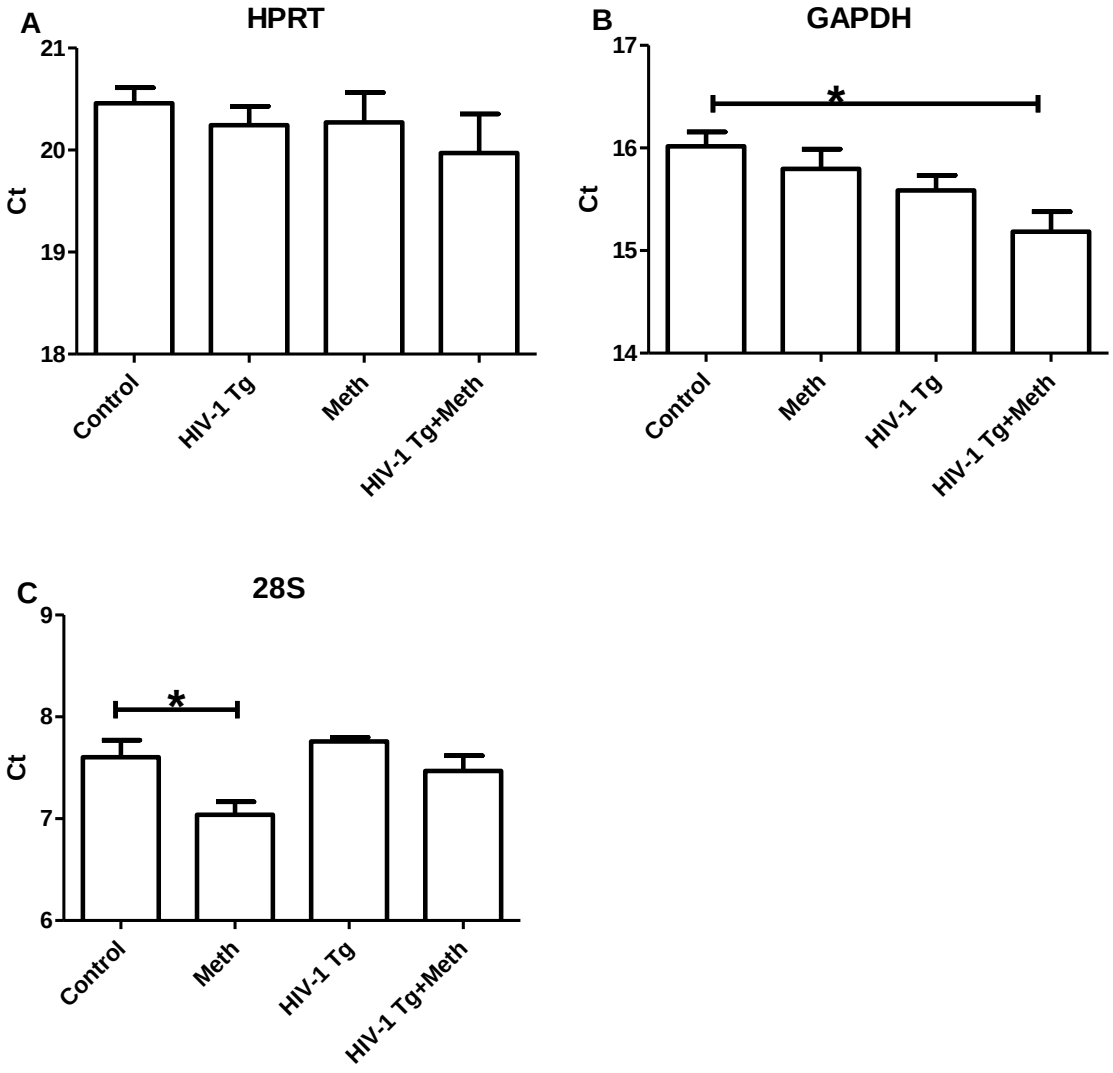

**Figure 3.3. xCT protein expression in the thalamus (A) , frontal cortex (B), and striatum (C).** * $p<0.05$, $^{\$}$ $p<0.05$ compared with rest of the groups, Mann Whitney test; values of $P_{Meth}$ and $P_{Interaction}$ were calculated using two-way ANOVA.

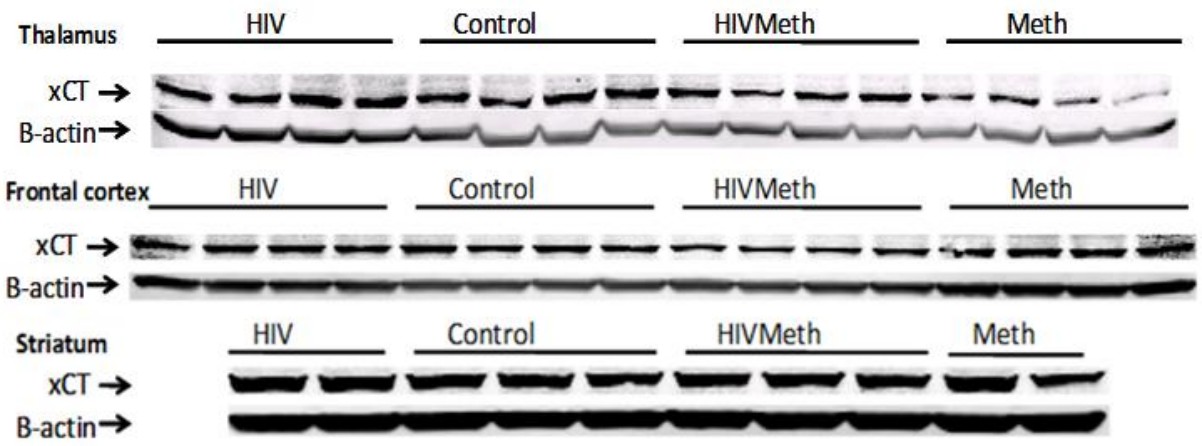


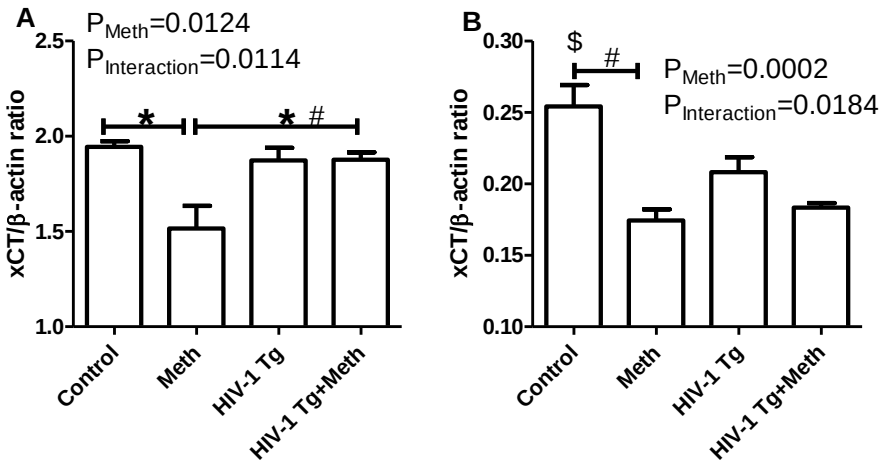





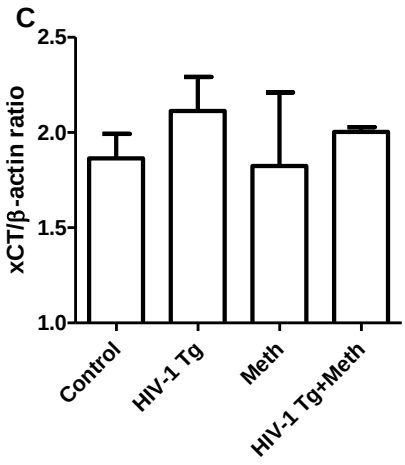

**Figure 3.4. Effects of HIV-1 transgenesis and methamphetamine on lipid peroxidation as indicated by 4-hydroxynonenal (HNE) content in the thalamus (A), frontal cortex (B), and striatum (C).** * $p<0.05$, ** $p<0.01$, t-test; value of $P_{Meth}$ was calculated using two-way ANOVA.

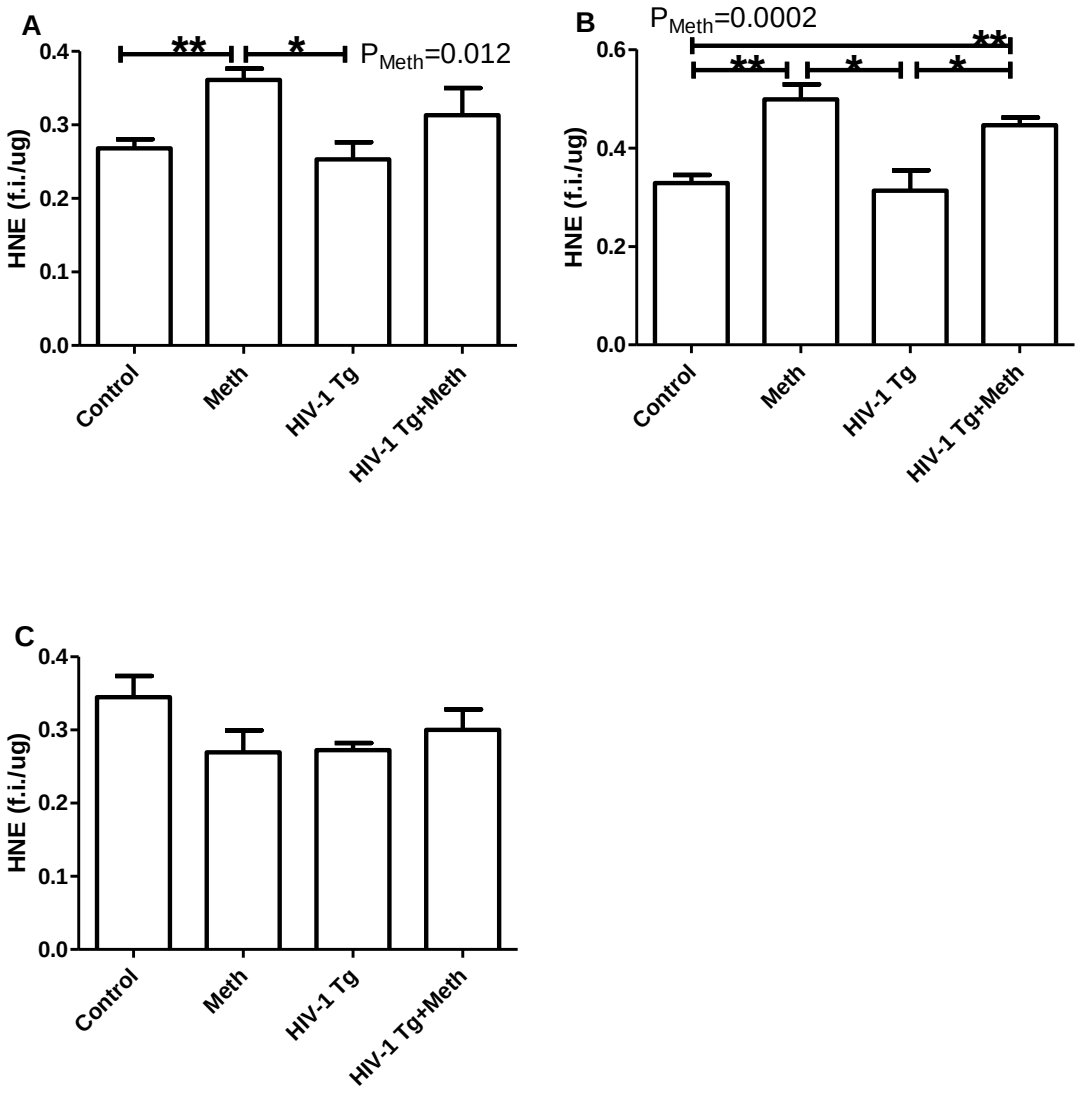

# Chapter 4

## Changes of Glutathione System in the Thalamus in Response to HIV-1 Transgenesis in Rats

## 4.1. Background

Situated between the cerebral cortex and midbrain, thalamus relays sensory and motor signals to the cerebral cortex. It also regulates sleep and wakefulness, memory, emotion, consciousness, awareness, and attention [191]. Combined keywords "HIV" and "thalamus" only brought up 56 articles in PubMed, suggesting the amount of study on thalamus in HIV infection is very limited. Contradictory results can be found in the existing studies. For example, some studies reported decreased thalamus volume in HIV patients [192,193], but others reported HIV did not change thalamus volume [194,195].

In Chapter 3, a higher GSH level was found in the thalamus compared with other brain regions in F344 and HIV-1Tg rats at 3 months, and GSH depletion in thalamus at this age caused compensatory transcriptional upregulation of enzymes involved in GSH metabolism, indicating that GSH may have a profound antioxidative role in this part of the brain. Previous studies also reported that HIV-induced changes of GSH in endothelial cells depended on the length [71] and dose [196] of viral protein exposure. Therefore in this chapter we studied the changes of GSH metabolism and GSH-dependent antioxidant enzymes in the thalamus of F344 and HIV-1Tg rats at an older age (10 months), and also extended the scope of the study to neuroinflammation and the basic conditions of neurons and astrocytes in the thalamus.

## 4.2. Methods

### 4.2.1 Animals and Dietary Treatment

Five (5) one-month old HIV-1 NL4-3 gag/pol transgenic rats (HIV-1 Tg) and 5 genetic background control Fisher 344 (F344) rats were purchased from Harlan Inc. (Indianapolis, IN) and housed at the Laboratory Animal Service facility of the University of Hawaii. The rats were maintained on a 12-hour light/dark schedule. Food and water were accessible to the animals *ad libitum*. Body weight and food consumption were monitored weekly. The experimental procedures were approved by the Institutional Animal Care and Use Committees (IACUC) of the University of Hawaii.

All animals were fed a standard diet purchased from Research Diets (New Brunswick, NJ). In this diet, 10% energy was from fat. In contrast to a high fat diet used in other experiments in the lab, this standard diet was called “low fat diet”. The HIV-1Tg rats in this experiment are noted as the “HLC” group, with “H” stands for HIV, “L” stands for “low fat diet”, and “C” stands for “control diet” which is in contrast to a supplemented diet in chapter 5. The F344 rats used in this experiment are noted as the “FLC” group, with “F” stands for F344.

### 4.2.2 Sample preparation

After 9 months, the rats were euthanized in a $CO_2$ induction chamber. Thalamus was dissected from the brain and stored at -80°C. The dissection procedure was carried out on ice. The thalamus tissue was then powderized on dry ice. An aliquot of the powder was sonicated in PBS (except for samples prepared for western blot), centrifuged at 18,000 x g for 10 min at 4°C, and the supernatant was collected. The protein concentration of supernatant was measured using Bradford assay (BioRad, catalog No. 500-0205). The samples were stored at -80°C until assay.

### 4.2.3 Chemicals and instruments

The chemicals and instruments used were the same as described in chapter 3 section 3.2.3.

### 4.2.4 GSH assay

GSH and GSSG assays were carried out using the GSH/GSSG-412 assay kit (Oxis International, Beverly Hills, CA, catalog number 21040). The results were normalized against protein concentration. The assay was carried out in triplicate.

### 4.2.5 GCS activity

The same procedure as described in chapter 3 section 3.2.8 was used in this experiment.

### 4.2.6 GGT activity

The same procedure as described in chapter 3 section 3.2.9 was used. The only difference was that in this experiment one unit of activity was defined as consumption of 1 mmol of GPNA per minute calculated from the expression (Vmax * $V_t/V_s$)/ (8.8* D), where 8.8 $mM^{-1}cm^{-1}$ is the extinction coefficient for GPNA at 410 nm.

### 4.2.7 HNE-His assay

The same procedure as described in chapter 3 section 3.2.15 was used.

### 4.2.8 GPx activity

The same procedure as described in chapter 3 section 3.2.13 was used. The only difference was that in this experiment one unit of enzyme activity was defined as a consumption of 1 mmol of NADPH per minute calculated from the expression (Vmax * Vt/Vs)/ (6.2* D), where 6.2 $mM^{-1}cm^{-1}$ is the extinction coefficient for NADPH at 340 nm.

### 4.2.9 GST activity

The same procedure as described in chapter 3 section 3.2.12 was used. The only difference was that in this experiment one unit of activity was defined as a consumption of 1 mmol of CDNB per minute calculated from the expression (Vmax * Vt/Vs)/(9.6* D), where 9.6 $mM^{-1}cm^{-1}$ is the extinction coefficient for glutathione-dinitrobenzene conjugate (GS-DNB) at 340 nm.

### 4.2.10 Western blot

Thalamus tissue powder was sonicated in 1M Tris (pH 7.5) membrane lysis buffer containing 1M NaCl, 1% Trition X-100, 5mM EDTA, proteinase inhibitor and phosphatase inhibitor. Supernatant was collected after 10 min centrifugation at 18,000 x g, 4°C. Protein concentration was measured by Bradford assay. Primary antibodies were purchased from Abcam (Cambridge, MA) included rabbit anti-GFAP (ab7260), rabbit anti-GGT7 (ab80903), mouse anti-MAP2 (ab11267), mouse anti-MRP1 (ab32574).

Mouse anti-NeuN was from Millipore (Billerica, MA) and mouse anti-β-actin was from Santa Cruz (Santa Cruz, CA). Secondary antibodies were from Li-Cor (Lincoln, NE).

4.2.11 Quantitative real-time PCR

RNA was extracted using Trizol and cleaned up using RNeasy mini kit (Qiagen, Valencia, CA). The reverse transcription kit for cDNA synthesis was from Applied Biosystems (Foster City, CA). SABiosciences syber® Green (PA-010-24) kits were used for quantitative PCR. The sequences of primers were: HPRT forward: ctcctcagaccgcttttcc, reverse: tcataacctggttcatcatcactaa; GusB forward: ctctggtggccttacctgat, reverse: cagactcaggtgttgtcatcg; GCS-HC forward: cgatgttcttgaaactctgcaa, reverse: ctggtctccagagggttgg; GCS-LC forward: ctgactcacaatgacccaaaag, reverse: gatgctttcttgaagagcttcct; GGT7 forward: tggcccaataggactgctaa, reverse: tccctggctgtaccgagtt; GGT6 forward: gccctgtggatcttccag, reverse: cagcgctgtggtggtaca; GGT 5 forward: gcatcctcctcaacaacga, reverse: accgttgaacctggcttgt; GGT 1 forward: tggttcgggtatgatgtgaa, reverse: ggcaaaagctggttgtgaag; GPx1 forward: cgacatcgaacccgatataga, reverse: atgccttaggggttgctagg; GPx4 forward: tgggaaatgccatcaaatg, reverse: cggcaggtccttctctatca; GSTα4 forward: tgaaccaggagtcatggaagt, reverse:actccagctgtagccagca; MRP1 forward: cacgagaactcatgacatttgaa, reverse: caggagcgaatgaactggtat.; xCT forward: tccatgaacggtggtgtgt, reverse: cccttctcgagatgcaacat; EAAC1 forward: gaactgcaaccacctattctca, reverse: actgcgtatcacaatcacagaga.

4.2.12 ELISA assays.

Multi-Analyte ELISArray Kits for rat from SABiosciences (Valencia, CA) were used for cytokine screening test. Rat IL-12 +p40 ELISA kits from Invitrogen (Grand Island, NV) were used for IL12 measurement.

4.2.13 Statistical analysis

Prism 5 (GraphPad Software Inc., La Jolla, CA) was used for statistical analysis. Differences among the means were analyzed using Student t-test. Two-way ANOVA

was used to analyze the difference caused by HIV-1 Tg, age and their interaction. Pearson correlation was used to test correlation among studied parameters. $p< 0.05$ was considered statistically significant.

## 4.3. Results

### 4.3.1 Energy/water consumption and body weight

A 30-week record of body weight and food/water consumption is shown in Figure 4.1. No differences of food intake were found between the F344 rats (FLC) and the HIV-1Tg rats (HLC) when compared by the record of each week (Figure 4.1A) or by the average of 30 weeks (Figure 4.1B). However, the water consumption was lower in the HLC group compared with FLC, Figure 4.1C and D ($p=0.01$, t-test). The growth curves of the two groups showed similar trend over the 30 weeks (Figure 4.1E). But at the end of the study (38 weeks), HLC rats were lighter than FLC rats by 12.6% ($p=0.0048$, t-test, Figure 4.1F). Wet brain weight was recorded and neither wet brain weight nor the ratio of brain weight over body weight showed differences between the two groups (Figure 4.1G and H).

### 4.3.2 HIV viral protein and Nrf2 gene expression at different ages

The profiles of gene expression of HIV viral proteins in different organs and brain regions in the HIV-1Tg rats have been reported to change with age [181]. In the present study, we examined the mRNA levels of gp120 and Tat in the thalamus of HIV-1Tg rats at 3 months and 10 months. Surprisingly, both viral proteins showed much lower mRNA expression in the older rats (-90% for gp120, and -89% for Tat; $p=0.02$ for both, Mann Whitney test), as shown in the Figure 4.2A and B. We also found that both age and HIV-1 Tg upregulated the gene expression of Nrf2 ($P_{age}=0.001$, $P_{HIV\text{-}1\ Tg}=0.03$, two-way ANOVA, Figure 4.2C), which is a transcription factor that responds to redox changes and regulates the expression of antioxidant and detoxification genes [197]. However, it is worth pointing out that the rats at the two age groups grew up at different locations. The 3-month rats were housed at the laboratory animal facility of Seton Hall University, NJ, and the 10-month rats were housed at the laboratory animal facility of the University of Hawaii, Kaka'ako campus. There might be subtle differences in the environments, and

more importantly, the 3-month rats were fed regular laboratory rodent chow, but the 10-month rats were fed a specially manufactured diet with casein as the protein source (refer to the control diet in Table 5.1). How the growing condition and/or diet may contribute to the differences in the aforementioned gene expression is not clear.

### 4.3.3. GSH and GSH metabolism

#### *4.3.3.1 GSH*

Chapter 3 shows that at 3 months HIV-1Tg was a causative factor of GSH depletion in the thalamus of the rats, and in response thalamus upregulated the expression of genes involved in GSH metabolism, such as GCS-HC, GS, and GGT7, but such upregulation did not result in increased enzyme activities. The present study shows that at 10 months, HIV-1 Tg rats had significantly higher GSH concentration in the thalamus than the F344 rats (+39%, p=0.0018, t-test, Figure 4.3A). This is a result of increases of both GSSG and rGSH (+27% for GSSG, and +42% for rGSH, p=0.0032 for both, t-test, Figure 4.3B and C) in the HLC group, and the ratio of GSSG/GSH remained the same in both groups (Figure 4.3D).

#### *4.3.3.2 GCS*

As the rate-limiting enzyme of GSH *de novo* synthesis, the gene expression, protein expression and activity of GCS were measured in the thalamus of the rats at 10 months. As shown in Figure 4.4, the GCS-HC protein expression was higher in the HLC group (+31%), but the difference between the two groups did not reach statistical significance (panel A). The GCS activity was significantly higher in the HLC group (+65%, p=0.0035, t-test, panel B). When the mRNA levels of both GCS heavy chain (panel D) and light chain (panel E) were measured, no differences were observed between the two groups.

#### *4.3.3.3 GGT*

GGT is the rate-limiting enzyme of extracellular GSH catabolism, and recycles cysteine for intracellular GSH synthesis. The gene and protein expression of selected GGT isoforms and the activity of GGT are shown in Figure 4.5. In a pilot study, the mRNA

level of GGT7 was found ~ 20 fold higher than those of the other isoforms (data not shown). In the present study, the GGT7 protein level was much lower in the HLC rats (-79%, p=0.008, t-test, panels A-B), but the GGT activity remained the same in the two groups (panel C). The gene expression of GGT7 and other GGT isoforms did not show differences between the two groups (panels D-G).

*4.3.3.4 Transporters*

GSH is synthesized in the cells, and transported to the extracellular space for decomposition. Multidrug resistance-associated proteins (MRPs) mediate efflux of GSH and GSSG. The protein and gene expression levels of MPR1 in the HLC group were comparable to those in the FLC group (Figures 4.7A-C). The gene expression of MRP2 did not change between the two groups (Figure 4.7D).

Cysteine is the limiting substrate for GSH synthesis, and it can be transported into the cells by excitatory amino acid carrier 1 (EAAC1), or by system $x_c^-$ in the form of cystine. The functional domain of system $x_c^-$ is xCT. The mRNA levels of EAAC1 and xCT were found similar between HLC and FLC (Figure 4.7E and F).

4.3.4 Lipid peroxidation and GSH-dependent antioxidant enzymes

HNE is a by-product of lipid peroxides and a commonly used oxidative stress marker. The concentration of HNE-histidine conjugate was 27% lower in the HLC group, but the difference between the two groups is not statistically significant (Figure 4.7A). Both GPx and GST use GSH as a substrate, and they prevent HNE accumulation by reducing lipid peroxides or conjugating HNE. Figures 4.7B-C show significant increases of GPx and GST activities in the thalamus of HIV-1 Tg rats compared with the F344 rats (for GPx, +56%, p=0.005, t-test; for GST, +67%, p=0.0004, t-test). GPx1 and GPx4 are two isoforms of GPx in the brain. GSTα4 is a major isoform of GST known to catalyze HNE conjugation [198,199,200,201]. When the mRNA levels of these genes were measured in the thalamus, no differences were found between the two groups (Figure 4.7D-F).

### 4.3.5 Inflammatory status in the thalamus

Neuroinflammation is associated with HIV infection. To evaluate the inflammatory status in the thalamus, we employed a Multi-Analyte ELISArray in the initial screening test. This array measured 12 cytokines simultaneously. In this assay, the same amount of protein was collected from the tissue lysate of each rat, and the samples from the same group were combined. The result is shown in Figure 4.8A. Among the 12 cytokines, the difference of IL12 was the largest between the 2 groups. Therefore IL12 was selected as a representative inflammatory cytokine, and the protein expression of IL12 in the thalamus of each rat was further measured using ELISA in duplicate. As shown in Figure 4.8B, the IL12 protein level in the thalamus of the HIV-1Tg rats was 5-fold lower than that in the F344 rats ($p=0.01$, t-test).

### 4.3.6 Neurons and astrocytes

To evaluate the changes of numbers and conditions of neurons and astrocytes in the thalamus, we examined the protein expression of neuronal nuclei (NeuN, neuron-specific nuclear protein), microtubule-associated protein 2 (MAP2, a neuron-specific cytoskeletal protein in rats and related to formation of neuronal dendrites), and glia fibrillary acidic protein (GFAP, expressed in astrocytes in CNS). As shown in Figure 4.9, no differences were found in the expression of NeuN and GFAP between the two groups (panels A and C), while a higher expression level of MAP2 was found in the thalamus of the HLC group (+65%, $p=0.0079$, Mann Whitney test, panel B).

### 4.3.7 Correlations

Correlations between the parameters measured in this study were evaluated by Pearson's linear correlation test, and summarized in Figure 4.10. GSH concentration positively correlated with GCS activity ($r=0.87$, $p=0.001$, panel A), suggesting increased GCS activity is a major causative factor of GSH upregulation in the thalamus of the HIV-1Tg rats. GSH concentration also positively correlated with GST activity ($r=0.75$, $p=0.01$, panel B), thus GST equipped with sufficient GSH can effectively execute antioxidant function, as evidenced by a negative correlation between GST and HNE (panel C).

Similar negative correlation was found between GPx and HNE (panel D). A strong positive correlation was found between GST and GPx (panel E). GCS activity was found positively correlated with GST and GPx activities, and negatively correlated with HNE concentration (panels F-H). Both HNE and IL12 positively correlated with GSSG/GSH ratio, suggesting they are responsive to the redox shifting in the thalamus. Interestingly, GPx seemed to have different functions in regulating IL12 production in the two groups of animals, i.e. it negatively correlated with IL12 in the F344 rats, but had a marginal ($p=0.051$) positive correlation with IL12 in the HIV-1Tg rats. The slopes of the regression lines of these two groups are significantly different ($p=0.002$). Furthermore, the protein expression of MAP2 positively correlated with GSH, GCS, GPx, and GST (panels L-O), but negatively correlated with IL12 (panel P), indicating the neuronal differentiation in the thalamus may be stimulated by GSH-centered antioxidants, but inhibited by neuroinflammation.

## 4.4 Discussion

At the age of 10 months, elevated antioxidant capacity (GSH, GPx and GST), and decreased neuroinflammation (IL12) were found in the thalamus of the HIV-1Tg rats compared with the F344 rats. The HIV-1Tg rats also showed lower lipid peroxidation (HNE) level, but the difference between the two groups was not significant. Correlation analysis showed that GSH upregulation was achieved through the increase of GCS activity, GPx and GST may directly contribute to the removal of HNE, and HNE and IL12 were responsive to the redox shift of GSH. Neuronal differentiation in the thalamus may be stimulated by GSH-centered antioxidants and inhibited by neuroinflammation. Collectively, this study demonstrated the significance of the GSH-centered system in preventing oxidative stress and regulating neuroinflammation and neuronal differentiation in the thalamus challenged by HIV viral proteins.

### 4.4.1 GSH regulation in the thalamus

The thalamus remains a less visited brain region in the research field of HIV neuro-disorders. Our studies emphasized the high abundance of GSH in the thalamus of HIV-1

Tg rats with F344 genetic background, and the age-dependent responses of the GSH-centered system to HIV viral protein expression. At 3 months, HIV-1Tg caused a 30% decrease of GSH content in the thalamus, but no increase of lipid peroxidation. This suggests that GSH is in the front line of antioxidant defense, and consumption of GSH contributes to the neutralization of excessive ROS generated by HIV viral proteins. At 10 months, the GSSG concentration in the thalamus of the HIV-1Tg rats increased by 27%, implicating increased transfer of the reducing power from GSH to GSH-dependent antioxidant enzymes, such as GPx and GST. The increase of GSSG was balanced by the upregulation of rGSH level, and the GSSG/GSH ratio remained unchanged compared to the F344 rats.

The increase of GCS activity was a major causative factor of GSH upregulation in the thalamus at 10 months. But the activity of this enzyme did not correlate with the gene or protein expression of it subunits, suggesting GCS activity in the thalamus is regulated post-translationally, for example by the binding ability and autophosphorylation of GCS-LC [202]. Reportedly, SIV-infected macaques had increased GCS activity in the liver and muscle tissues [167], and Tat transgenic mice showed lower gene and protein expression of GCS-LC in the liver [168].

In previous publications, HIV infection and HIV viral protein exposure were associated with GSH depletion in CSF (Chapter 2 and [29]), hippocampus and posterior cerebral cortex [35], and brain microvascular endothelial cells [71,196], which are in contrast to the finding of the present study highlighting biphasic changes of GSH concentration in the thalamus of the HIV-1Tg rats. Such differences may be explained by tissue specific regulatory mechanisms, and the time points selected in each study.

### 4.4.2 HIV and GGT regulation

Previously, increased GGT activity was found in the periphery of both HIV naïve patients and patients with antiretroviral therapy [159,160], and use of the antiretroviral drug NVP increased GGT activity in liver [160]. Region-specific elevation of GGT activity was found in the brain with Parkinson's disease [203]. In Chapter 3, GGT activity was found

increased in the thalamus of the HIV-1Tg rats at 3 months, which was consistent with GGT7 gene upregulation. No changes of GGT activity and GGT7 gene expression were observed at 10 months, but the protein expression of GGT7 was significantly decreased in the HIV-1Tg rats compared with the F344 rats. GGT7 was first isolated from a rat brain cDNA expression library and found only expressed in the nervous system [62]. Our pilot study showed the mRNA level of GGT7 was ~20-fold higher than the other GGT isoforms in the brain. The significance of GGT7 in the CNS and its transcription and translation regulation warrant further study.

### 4.4.3 GSH, cysteine, and cystine transporters

As transporters of GSH, the MRPs have not been sufficiently studied in the brain. MRP1 protein is found in astrocytes and microglia, but not neurons [63]. MRP1 mediates GSH efflux from astrocytes. Once outside of the astrocytes, GSH either reduces extracellular oxidative stress, or supports *de novo* GSH synthesis in neurons by providing substrates after going through degradation. GSH export from astrocytes was not completely blocked during MRP1 inhibition, suggesting MRP1 is not the only transporter of GSH [204]. It has been reported that gp120 upregulated gene and protein expression of MRP1 in primary rat astrocytes [166], and HNE upregulated MRP1 protein expression in bovine aortic endothelial cells [205]. However, in the present study, no significant changes were observes in the gene and protein expression levels of MRP1 and MRP2. At this time point, the lipid peroxidation in the thalamus seemed to be lower in the HIV-1Tg rats compared to the F344 rats due to the upregulation of GSH-centered antioxidant system, and this is the major difference between the present and the previously reported experimental conditions, with the later involved in oxidative stress.

Other transporters play roles in GSH metabolism are system $x_c^-$ and EAAC1. As mentioned in Chapter 3, system $x_c^-$ is a membrane antiporter transporter for cystine/glutamate. It consists of a light catalytic chain (xCT) and a heavy regulatory chain (4F2) [49]. In the CNS, xCT is considered as the determinant protein for the system $x_c^-$ activity [49]. Increased expression of xCT and hence higher availability of cysteine for GSH biosynthesis has been considered as a response to oxidative stress [186]. In

cultured primary microglia, Tat treatment increased the expression of xCT and glutamate release in a dose dependent manner [166]. EAAC1 (also known as EAAT3) is one of the neuron membrane excitatory amino acid transporters (EAAT), which takes up extracellular glutamate and cysteine competitively [64]. EAAC1 knockout mice showed significantly lower GSH levels in the brain [206]. In the present study, no changes were found on the gene and/or protein expression levels of xCT and EAAC1 in the thalamus of the HIV-1Tg rats.

### 4.4.4 Oxidative stress, neuroinflammation, and neuronal differentiation

HIV-induced lipid peroxidation in the brain has been reported to be region-specific [33] and associated with the severity of HANDs [32]. Exposing brain endothelial cells to Tat caused ROS generation dose-dependently [196]. In the present study the HNE-his concentration in the thalamus of the HIV-1Tg rats was 27% lower than the F344 rats, and this decrease of lipid peroxidation is clearly correlated with GPx and GST activities, demonstrating the effectiveness of the GSH-dependent antioxidant enzymes in the amelioration of oxidative stress during HIV viral protein exposure.

In HIV seropositive patients, decreased GPx activity was found in the CSF [207], and increased GPx activity was detected in the plasma [207,208,209,210]. When exposed to gp120 or Tat, the GPx activity decreased in brain endothelial cells [71]. The GPx activity in cortical cells increased after a 2-hour gp120 exposure, and normalized after 4 hours and maintained at the baseline after 24 hours [70]. Few reports can be found on the changes of GST in the context of HIV infection. Lower GST activity in the plasma of HIV patients compared to control has been documented [211]. Decreased GST activity was observed in other brain diseases, such as aging and Alzheimer's disease [212], and increased GST activity prevented neuron loss in an animal model of Parkinson's disease [213].

IL12 is a proinflammatory cytokine secreted by dendritic cells, macrophages and B cells [214]. It stimulates naïve T cells into T helper type 1 cells through Jak-STAT pathway which transcribes cytokines for T cell differentiation. Decreased IL12 expression has

been reported in the monocytes of HIV patients [215,216], and the release of IL12 from dendritic cells was inhibited by the plasma of HIV patients [214]. In the present study, an array of pro-inflammatory cytokines have been found decreased in the thalamus of the HIV-1Tg rats in a pilot screening, indicating a generally lower inflammatory status. When IL12 was selected for further assay, its concentration was found 84% lower in the HIV-1Tg thalamus than in the control. The concentration of IL12 seemed to respond to the redox status of GSH and the activity of GPx. In other studies, increased IL12 production has been induced by GSH in monocytes [217], by GSH precursor in splenocytes of Tat-exposed mice [218], and by low dose GSH precursor in macrophages [219]. IL12p40 knockout mice showed decreased GPx activity in lungs [220]. However, patients with systemic lupus erythematosus showed low GSH and GPx activity but high IL12 concentrations in erythrocyte hemolysate [221].

The protein expression levels of GFAP and NeuN were similar in the thalamus of the F344 rats and the HIV-1Tg rats, suggesting the lack of astrocyte activation and neuron loss in the transgenic rats at this time point. Several studies have shown decreased neuronal dendritic branches in the hippocampus of HIV-1 infected patients [10,222,223], but our result showed increased MAP2 protein in the thalamus of the HIV-1Tg rats, implicating a higher level of neuronal differentiation in this brain region. Correlation analysis indicates that MAP2 expression may be enhanced by GSH and the activities of GCS, GPx, and GST, but inhibited by IL12. In future studies, this correlation will be further confirmed using immunocytochemistry.

### 4.5 Conclusion

In summary, this is among the few studies that elucidate the redox, neuroinflammation, and cellular changes in the thalamus in the context of HIV viral protein exposure, and highlight the regulatory and protective roles of GSH and GSH-centered enzymes in this brain region. There are more questions revealed than answered in this study. Future investigations will be directed to understanding the regulatory mechanisms of the key players in this picture and the intrinsic relationship among redox shifting, neuroinflammation and neuron cell differentiation.

**Figure 4.1. Food and water consumptions and body weight of the animals.** (A) Food consumption of F344 rats (FLC) and HIV-1 transgenic rats (HLC) over 30 weeks. (B) Average energy consumption of 30 weeks. (C) Average water consumption per rats per day from week 8 to week 30. (D) Average water consumption of 22 weeks. (E) Growth curves of the animals over 30 weeks. (F) Average body weight before animal scarification. (G) Wet brain weight. (H) Percentage of brain weight over body weight. *p<0.05, **P<0.01, t-test.

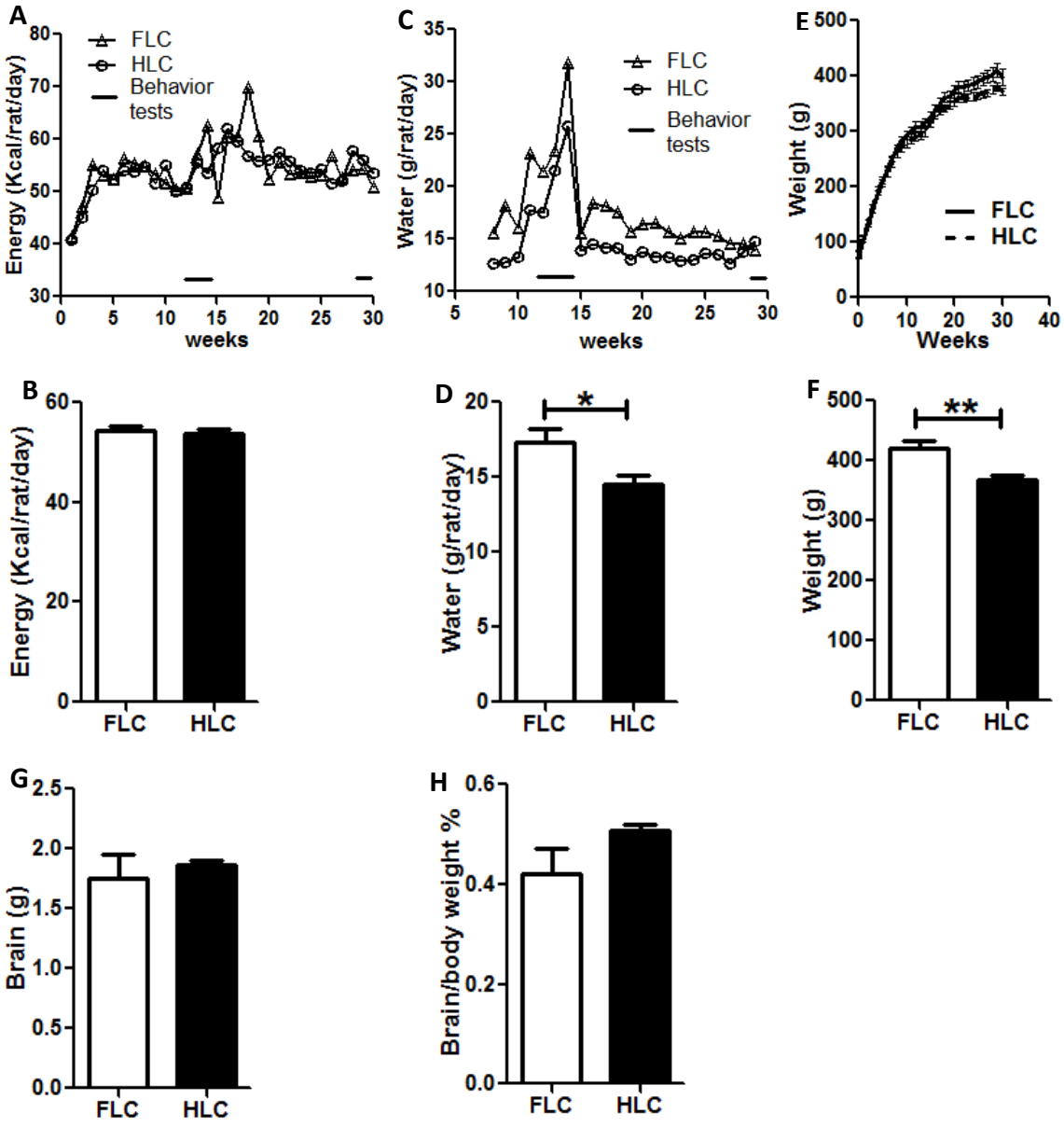

**Figure 4.2. HIV viral protein gp120 (A), Tat (B), and Nrf2 (C) mRNA level in the thalamus of 3-month (n=4) and 10-month (n=5) old rats**. *p<0.05, t-test. P values in panel C were calculated from two-way ANOVA.

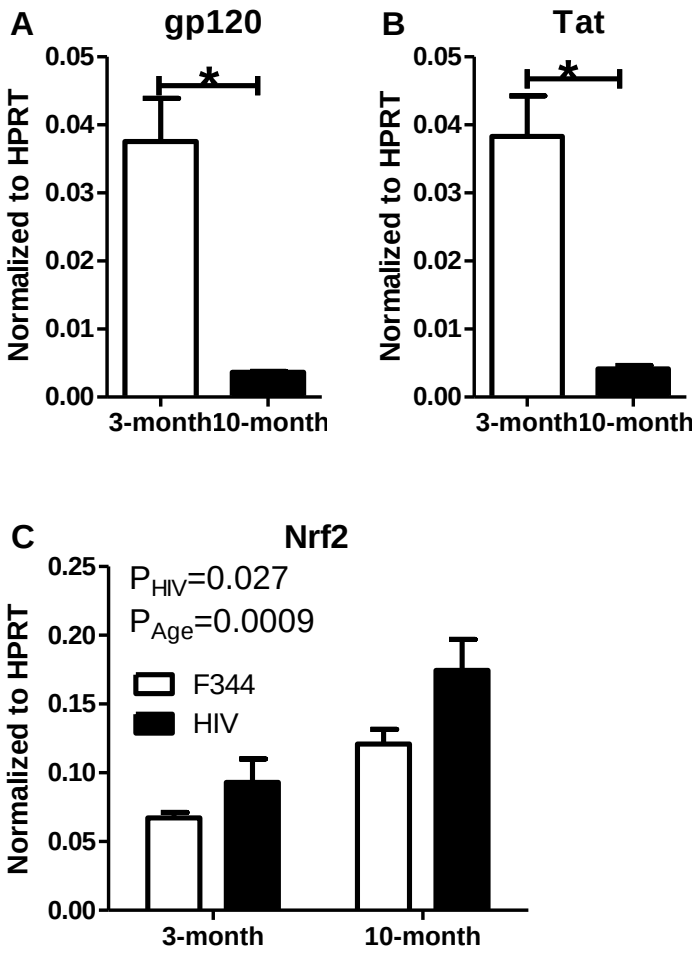

**Figure 4.3. The concentrations of total GSH (panel A), oxidized GSH (GSSG, panel B), reduced GSH (rGSH, panel C), and the ratio of GSSG/GSH (panel D) in the thalamus of F344 rats (FLC) and HIV-1Tg rats (HLC).** ** $p<0.01$, t-test.

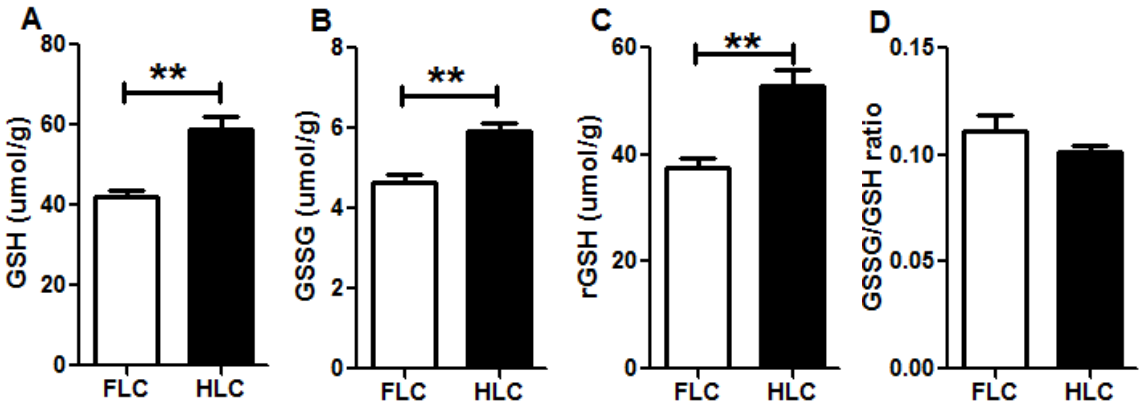

**Figure 4.4. γ-Glutamylcysteine synthetase (GCS) expression and activity in the thalamus of F344 rats (FLC) and HIV-1Tg rats (HLC).** (A) Western blot image of protein expression of the catalytic domain of GCS (GCS-HC). (B) Relative quantification of GCS-HC protein expression. (C) GCS activity. (D) Relative quantification of gene expression of GCS-HC. (E) Relative quantification of gene expression of GCS light chain (GCS-LC). ** p<0.01, t-test.

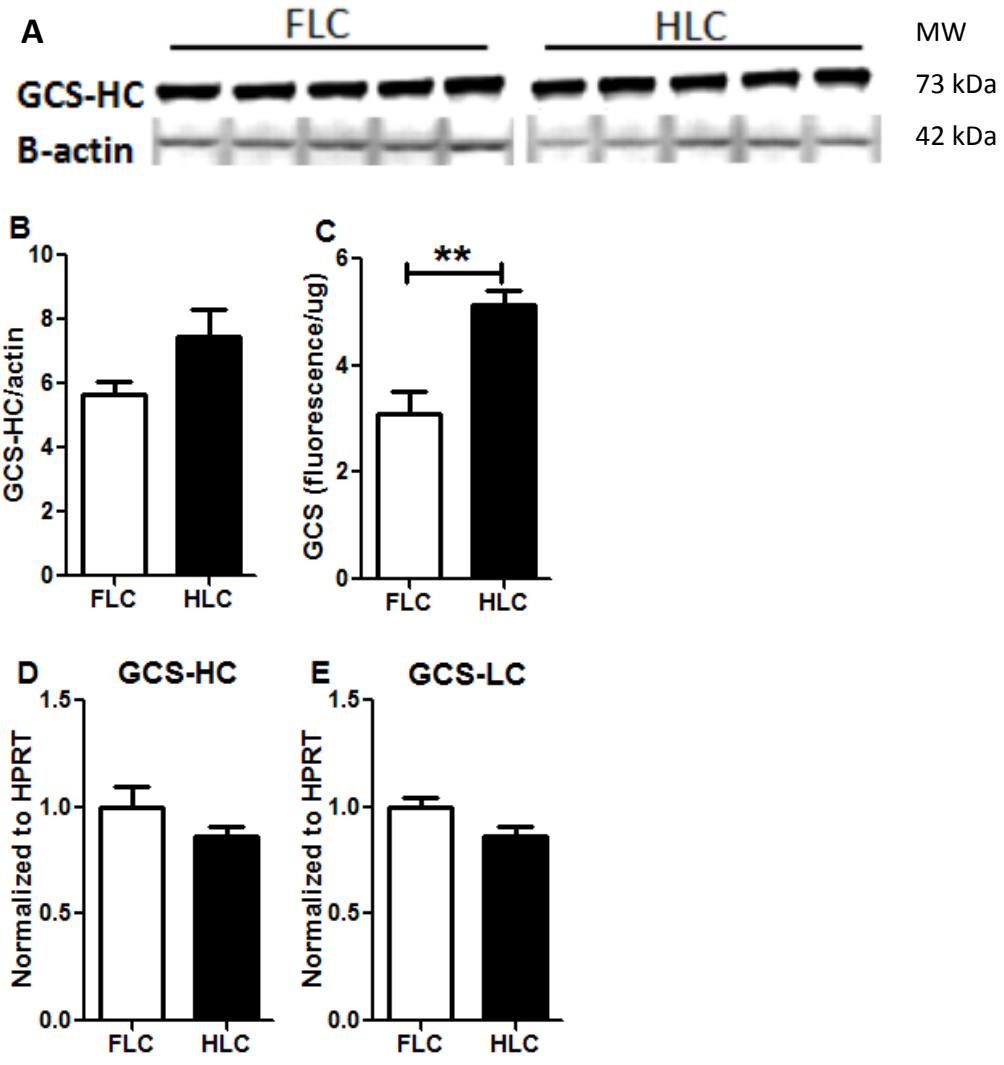

**Figure 4.5. γ-Glutamyl transferase (GGT) expression and activity in the thalamus of F344rats (FLC) and HIV-1Tg rats (HLC). (**A) Western blot of protein expression of GGT isoform 7 (GGT7). (B) Relative quantification of GGT7 protein expression. (C) GGT activity. (D-G) Relative quantifications of gene expression of GGT isoforms 7, 6, 5 and 1, respectively. ** p<0.01, Mann Whitney test.

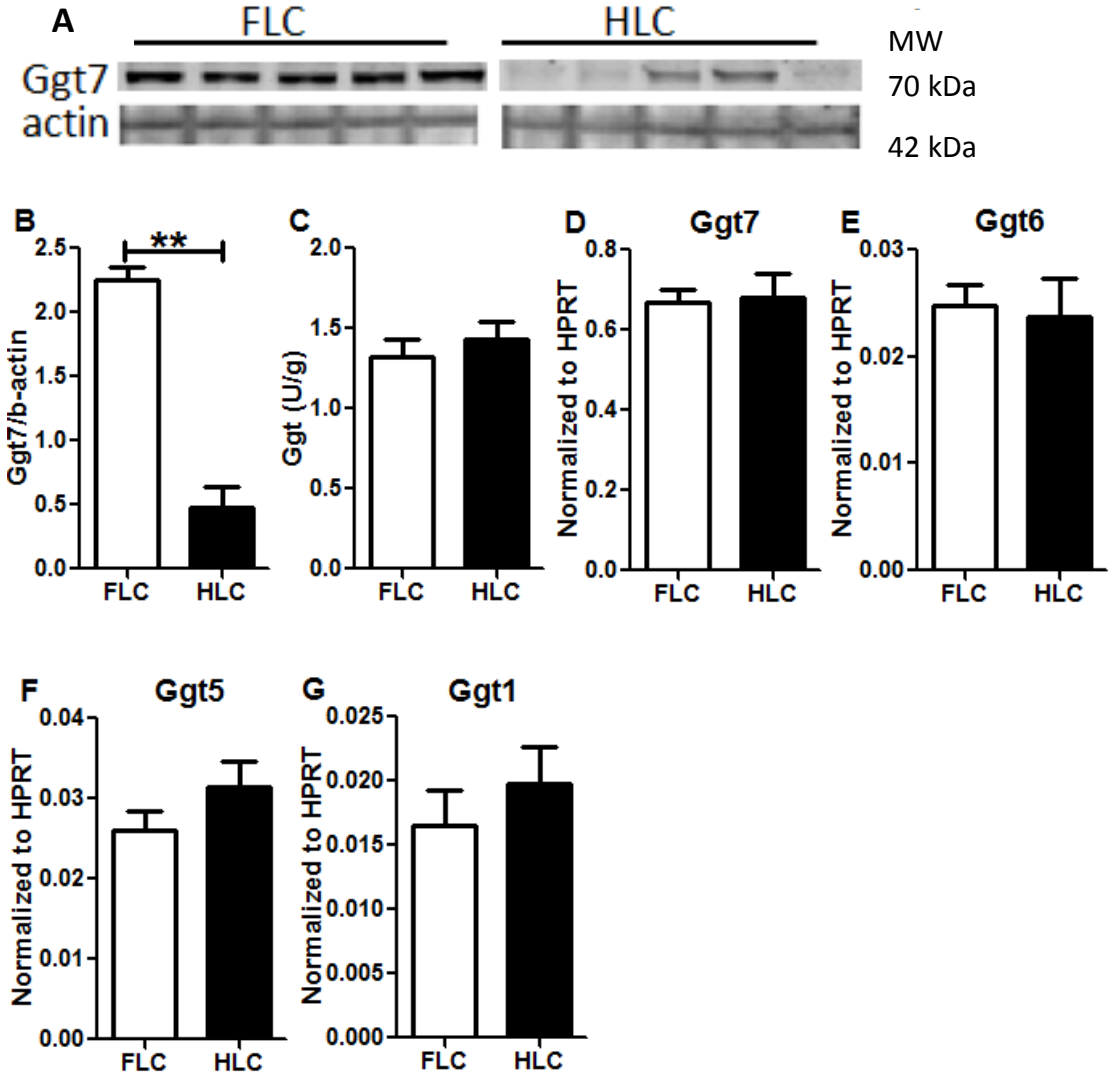

**Figure 4.6. Lipid peroxidation (panel A) and enzymatic activities of glutathione peroxidase (GPx, panel B) and glutathione-S-transferase (GST, panel C) in the thalamus of F344 rats (FLC) and HIV-1Tg rats (HLC).** Panels D-F show the mRNA expression of GPx4, GPx1 and GSTa4, respectively. **p<0.01, ***p<0.001, t-test.

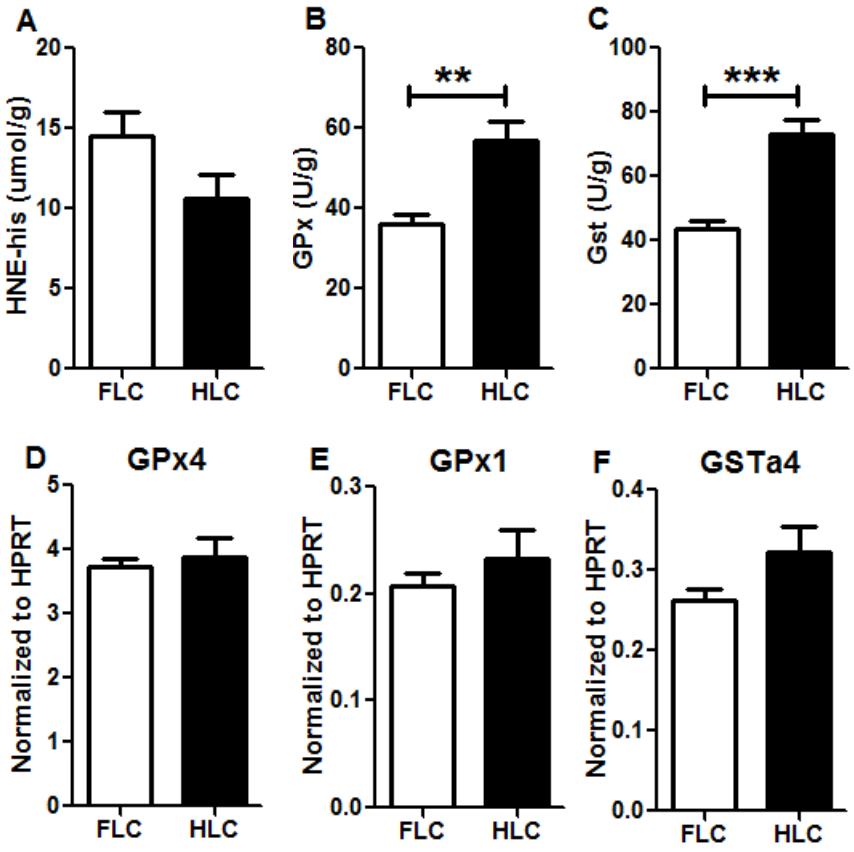

**Figure 4.7. Gene and protein expressions of transporters involved in GSH metabolism in the thalamus of F344 rats (FLC) and HIV-1Tg rats (HLC).** (A) Western blot image of multidrug resistance-associated proteins 1 (MRP1). (B) Relative quantification of MRP1 protein expression. (C-F) Relative gene expression levels of MRP isoforms 1 and 2, system $x_c$- catalytic domain (xCT), and excitatory amino acid carrier 1 (EAAC1), respectively.

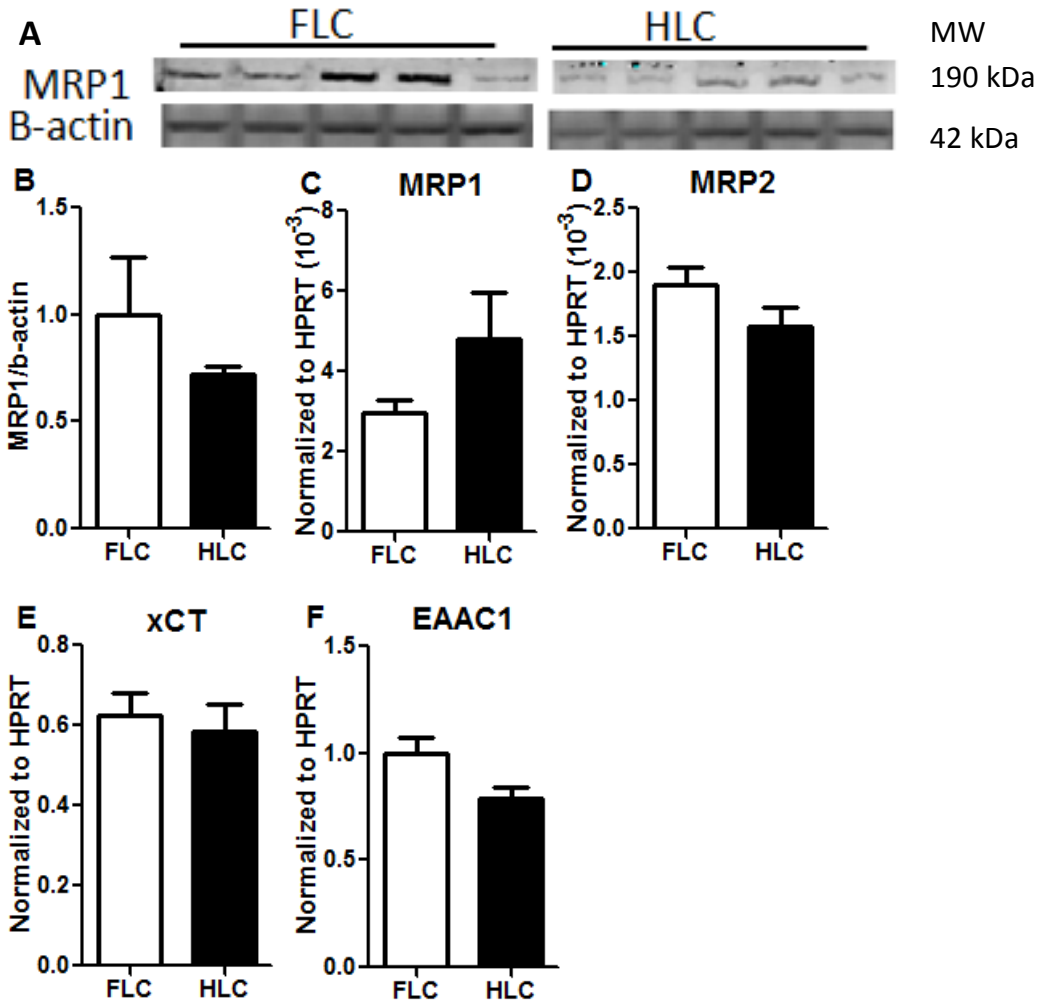

**Figure 4.8. Protein concentrations of 12 cytokines (panel A) and interleukin 12 (IL12, panel B) in the thalamus of F344 rats (FLC) and HIV-1 Tg rats (HLC).** * $p<0.05$, t-test.

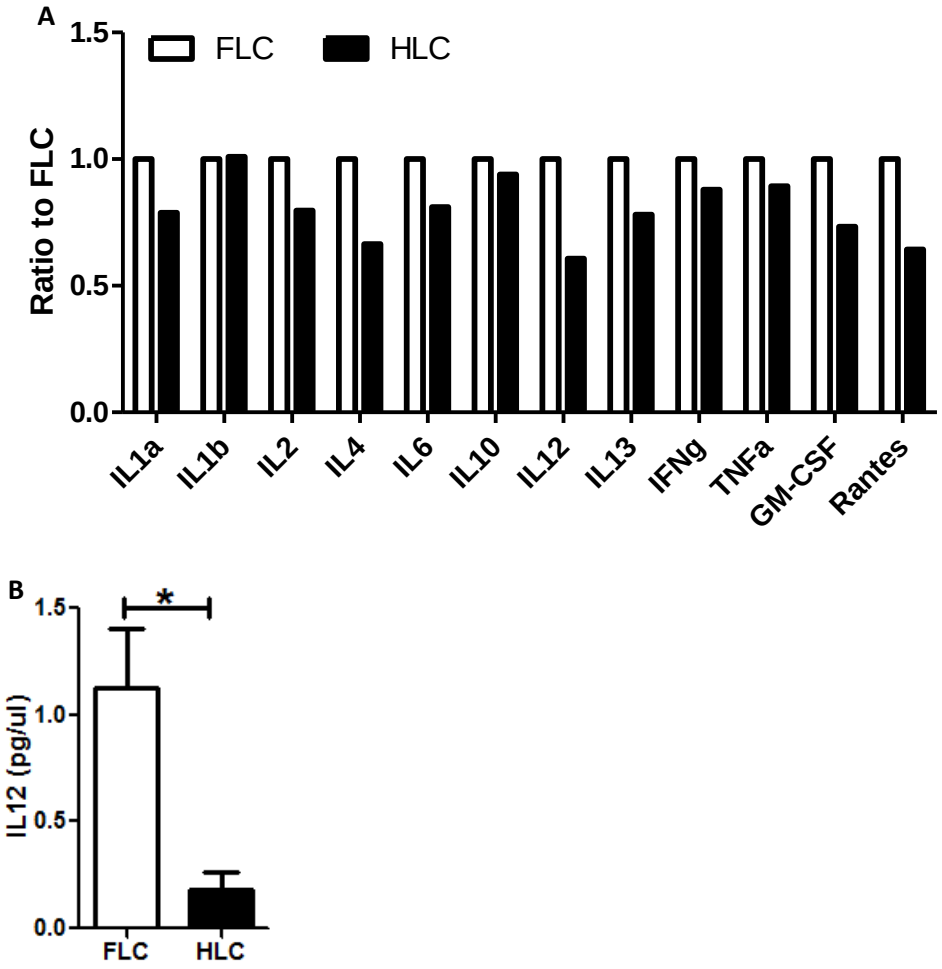

**Figure 4.9. The relative expression of glia fibrillary acidic protein (GFAP, panel A), neuronal nuclei (NeuN, panel B), and microtubule-associated protein-2 (MAP2, panel C) in the thalamus of F344 rats (FLC) and HIV-1Tg rats (HLC).** ** p<0.01, Mann Whitney test.

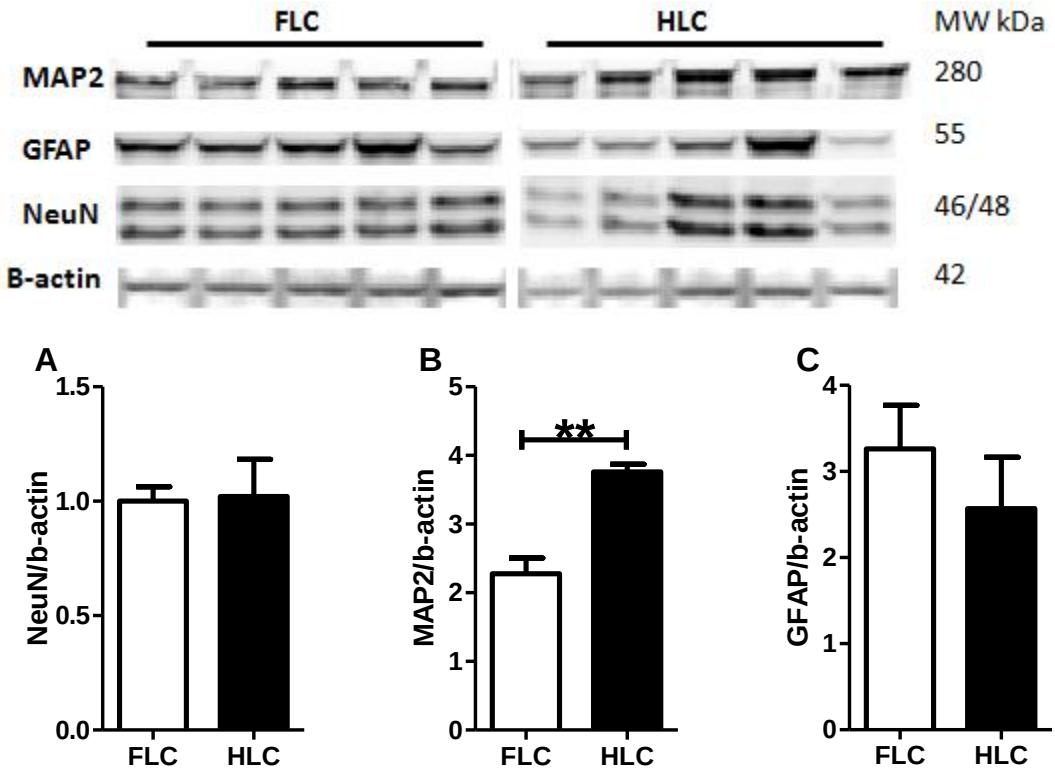

**Figure 4.10. Correlations among parameters involved in GSH metabolism and antioxidant function, oxidative stress, neuroinflammation, and neuronal differentiation in the thalamus of F344 rats (FLC) and HIV-1Tg rats (HLC).** Pearson correlation test was used in the statistical analysis. Abbreviation: GSH, glutathione; GCS, γ-glutamylcysteine synthetase; GST, glutathione-S-transferase; GPx, glutathione peroxidase; HNE-his, 4-hydroxynonenal and histidine conjugates; IL12, interleukin 12; MAP2, microtubule-associated protein-2.

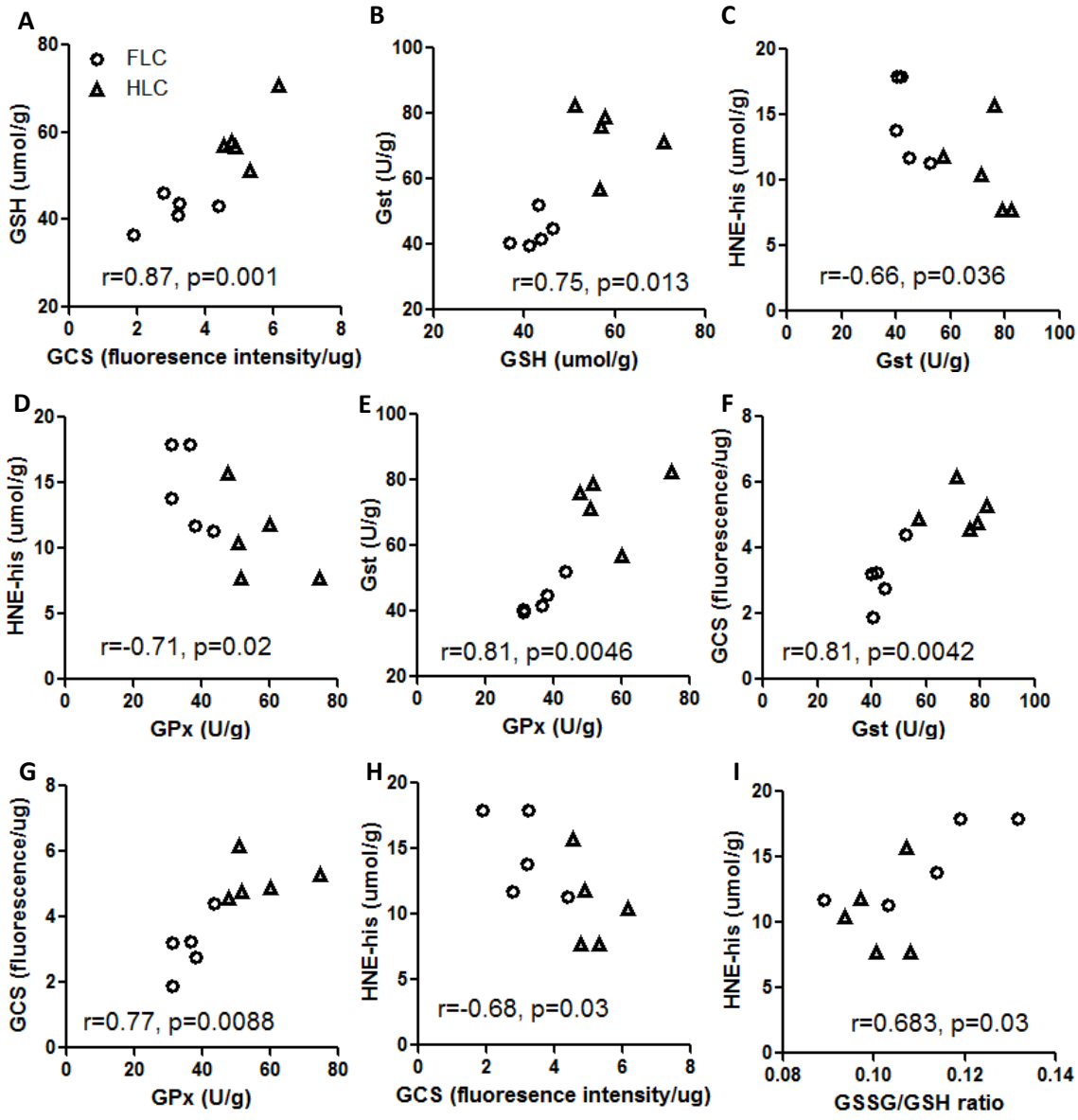

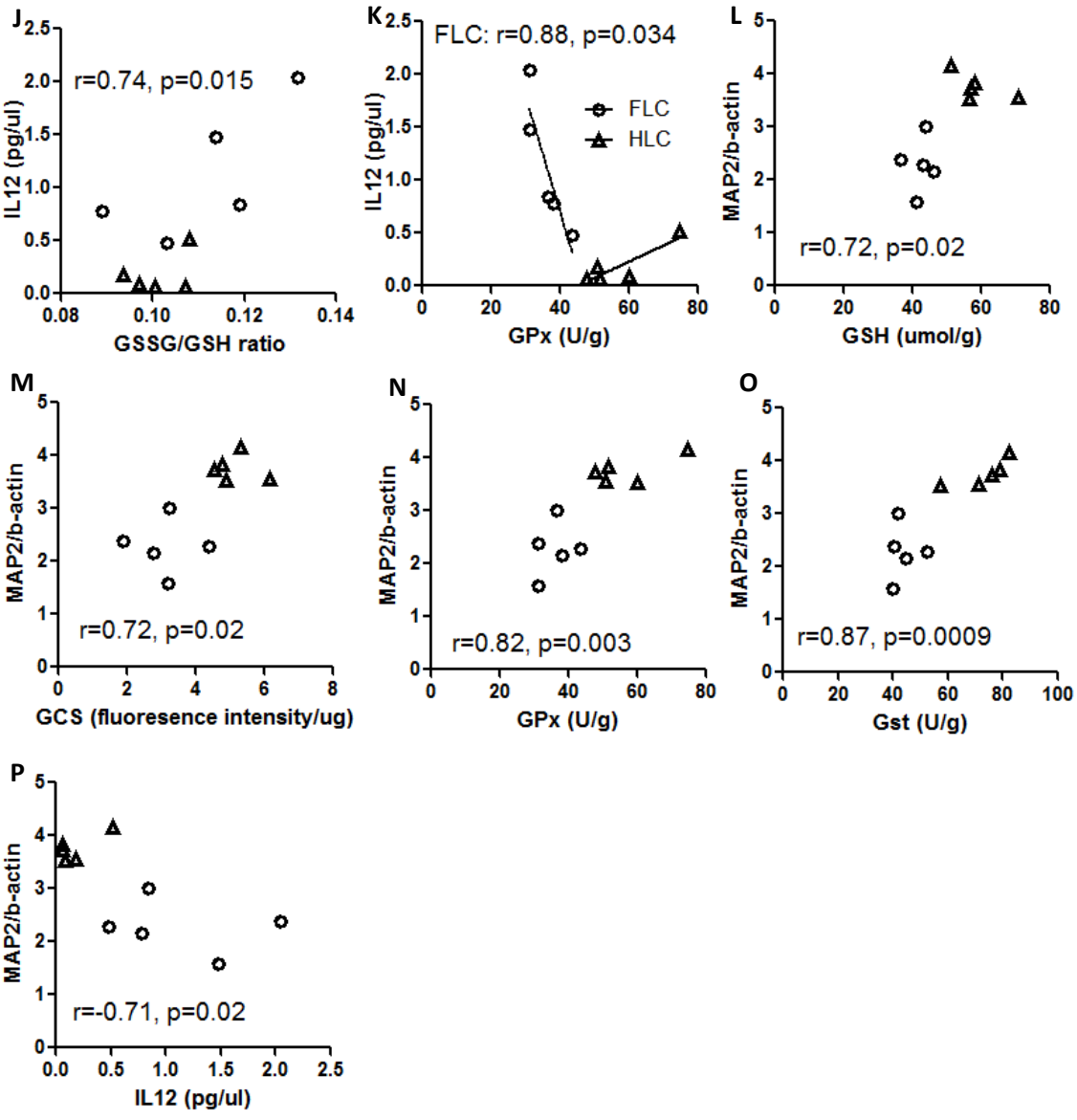
J
r=0.74, p=0.015
IL12 (pg/ul)
GSSG/GSH ratio
K
FLC: r=0.88, p=0.034
FLC
HLC
IL12 (pg/ul)
GPx (U/g)
L
r=0.72, p=0.02
MAP2/b-actin
GSH (umol/g)
M
r=0.72, p=0.02
MAP2/b-actin
GCS (fluoresence intensity/ug)
N
r=0.82, p=0.003
MAP2/b-actin
GPx (U/g)
O
r=0.87, p=0.0009
MAP2/b-actin
Gst (U/g)
P
r=-0.71, p=0.02
MAP2/b-actin
IL12 (pg/ul)

# Chapter 5

## Hippocampal Inflammation in HIV-1 Transgenic Rats and the Anti-inflammatory Effect of *Phyllostachys Edulis* Extract

## 5.1 Background

Antiretroviral drugs suppress HIV replication, but they cannot efficiently penetrate the blood-brain-barrier, and therefore HIV-related neurological disorders remain a major clinical challenge. Besides standard medical care, dietary supplements and use of natural products are convenient and cost-effective alternatives in the prevention and management of diseases [127]. In this project, we investigated the potential protective effect of bamboo *Phyllostachys edulis* extract (BEX) as a dietary supplement on HIV viral protein-induced neuroinflammation in the brain of HIV-1Tg rats.

Varied extracts derived from bamboo plants have been used in Traditional Chinese Medicine to treat inflammation, hypertension, cough and insomnia [224]. *Phyllostachys edulis*, also known as Moso or Maozhu, is one of the fastest growing plants in the world. It is a "running bamboo" with large biomass and wide geographical distribution. The leaves of *P. edulis* are the by-products of the bamboo timber industry. A patented procedure has been developed in China to utilize this "industrial waste" to produce the BEX, which was used in this project. In our previous studies, we have shown that BEX as a dietary supplement had anti-inflammation and anti-anxiety function in mice [225,226,227], and the anti-inflammatory effect of BEX was partially mediated by inhibiting the activation of nuclear factor kappa-light-chain-enhancer of activated B cells (NFκB) [228].

NFκB is a nuclear transcription factor expressed in many types of cells. NFκB regulates the expression of more than 400 genes, including cytokine/chemokines and their modulators [229,230,231], immunoreceptors [232], proteins involved in antigen presentation [233], cell adhesion molecules [234], stress response genes [235], and cell surface receptors [236]. Abnormal NFκB activity is involved in the pathogeneses of many diseases, such as chronic inflammation, cancer, arthritis, asthma, neurodegenerative diseases, and heart disease.

NFκB consists of five subunits: RelA (p65), RelB, c-Rel, NFκB1 (p50/105) and NFκB2 (p52/p100), and it functions as a dimer. One of the most common NFκB dimers is p50-

p65 heterodimer [237]. In normal conditions, NFκB binds the inhibitor of κB (IκB) and stays in the cytoplasm. When stimulated, NFκB dissociates with IκB and translocates to the nucleus, where it functions as a transcription factor. NFκB can be activated by many stimuli, such as proinflammatory cytokines, virus and viral proteins, chemical stress, oxidative stress, and environmental hazards [238].

Interleukin 1 beta (IL1β) and tumor necrotic factor alpha (TNFα) are target genes of NFκB, and they can also stimulate NFκB activation forming a positive feedback circle. Although both cytokines have neuroprotective functions, their chronic release in the brain from activated macrophage/microglia during HIV infection results in neuronal damage, mainly through inflammation-related ROS generation and calcium influx [239]. They also increase monocyte infiltration through the BBB, which further enhances neuroinflammation [239].

Our unpublished data also showed that BEX inhibited endoplamic reticulum (ER) stress. ER stress is caused by accumulation of unfolded proteins that can be induced by glucose deprivation, viral infection, oxidative stress, and other factors [240]. Unfolded protein response (UPR) is an adaptive program for ER stress. UPR can attenuate protein synthesis and upregulate genes that promote protein folding or disposal. The acute response of UPR is protective, but the chronic response may lead to cell death. Many cell types can survive ER stress by diluting the ER through cell replication, but the neuron is more vulnerable to ER stress due to its limited replication ability [241]. ER dysfunction is a common pathway of many neurological diseases, such as Alzheimer's disease, Parkinson's disease, Huntington's disease, and brain trauma [242]. Several studies showed impaired ER function associated with HIV infection and antiretroviral drug treatment [241,243,244]. The increase of ER stress response in the brain of HIV-infected patients was also reported [241].

Protein kinase R-like endoplasmic reticulum kinase (PERK) is one of the ER stress sensor proteins. Under stressed conditions, PERK is released from bindingimmunoglobulin protein (BiP, or glucose-regulated protein 78, GRP78) and forms a dimer. The autophosphorylated dimer phosphorylates eukaryotic initiation factor 2α

(eIF2α), which decreases the rate of protein synthesis by blocking formation of methionine-charged tRNA [242]. X-box binding protein 1 (XBP1) is a transcription factor upregulated in ER stress response. The activated XBP1 enhances the transcription of ER-located chaperones, which prevent protein aggregation and retain $Ca^{2+}$ in the ER lumen [240].

The aims of this chapter were to study the impact of HIV-1Tg on the hippocampus in terms of oxidative stress and inflammation, evaluate protective effects of BEX dietary supplement, and explore the mechanistic roles of NFκB and ER stress in HIV viral protein-caused neuroinflammation.

## 5.2 Methods

### 5.2.1 Animals and Dietary Treatment

Ten (10) one-month old HIV-1 NL4-3 gag/pol transgenic rats (HIV-1 Tg) and 5 genetic background control Fisher 344 (F344) rats were purchased from Harlan Inc. (Indianapolis, IN) and housed at the Laboratory Animal Service facility of the University of Hawaii. The rats were maintained on a 12-hour light/dark schedule. Food and water were accessible *ad libitum*. Body weight and food consumption were monitored weekly. The experimental procedures were approved by the Institutional Animal Care and Use Committee (IACUC) of the University of Hawaii.

Five (5) F344 rats (FLC group) and 5 HIV-1 Tg rats (HLC group) were fed a standard diet with 10% calories from fat. The meaning of the abbreviated group names have been explained in chapter 4. Meantime 5 HIV-1 Tg rats were fed the standard diet with 1% (w/w) BEX supplement (HLB group, "B" stands for "BEX"). Both diets were purchased from Research Diets (New Brunswick, NJ). The dietary composition is listed in Table 5.1 [245].

BEX used in this study was provided by Golden Basin LLC (Kailua, HI). BEX was produced by Golden Basin Bio-Tech (Hunan, China) through a patented procedure (Chinese invention patent, CN 1287848A). Briefly, twigs of *Phyllostachys edulis* no

longer than 2 feet were washed in water and air dried, ground and infused with 70-90% ethanol twice. The ethanolic extract was concentrated by vacuuming to obtain BEX. According to the manufacturer, BEX contains 50% water, 20% saccharides, 10% protein and 20% others [245].

5.2.2 Sample preparation

The hippocampal tissues were processed in the same way as the thalamus tissues described in Chapter 4 section 4.2.

5.2.3 GSH, GSSG, GPx, GGT, GST and HNE assays, and western blot

These procedures were carried out in the same way as described in Chapter 4 section 4.2. The primary antibodies used were rabbit anti-GFAP (ab7260, Abcam) and rabbit anti-p65 (ab7970, Abcam).

5.2.3 qPCR

The qPCR procedure was carried out in the same way as described in Chapter 4 section 4.2. The sequences of primers used were: beta-actin (β-actin): forward: cccgcgagtacaaccttct, reverse: cgtcatccatggcgaact; glucuronidase beta (GusB) forward: ctctGGTggccttacctgat, reverse: cagactcaggtgttgtcatcg; hypoxanthine guanine phosphoribosyl transferase (HPRT) forward: ctcctcagaccgcttttcc, reverse: tcataacctggttcatcatcactaa; TATA box binding protein (TBP) forward: cccaccagcagttcagtagc, reverse: caattctgggtttgatcattctg; beta-2-microglobulin (B2M); glucose-6-phosphate dyhydrogenase (G6PH); interleukin 1 beta (IL1β) forward: tgtgatgaaagacggcacac, reverse: cttcttctttgggtattgtttgg; tumor necrosis factor α (TNFα) forward: tgaacttcggggtgatcg, reverse: gggcttgtcactcgagtttt; PERK forward: gaagtggcaagaggagatgg, reverse: gagtggccagtctgtgcttt; XBP1 forward: ctcagaggcagagtccaagg, reverse: gaggcgcacgtagtctgagt.

5.2.4 Statistical analysis

Prism 5 (GraphPad Software Inc., La Jolla, CA) was used for statistical analysis. Differences among the means were analyzed using Student t-test and one-way ANOVA. $P < 0.05$ was considered statistically significant.

## 5.3 Results

5.3.1 Food consumption, body weight, and brain weight

A 30-week record of energy consumption and body weight is summarized in Figure 5.1. No differences of energy intake were observed among the 3 groups at any time point (Figure 5.1A) or on average (Figure 5.1B) over the 30-week period. The growth of animals showed similar trends in the 3 groups over the first 30 weeks (Figure 5.1C). But at the end of the study (38 weeks), both HLC and HLB rats were lighter than the FLC rats ($p=0.0053$, one-way ANOVA, Figure 5.1D). Wet brain weight was recorded and neither wet brain weight nor the ratio of brain weight over body weight showed differences among the 3 groups (Figure 5.1E and F). Therefore, BEX supplement did not affect food intake, growth, and general brain development of the HIV-1 Tg rats.

5.3.2 GSH-centered antioxidant system and lipid peroxidation in the hippocampus

GSH consists of oxidized GSH (GSSG) and reduced GSH (rGSH). Total GSH and GSSG were measured in the hippocampal samples and rGSH was calculated ([rGSH]=[GSH]-2*[GSSG]). HLC had a lower content of GSSG than the other two groups (-23% vs. FLC, $p=0.01$; -22% vs. HLB, $p=0.035$; t-test; Figure 5.2B). Similarly, HLC group also showed the lowest GSH and rGSH readings among the 3 groups (Figure 5.5A and C), but the differences were not statistically significant. The ratios of GSSG/GSH were comparable among the 3 groups, indicating the redox status of GSH was not affected.

The HLB group showed a trend of having a higher GGT activity in the hippocampus (+39% vs. FLC, $p=0.058$; +44% vs. HLC, $p=0.053$; t-test; Figure 5.2E). In contrast, the GPx activity was lower in HLB group than in HLC group (-40% vs. HLC, $p=0.03$, t-test, Figure 5.2F). No differences were detected in the GST activity among the 3 groups

(Figure 5.2G). The highest HNE concentration was found in HLB, followed by FLC and HLC, and the differences between each two groups were significant ($p<0.0001$, one-way ANOVA; $p<0.05$, HLB compared with HLC or FLC, Bonferroni's post hoc; Figure 5.2H).

### 5.3.3 Inflammation markers in the hippocampus

Protein expression of glia fibrillary acid protein (GFAP, an astrocyte activation marker) and NFκB subunit p65 were measured using western blot to evaluate the inflammation status of the hippocampus (Figure 5.3). A dramatic increase (approximately 5 folds) of GFAP expression was observed in the HLC group compared to FLC ($p=0.008$, Mann-Whitney test), and this increase was effectively abolished by BEX supplementation (HLB vs. HLC, $p=0.008$, Mann Whitney test). Similarly, a trend of lower p65 expression was found in the HLB group compared to the HLC group (-59%, $p=0.056$, Mann-Whitney test).

### 5.3.4 Gene expression of IL1β and TNFα in the hippocampus

The relative mRNA levels of inflammatory cytokines IL1β and TNFα were measured in the hippocampal samples using quantitative real-time PCR (qPCR). To evaluate the reliability of housekeeping genes, we compared the cycle thresholds (Ct values) of 6 commonly used housekeeping genes among the 3 groups of rats, with the same amount of cDNA in the qPCR mixes. These housekeeping genes were β-actin, GusB, HPRT, TBP, B2M and G6PD. As shown in Figure 5.4A, the Ct values of these genes were consistently higher in the HLB group compared to the other 2 groups, and the reason behind this phenomenon is not clear. β-actin was used as housekeeping genes in the final test. As shown in Figure 5.4B and C, when the target genes were normalized against β-actin, higher IL1β mRNA level was found in the HLC group compared to the FLC group (+90%, $p=0.004$, Kruskal Wallis test) and the HLB group (+170%, $p<0.01$, Dunn's post-hoc); higher TNFα mRNA level was found in the HLC group compared to the HLB group (+113%, $p=0.03$, Mann Whitney's test). It is worth pointing out that such differences are not caused by the higher Ct values of the housekeeping genes in the HLB

group (Figure 5.4A), since normalization against a higher Ct value of the housekeeping gene will result in higher relative abundance of the target gene (mRNA $ratio_{target/housekeeping} = 2^{Ct\ housekeeping}/2^{Ct\ target}$).

### 5.3.5 Gene expression of ER stress markers

The mRNA levels of PERK and XBP1 were measured using qPCR to evaluate the ER stress in the hippocampus (Figure 5.5). Using β-actin as a housekeeping gene, the relative mRNA level of PERK was significantly lower in the HLB group compared to the HLC group (-42%, $p=0.03$, Kruskal Wallis test; $p<0.05$, Dunn's post-hoc); and the mRNA level of xBP1 was significantly lower in HLB group than the FLC group (-32%, $p=0.006$, Kruskal Wallis test; $p<0.01$, Dunn's post-hoc).

## 5.4 Discussion

This study showed that HIV viral protein expression induced neuroinflammation in the hippocampus of the transgenic rats, and such inflammation was effectively prevented by BEX dietary supplementation. Two selected ER stress markers also showed the lowest gene expression level in the HLB group, indicating potential links between ER stress and neuroinflammation. Meanwhile, the HLB groups showed the highest level of lipid peroxidation, which may be partially due to the low GPx activity and high GGT activity in this group. In this study oxidative stress and neuroinflammation did not converge in hippocampus.

### 5.4.1 HIV-induced changes in hippocampus

Compared with other brain regions, higher levels of neuroinflammation have been found in the hippocampus of HAART-treated HIV patients [246,247], as evidenced by the increases of CD68+ monocyte/macrophages and GFAP-positive astrocytes [247]. *In vitro* studies showed HIV viral protein can induce oxidative stress in hippocampal neurons through increasing mitochondrial ROS generation [27], but hippocampal oxidative stress has not been recorded in HIV patients.

In the present study, HIV-1Tg caused moderate GSH depletion in the hippocampus, but did not affect the redox status of GSH, nor the activities of GSH-dependent antioxidant enzymes such as GPx and GST. This is in contrast to the systematic upregulation of GSH and GSH-centered enzymes in the thalamus of the HIV-1Tg rats, as presented in Chapter 3. Despite the lack of response of the GSH system to the viral protein expression, the HNE concentration in the hippocampus of the HLC group was significantly lower than that in the FLC group, suggesting that other antioxidant systems (such as SOD, catalase, or small non-protein molecules) may have been upregulated by the viral proteins in a overcompensatory manner in the hippocampus and contributed to the decreased lipid peroxidation. Furthermore, in contrast to the lower level of inflammation in the thalamus of the HIV-1Tg rats, the inflammatory markers in the hippocampus of these rats were significantly elevated. Collectively, Chapters 3 and 4 illustrate that HIV viral protein induced redox and inflammatory changes in the brain are region-specific.

### 5.4.2 Effects of BEX on GSH metabolism

In the present study, the concentrations of GSH, GSSG, and rGSH in the hippocampus of the HLC group appeared to be lower than those in the FLC group, and BEX supplement to the HIV-1Tg rats abolished these differences. The GSSG/GSH ratios were comparable among the three groups. Our previous study showed that when C57BL/6J mice were treated with standard (10% energy from fat) or high fat (45% energy from fat) diets, the high fat diet increased GSH concentrations in both forebrain and hindbrain, and BEX supplement (same dose as in the present study) normalized the GSH contents in both regions to the control levels, and also decreased GSSG/GSH ratio in the hindbrain (unpublished data). In contrast, BEX supplement in both standard and high fat diets increased the GSSG/GSH ratio in the whole blood of mice [245]. These results implicate that BEX can regulate GSH homeostasis in both CNS and peripheral. Other researchers reported that 3-O-caffeoyl-1-methylquinic acid, a compound found in the leaves of *Phyllostachys edulis*, increased the levels of GSH, GSSG, and GSSG/GSH ratio in a dose and time-dependent manner in endothelial cells through Nrf2 activation [248]. Our unpublished data also showed the ethanol-soluble fraction of BEX can activate Nrf2 in multiple cell lines.

The present study also showed that BEX increased GGT activity and decreased GPx activity in the hippocampus of HIV-1Tg rats. GGT generates cysteinylglycine (CysGly), which facilitates hydroxyl radicals ($^{\bullet}$OH) production through Fenton reaction, and initiates the chain reaction of lipid peroxidation [55]. Meanwhile, the resultant lipid peroxides may not be removed efficiently due to the decrease of GPx activity, leading to the accumulation of lipid peroxidation markers such as HNE. However, the increased lipid peroxidation in the hippocampus of the HLB group did not converge with increased neuroinflammation, but rather co-occurred with inhibition of neuroinflammation, as discussed below.

### 5.4.3 BEX and Neuroinflammation

BEX inhibits obesity-induced systemic periphery inflammation in mice [226], possible through preventing the activation of NFκB and AP-1 pathways [225]. Bioactivity-guided fractionation revealed that flavonoids such as tricin and 7-O-methyltricin are among the anti-inflammatory compounds in BEX [249]. In the present study, the prominent increase of GFAP protein expression in the hippocampus of the HLC group indicates increased astrogliosis [250], and this astrogliosis was effectively reduced by BEX treatment. Compared with HLC group, HLB group also showed lower protein expression of p65, implicating potentially lower activity of the NFκB pathway. Along this line, the qPCR results also showed lower mRNA levels of IL1β and TNFα in HLB group. Thus BEX may have an inhibitory role in HIV-induced neuroinflammation.

### 5.4.4 BEX and ER stress

HIV infection can induce ER stress. For example, higher protein expression of ER stress sensors BiP and activation transcription factor (ATF6β) were found in the brain of HIV patients [241]. Our unpublished data showed that the ethanol soluble fraction of BEX effectively inhibited the gene expression of an array of ER stress sensors, including BiP, XBP1, and ATF6, under a lipotoxic condition in muscle cells. In the present study, lower mRNA levels of PERK and XBP1 were found in the hippocampus of the HLB group compared to the HLC group, suggesting potential anti-ER stress function of BEX in the

brain. It is worth mentioning that in contrast to Figure 5.3, which shows the dramatic differential protein expressions in tissue lysates prepared in a membrane lysis buffer, no differences were observed when PBS was used to prepare the tissue lysates (data not shown). This suggests that the newly synthesized proteins in the hippocampus of the HLC group may be accumulated in the ER lumen, which is in accordance with the hallmark of ER stress.

To confirm the presence of ER stress in the hippocampus of the HIV-1Tg rats, and to further demonstrate the anti-ER stress effect of BEX, expression and phosphorylation of proteins involved in the unfold protein response (UPR), such as BiP, ATF6β, XBP1, ATF4, should be studied.

**Table 5.1. The composition of the standard (control) diet and the BEX supplemented diet.**

| Diet | Control | | Bex | |
|---|---|---|---|---|
| | g | kJ | g | kJ |
| Ingredients | | | | |
| Casein, 80 mesh | 200 | 3349 | 200 | 3349 |
| $_{L}$-Cystine | 3 | 50 | 3 | 50 |
| Maize starch | 315 | 5275 | 315 | 5275 |
| Maltodextrin 10 | 35 | 586 | 35 | 586 |
| Sucrose | 350 | 5862 | 350 | 5862 |
| Cellulose BW200 | 50 | 0 | 50 | 0 |
| Soybean oil | 25 | 942 | 25 | 942 |
| Lard | 20 | 754 | 20 | 754 |
| Mineral mix S10026 | 10 | 0 | 10 | 0 |
| Dicalcium phosphate | 13 | 0 | 13 | 0 |
| Calcium carbonate | 5.5 | 38 | 5.5 | 38 |
| Potassium citrate, $1H_2O$ | 16.5 | 0 | 16.5 | 0 |
| Vitamin mix V10001 | 10 | 167 | 10 | 167 |
| Choline bitartrate | 2 | 0 | 2 | 0 |
| Bamboo extract (dry mass) | 0 | 0 | 11 | 0 |
| Water from bamboo extract | 0 | 0 | 11 | 0 |
| FD&C Yellow Dye #5 | 0.05 | 0 | 0.025 | 0 |
| FD&C Red Dye #40 | 0 | 0 | 0 | 0 |
| FD&C Blue Dye #1 | 0 | 0 | 0.025 | 0 |
| Total | 1055 | 17000 | 1077 | 17000 |

**Figure 5.1. Food consumption and body weight of the experimental animals.** (A) Food consumption of F344 rats (FLC), HIV-1 transgenic rats (HLC) and BEX-fed HIV-1 Tg rats (HLB) over 30 weeks. (B) Average energy consumption of 30 weeks. (C) Body weight over 30 weeks. (D) Average body weight before animal scarification. (E and F) Wet brain weight and percentage of brain weight over body weight. * $p<0.05$, Bonferroni's post-hoc.

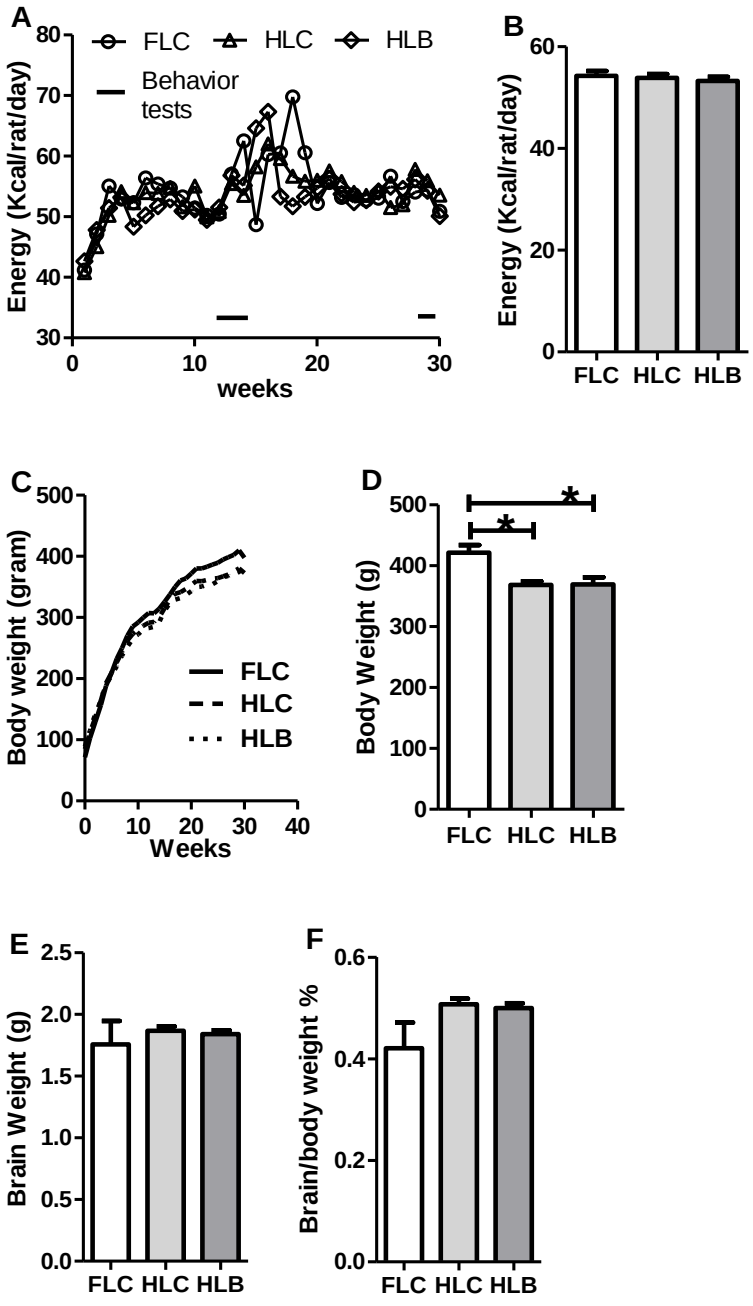

**Figure 5.2. Concentrations of GSH and HNE, and activities of GSH-centered enzymes in the hippocampus of F344 rats (FLC), HIV-1Tg rats (HLC), and HIV-1Tg rats fed bamboo extract-supplemented diet (HLB).** (A) GSH concentration. (B) GSSG concentration. (C) Reduced GSH (rGSH) concentration. (D) GSSG/GSH ratio. (E) GGT activity. (F) GPx activity. (G) GST activity. (H) HNE-his concentration. * $p<0.05$, t-test; $^{\wedge}p<0.1$, t-test; $^{\#}$ $p<0.05$, Bonferroni's post-hoc; p value in panel B was calculated from one-way ANOVA.

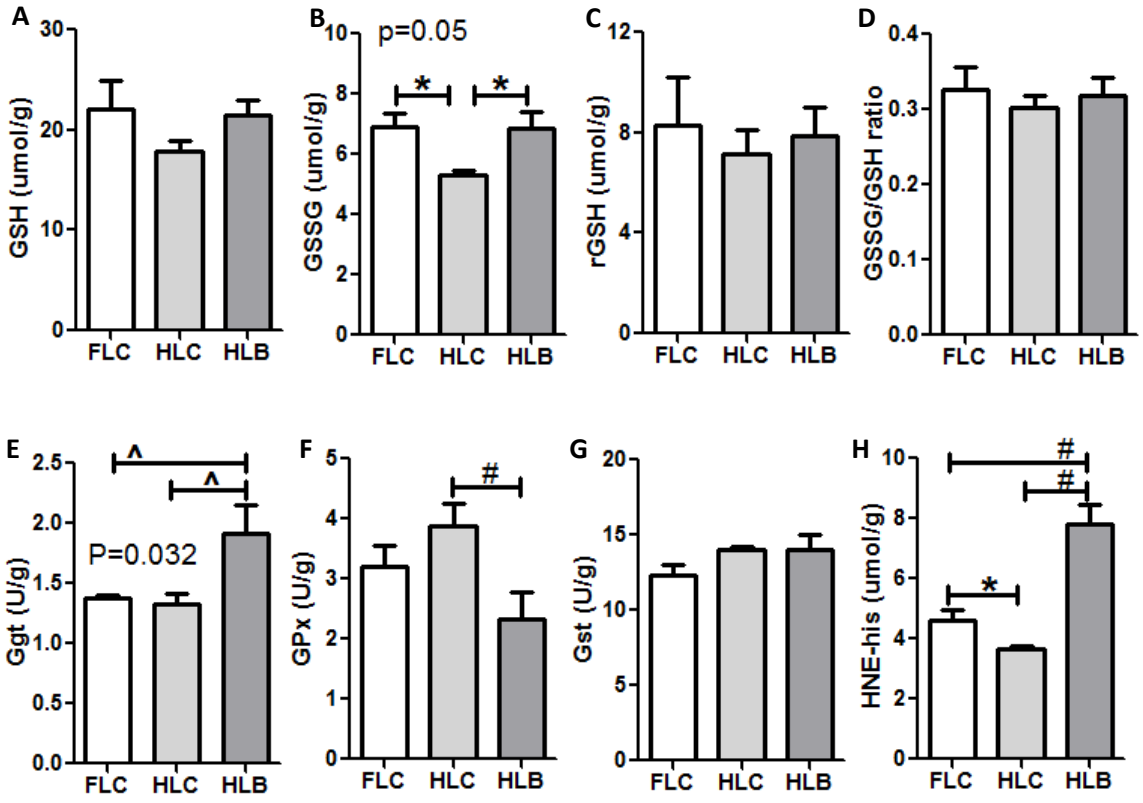

**Figure 5.3. Protein expression of neuroinflammation markers in the hippocampus of F344 rats (FLC), HIV-1Tg rats (HLC) and BEX-fed HIV-1Tg rats (HLB).** (A) Protein expression of GFAP detected by western blotting and relative densitometric quantification. Note that FLC vs. HLC and HLC vs. HLB were compared in two separate gels, and the HLC group was used for signal normalization between the two gels. (B) Protein expression of p65 detected by western blotting and relative densitometric quantification. ** p<0.01, ^ p<0.1, Mann Whitney test;. All samples were prepared in a membrane lysis buffer.

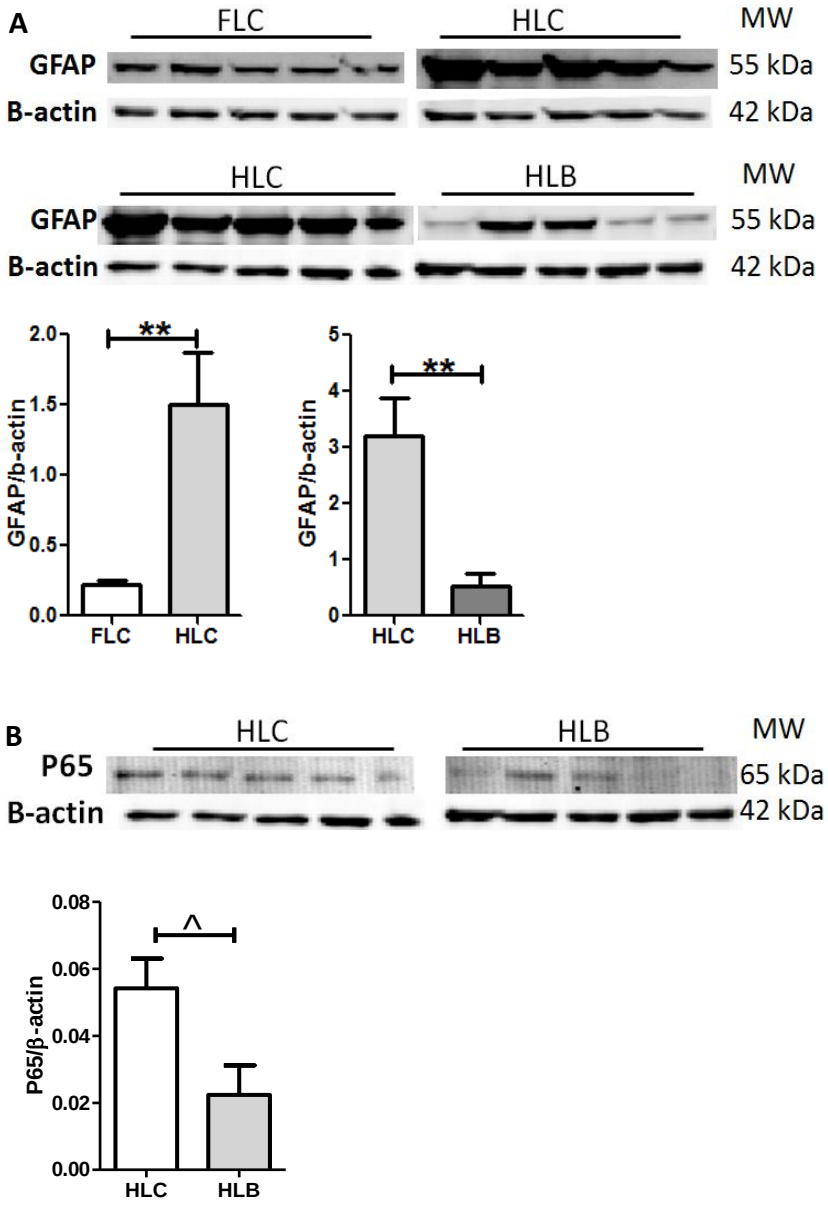

**Figure 5.4. mRNA expression of housekeeping genes and cytokines IL1β and TNFα in the hippocampus of F344 rats (FLC), HIV-1Tg rats (HLC) and BEX-fed HIV-1Tg rats (HLB).** (A) Cycle threshold of housekeeping genes, * $p<0.05$, t-test. (B) mRNA expression of IL1 β. (C) mRNA expression of TNFα. * $p<0.05$ Mann Whitney test; # $p<0.05$, Dunn's post-hoc.

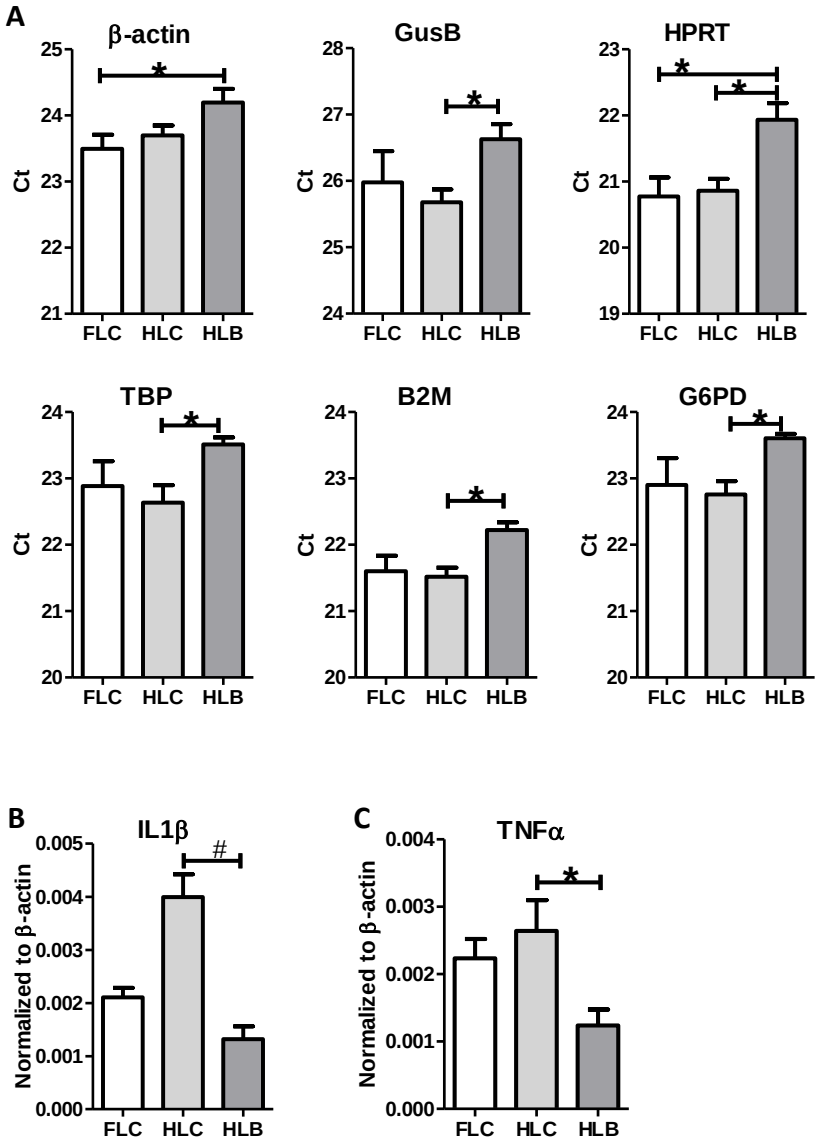

**Figure 5.5. mRNA expression of ER stress markers in the hippocampus of F344 rats (FLC), HIV-1Tg rats (HLC) and BEX-fed HIV-1Tg rats (HLB).** # $p<0.05$, Dunn's post-hoc test.

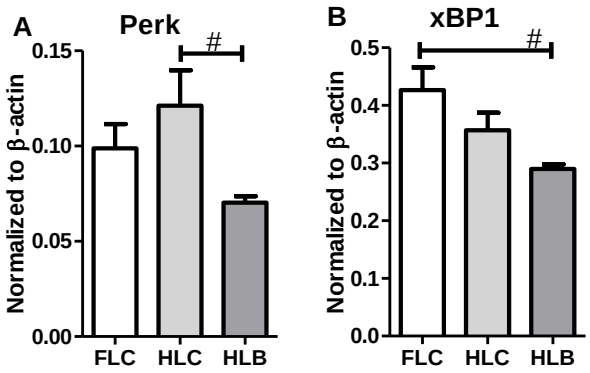

# Chapter 6

# Concluding Remarks and Future Directions

This study examined the changes of antioxidant, oxidative stress and inflammation in the CNS in the context of HIV infection, and evaluated the modulatory effects of Meth exposure and dietary supplement of bamboo *Phyllostachys edulis* extract. It was found that in human CSF, GSH depletion co-occurred with oxidative stress in HIV seropositive patients, and upregulation of GSH and GPx may have contributed to the amelioration of lipid peroxidation in the CSF of Meth users. These results emphasize on the importance of the GSH-centered antioxidant system in the extracellular environment of the CNS in both HIV infection and Meth abuse.

Using the HIV-1Tg model, we observed that HIV-1 transgenesis affected the redox status in the brain in region-specific and age-dependent manners. Among several brain regions studied, the thalamus was found to have the highest GSH content. GSH biosynthesis and GSH-dependent antioxidant enzymes in the thalamus were highly responsive to the viral protein expression, and also seemed to regulate the production of inflammatory cytokine IL12 and neuronal differentiation as indicated by MAP2 expression. In contrast, little changes were found in the GSH system in the hippocampus of the HIV-1Tg rats, but increased neuroinflammation markers such as GFAP and p65 were detected. Interestingly, these increases were only found in the samples prepared in membrane lysis buffer, but not in those prepared in PBS, implicating the newly synthesized proteins may be compartmented in the cells, as seen under ER stress conditions. Dietary supplementation of BEX normalized the inflammatory and ER stress status in the hippocampus, implicating potential therapeutic effect on HANDs of this natural product.

In conclusion, this study highlighted the significance of GSH and GSH-dependent antioxidant enzymes in regulating the redox status in the CSF and in the brain tissues (especially thalamus) during HIV infection, documented HIV viral protein-induced inflammation in the hippocampus, and suggested potential anti-neuroinflammatory effect of the BEX. The regulatory pathways of the GSH-centered antioxidant system in the CNS, and potential pharmaceutical interventions through the mechanisms, warrant detailed investigation. Other less studied topics, such as the role of the GSH system in the regulation of neuroinflammation and neuronal differentiation need to be further established. The high level of inflammation in the hippocampus of the HIV-1Tg rats also

calls for more attention, since this may contribute to the pathogenesis of HAND. Last but not least, the active compounds and the mechanism underlying the anti-neuroinflammatory function of the bamboo extract deserve further investigation for the development of a CAM-based cost effective HIV treatment.

# Appendices

In the appendices, the ID of each group of rats consists of three letters, and the meaning of each letter is explained below: For the first letter, “F” stands for F344 rats and “H” stands for HIV-1 Tg rats. For the second letter, “H” stands for high fat diet (45% calories from fat, Research Diet catalog number D12451) and “L” stands for low fat diet (10% calories from fat, Research Diet catalog number D12450B). For the third latter, “C” stands for control diet, “B” stands for BEX supplement (11 grams of BEX dry mass per 4057 Kcal, or 1% w/w) and “S” stands for selenium supplement (sodium selenite, 16ppm or 92.5uM in drinking water). N=6 for FHB and N=5 for the other groups. Dietary treatment started at 5 weeks, and samples harvested at 10 months.

## Appendix A. Levels and correlations of GSH-centered enzymes, neuronal proteins and inflammatory marker IL12 in the thalamus.

**Appendix A1. GSH, GSH-centered proteins and IL12 level in the thalamus.**

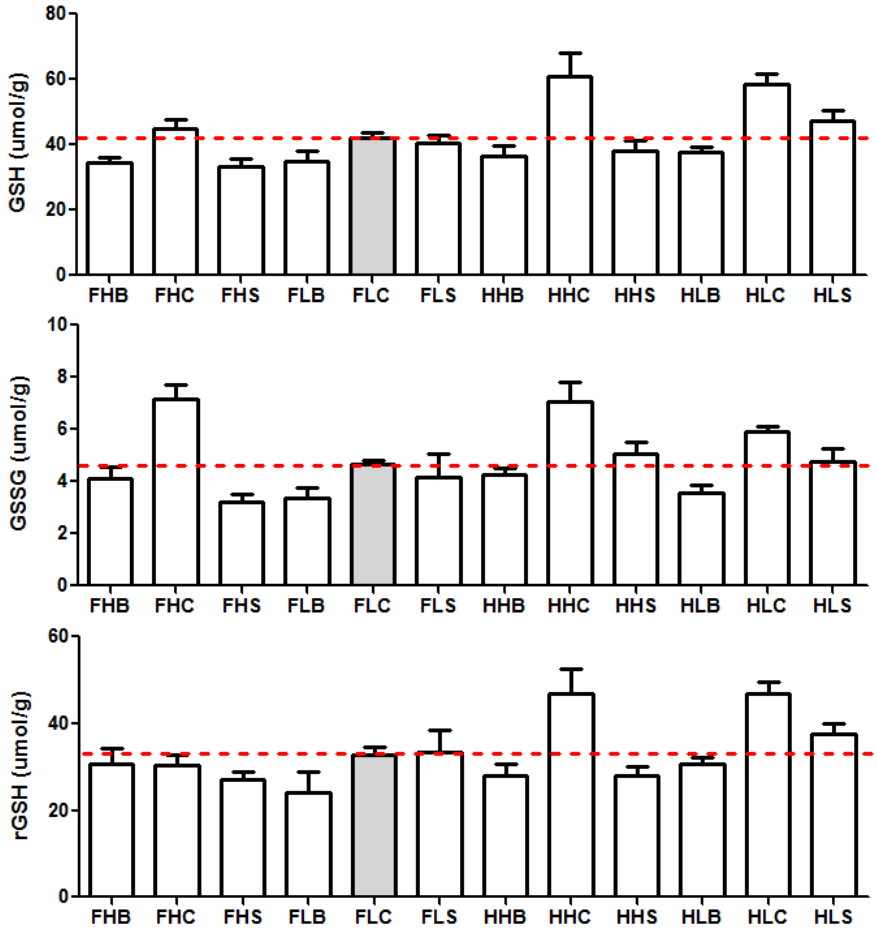

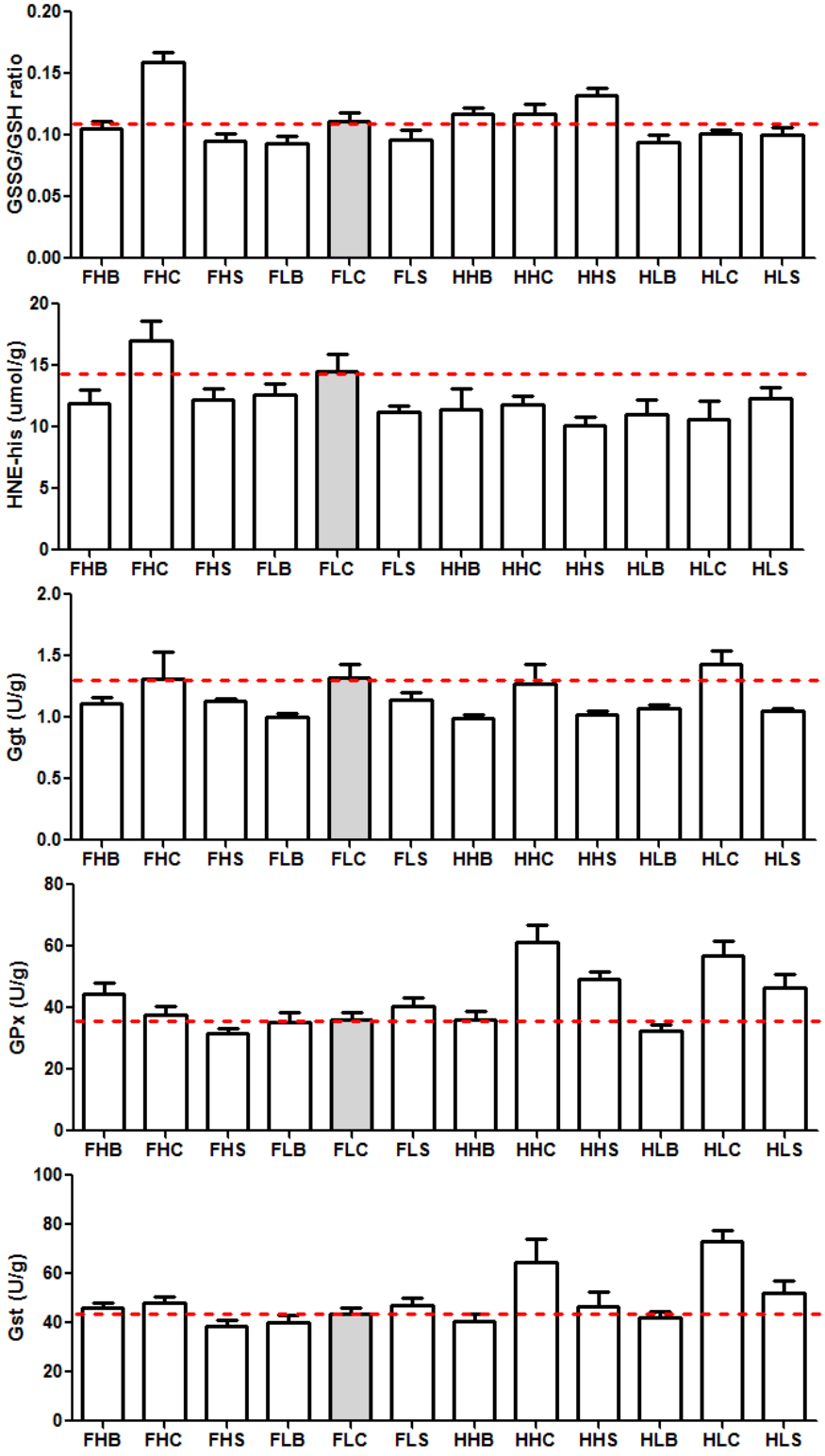
GSSG/GSH ratio
0.20
0.15
0.10
0.05
0.00
HNE-his (umol/g)
20
15
10
5
0
Ggt (U/g)
2.0
1.5
1.0
0.5
0.0
GPx (U/g)
80
60
40
20
0
Gst (U/g)
100
80
60
40
20
0
FHB FHC FHS FLB FLC FLS HHB HHC HHS HLB HLC HLS

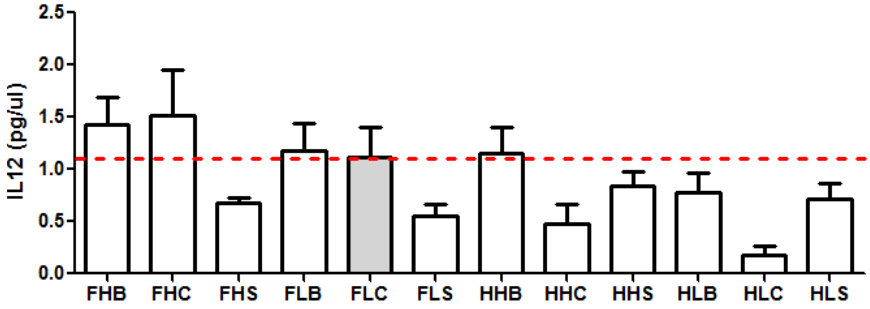
IL12 (pg/ul)
2.5
2.0
1.5
1.0
0.5
0.0
FHB
FHC
FHS
FLB
FLC
FLS
HHB
HHC
HHS
HLB
HLC
HLS

**Appendix A2**. **Correlations among parameters involved in GSH metabolism and antioxidant function, oxidative stress and neuroinflammation in thalamus.** The green round dots represent F344 rats (N=31) and red square dots represent HIV-1 Tg rats (N=30).

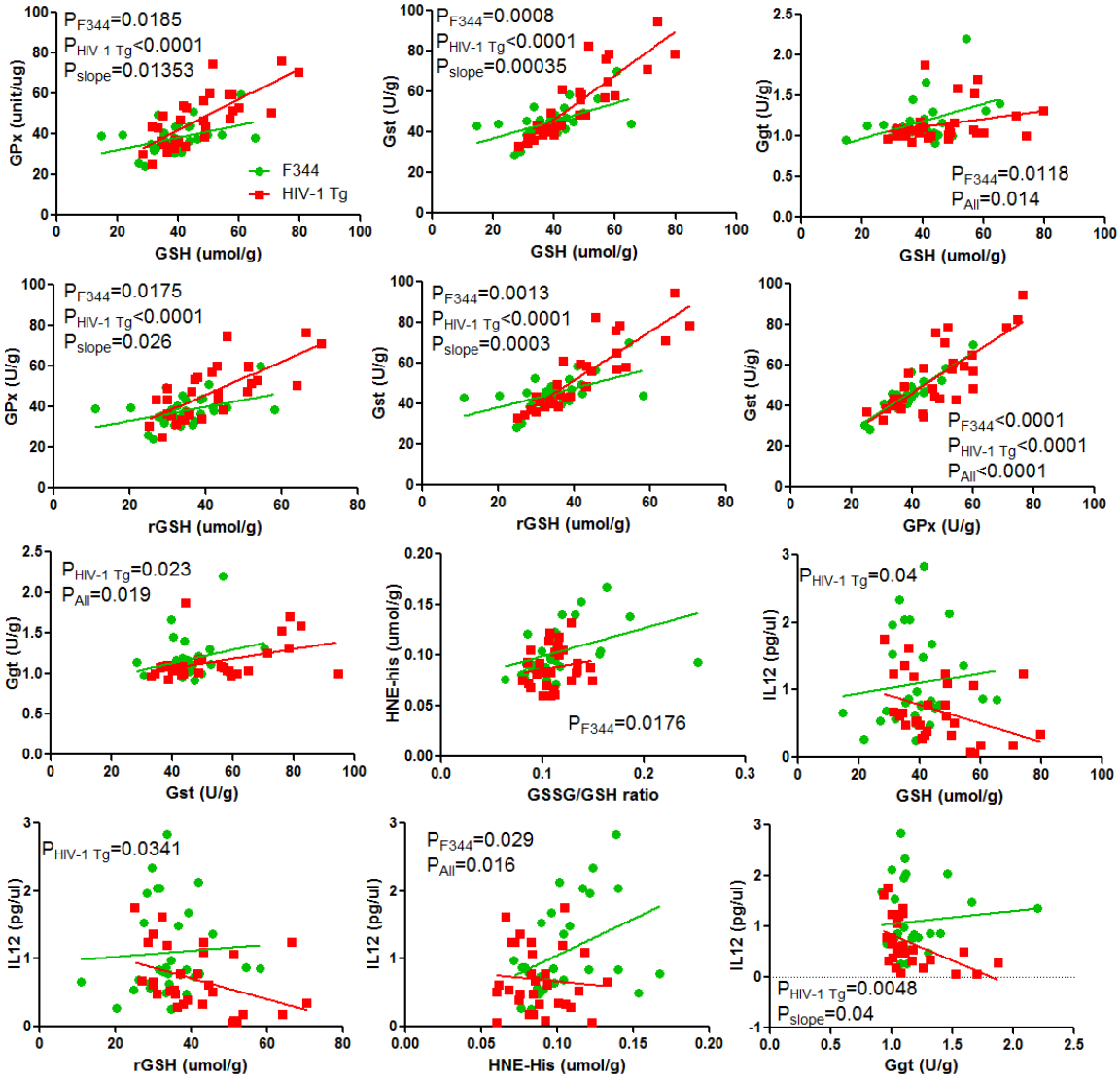

**Appendix A3**. **Glutathione levels in the thalamus of control F344 and HIV-1 Tg rats treated low and high fat diet.** A, B, C, and D are the figures of tGSH, GSSG, rGSH and GSSG/tGSH ratio, respectively. T-test: *, P≤0.05; **, P<0.01; $, P<0.05 compared with rest of groups. Two-way ANOVA: $P_{HIV}$ and $P_{Fat}$. Bonferroni post-hoc: #, P<0.05. F344 HIV-1 Tg

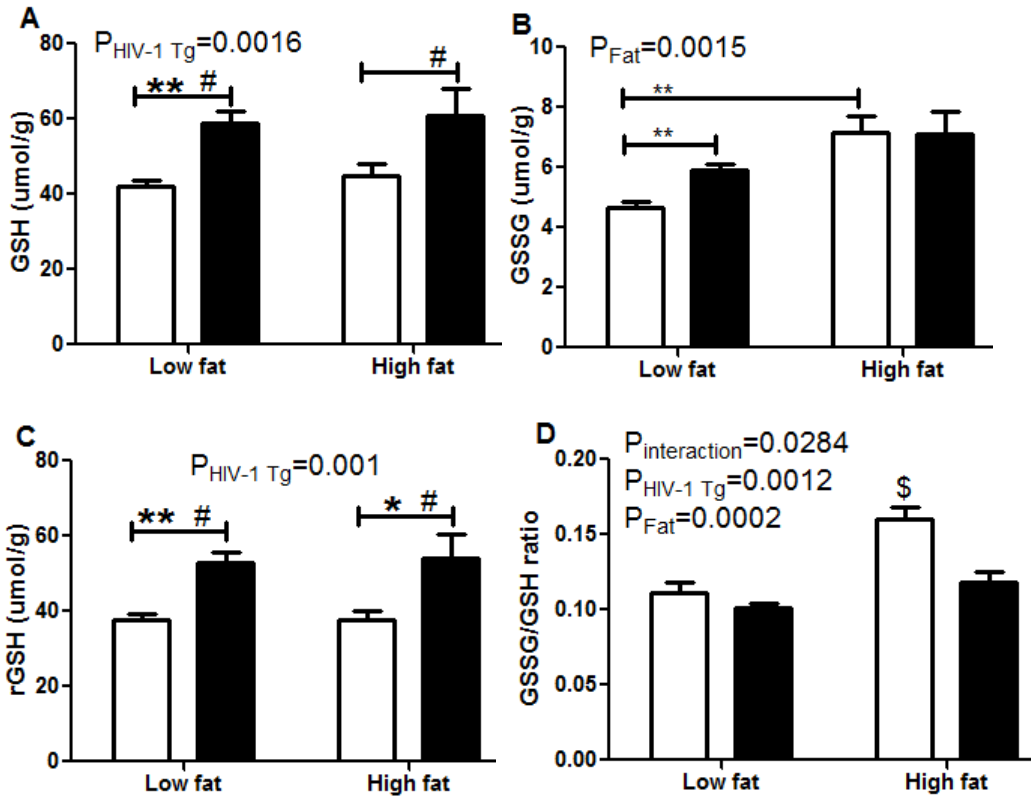

**Appendix A4**. **Activity and expression of GCS and Ggt in the thalamus of control F344 and HIV-1 Tg rats treated low and high fat diet.** A and B, activity of GCS and Ggt; C, protein expression of GCS catalytic heave chain (GCS-HC) and Ggt isoform 7 (Ggt7); D and E, GCS-HC and Ggt7 protein expression normalized against beta-actin; F-I, mRNA levels of GCS and Ggt isoforms. FLC, F344 rats fed low fat; FHC, F344 rats fed high fat; HLC, HIV-1 Tg rats fed low fat; HHC, HIV-1 Tg rats fed high fat. T-test: *, P<0.05; $, P<0.05 compared to rest of groups. Two-way ANOVA: $P_{HIV}$ and $P_{Fat}$. Bonferroni post-hoc: #, P<0.05. F344 HIV-1 Tg

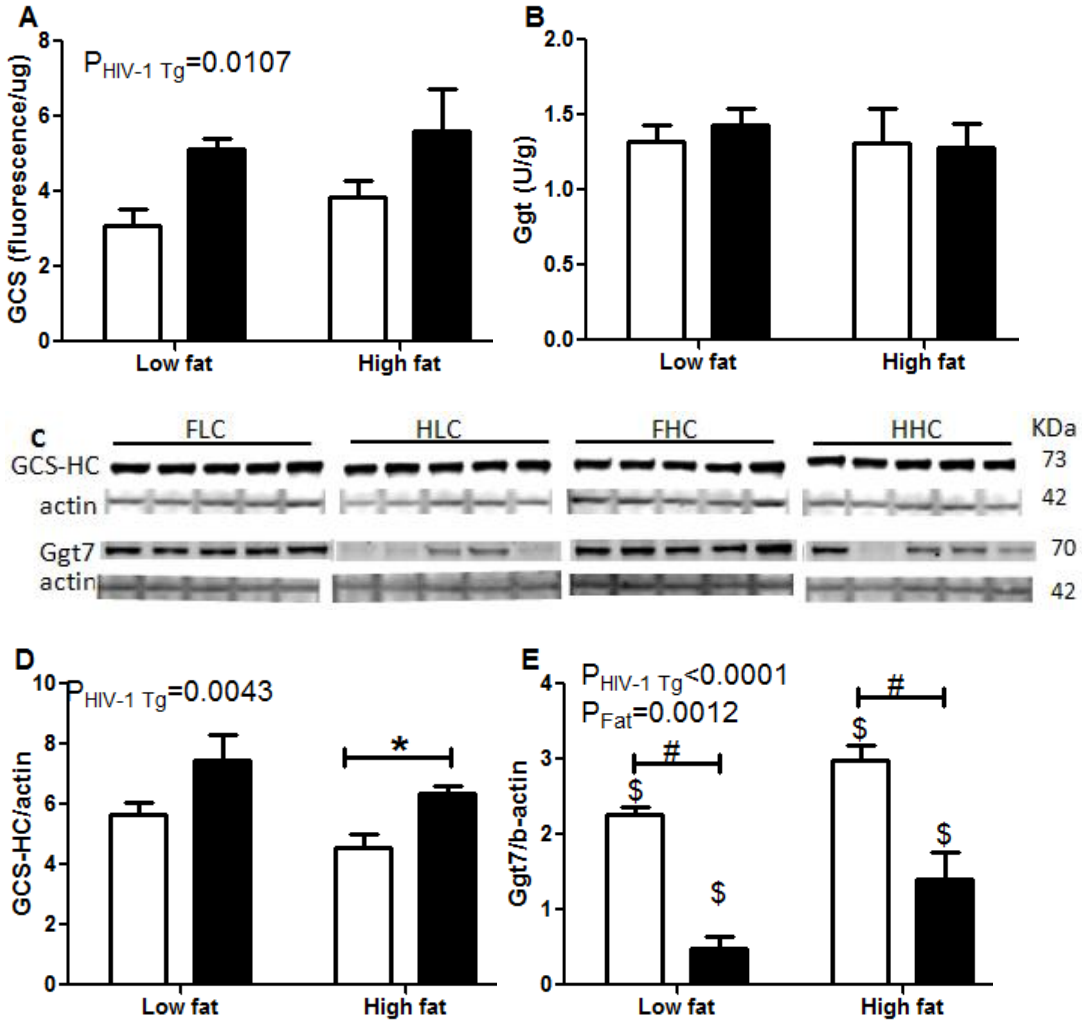

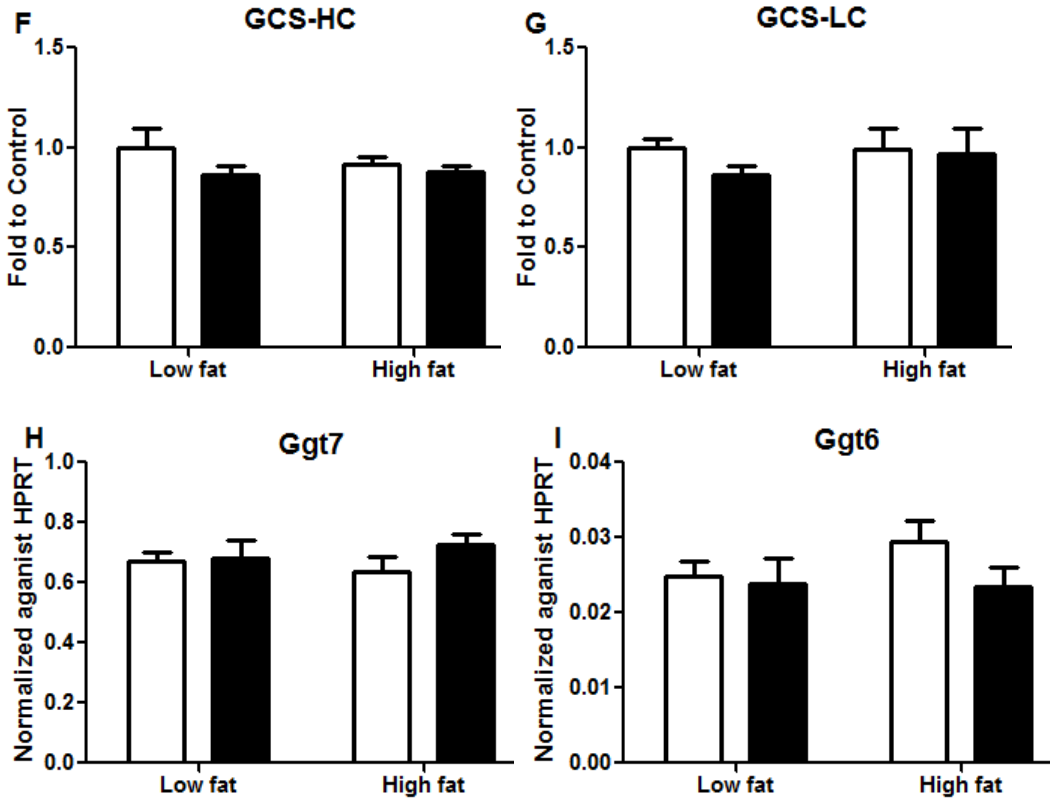
F
GCS-HC
Fold to Control
1.5
1.0
0.5
0.0
Low fat
High fat
G
GCS-LC
Fold to Control
1.5
1.0
0.5
0.0
Low fat
High fat
H
Ggt7
Normalized aganist HPRT
1.0
0.8
0.6
0.4
0.2
0.0
Low fat
High fat
I
Ggt6
Normalized aganist HPRT
0.04
0.03
0.02
0.01
0.00
Low fat
High fat

**Appendix A5. Lipid peroxidation and related antioxidant enzymes in the thalamus of control F344 and HIV-1 Tg rats treated with low and high fat diet.** A, 4-Hydroxynonenal His conjugate (HNE-His) level; B and C, activities of glutathione peroxidase (GPx) and glutathione – S- transferase (Gst); D-F, mRNA levels of GPx and Gst isoforms. T-test: *, P<0.05; **, P<0.01. Two-way ANOVA: $P_{HIV}$. Bonferroni post-hoc: #, P<0.05. F344 HIV-1 Tg

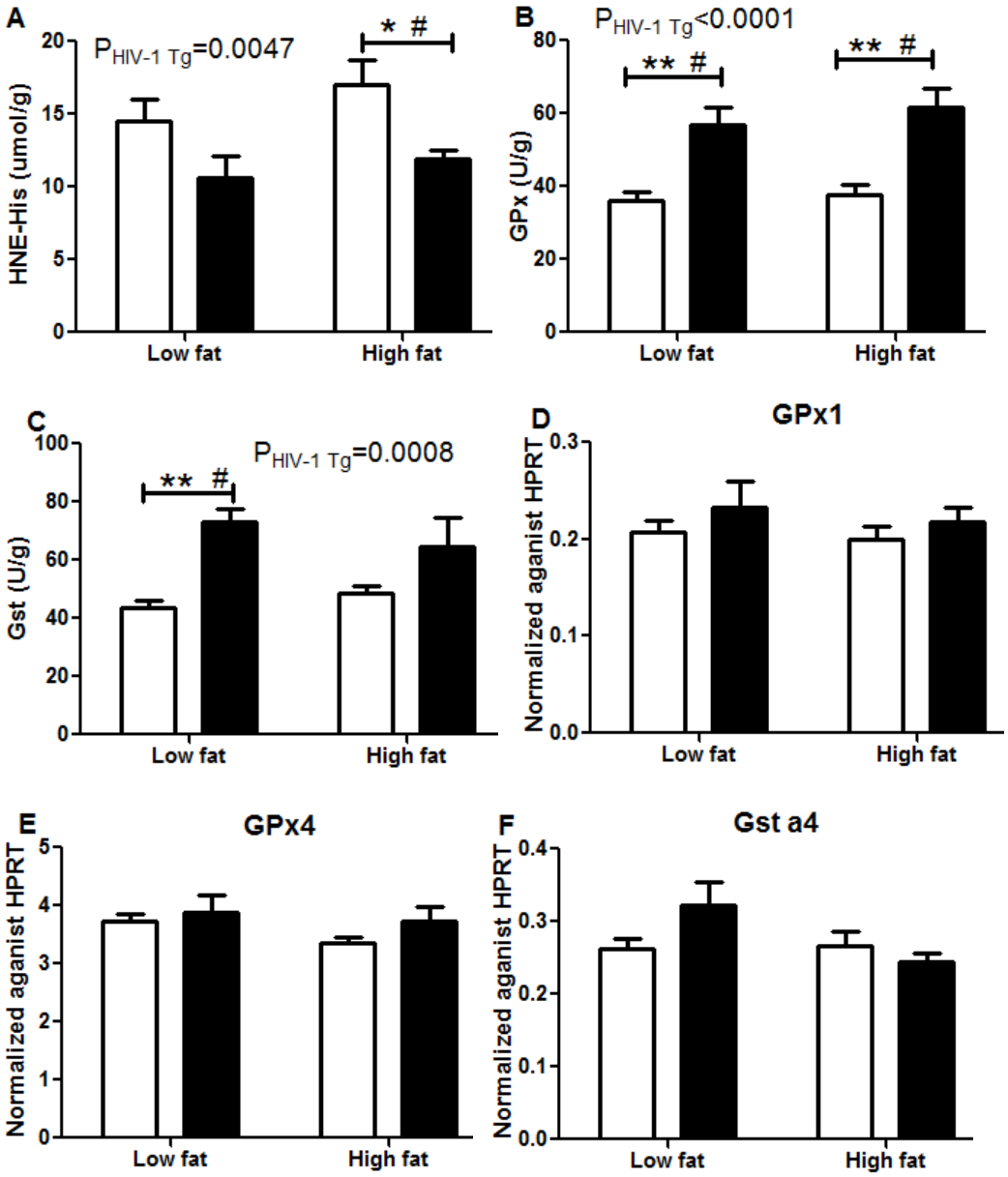


**Appendix A6. Expression of GSH-related transporters in the thalamus of control F344 and HIV-1 Tg rats treated low and high fat diet.** A, Expression of multidrug resistance protein 1 (MRP1) and the expression normalized to beta-actin; B- D, mRNA level of MRP1, system xC catalyze domain (xCT) and excitatory amino acid carrier 1 (EAAC1). FLC, F344 rats fed low fat;

FHC, F344 rats fed high fat; HLC, HIV-1 Tg rats fed low fat; HHC, HIV-1 Tg rats fed high fat. T-test: *, P<0.05; **, P<0.01. Two-way ANOVA: $P_{HIV}$.

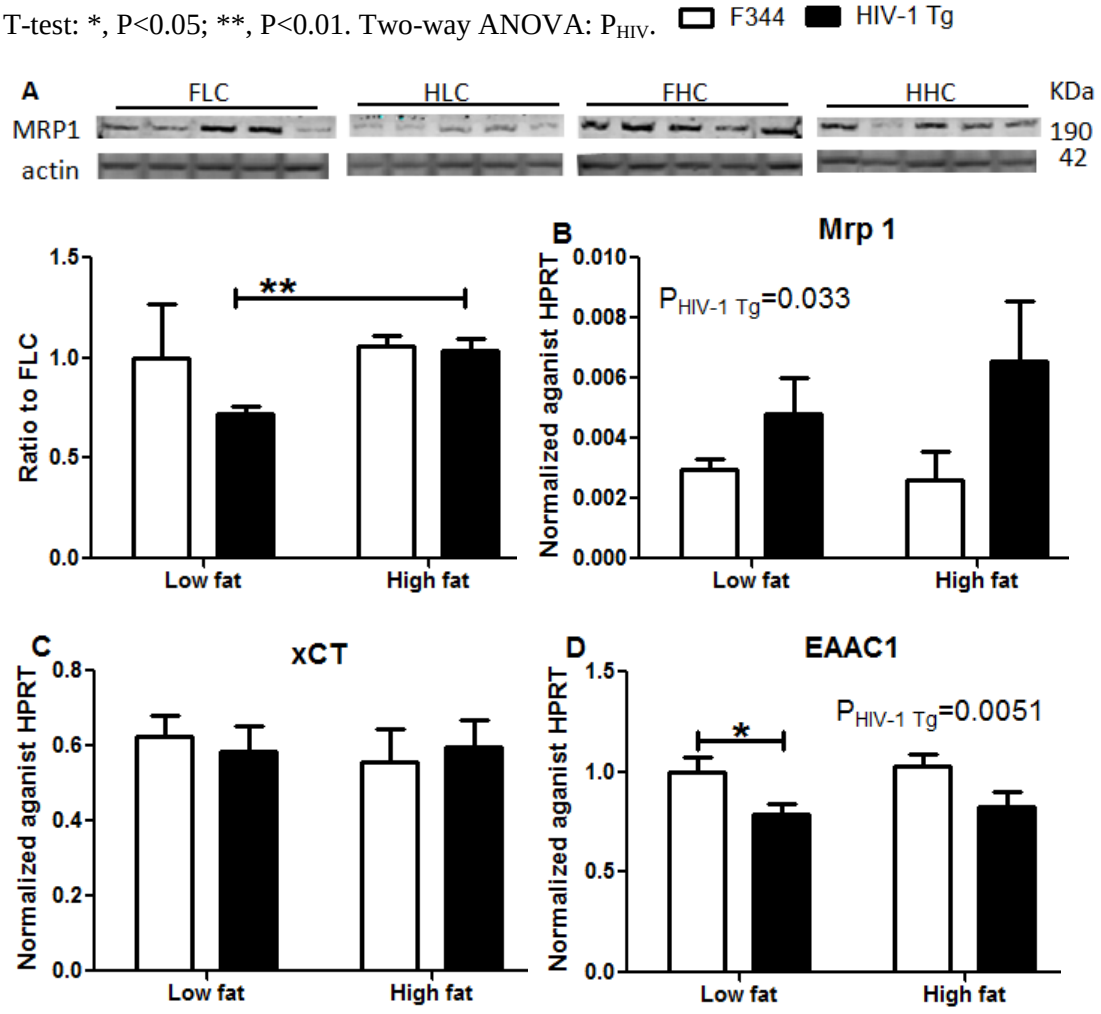

**Appendix A7. Protein expression of neuronal nuclei (NeuN), microtubule-associated protein 2 (MAP2) and glial fibrillary acidic protein (GFAP) in the thalamus of control F344 and HIV-1 Tg rats treated low and high fat diet.** A, Western blot images of MAP2, NeuN, GFAP; B-D, densitometric quantification of protein expression, normalized to beta-actin. FLC, F344 rats fed low fat; FHC, F344 rats fed high fat; HLC, HIV-1 Tg rats fed low fat; HHC, HIV-1 Tg rats fed high fat. T-test: *, P<0.05. Two-way ANOVA: $P_{HIV}$ and $P_{Fat}$. Bonferroni post-hoc: #, P<0.05.

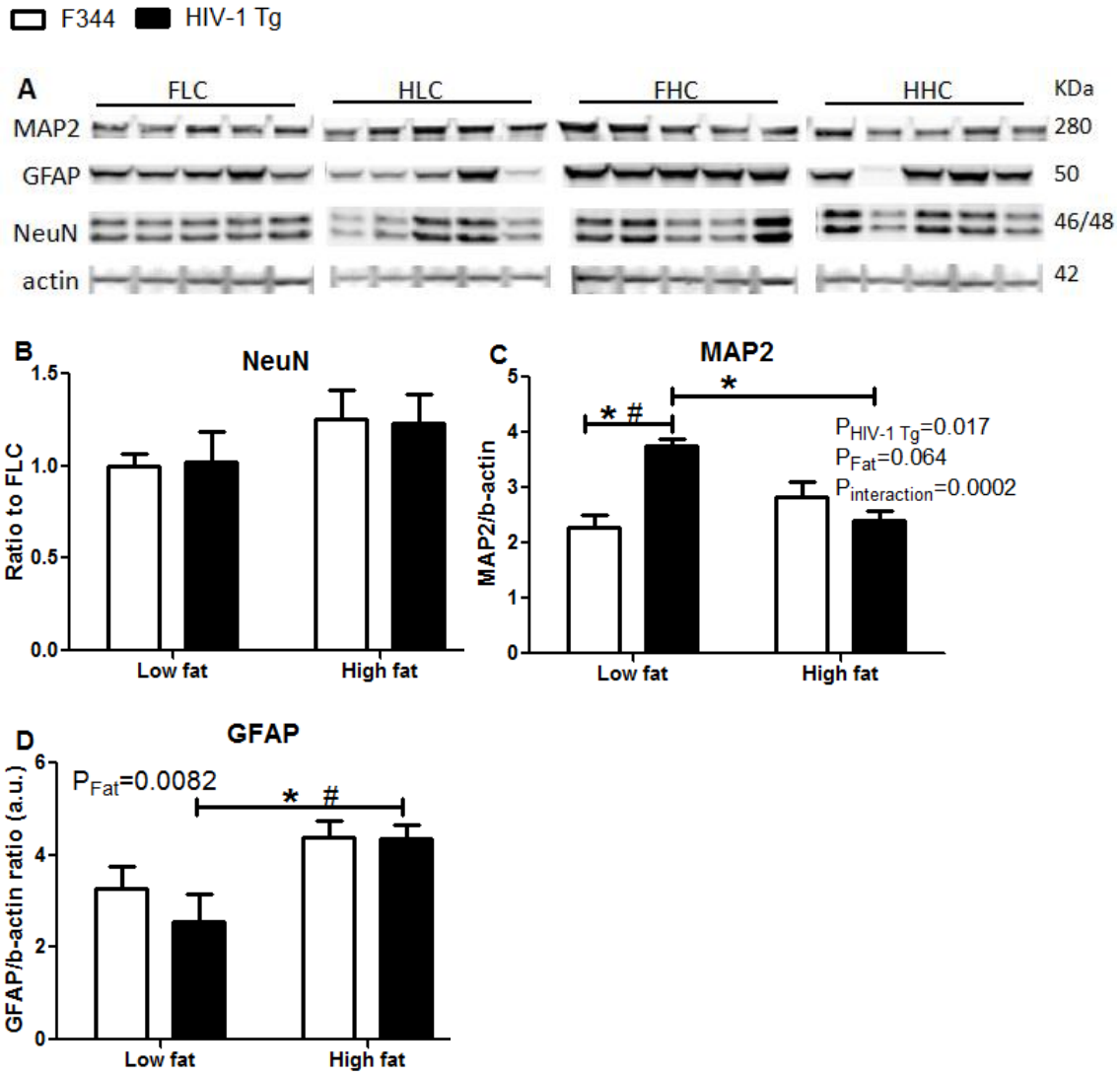

**Appendix A8. Correlations among antioxidants, lipid peroxidation and IL12 in the thalamus of control F344 and HIV-1 Tg rats treated low and high fat diet.**

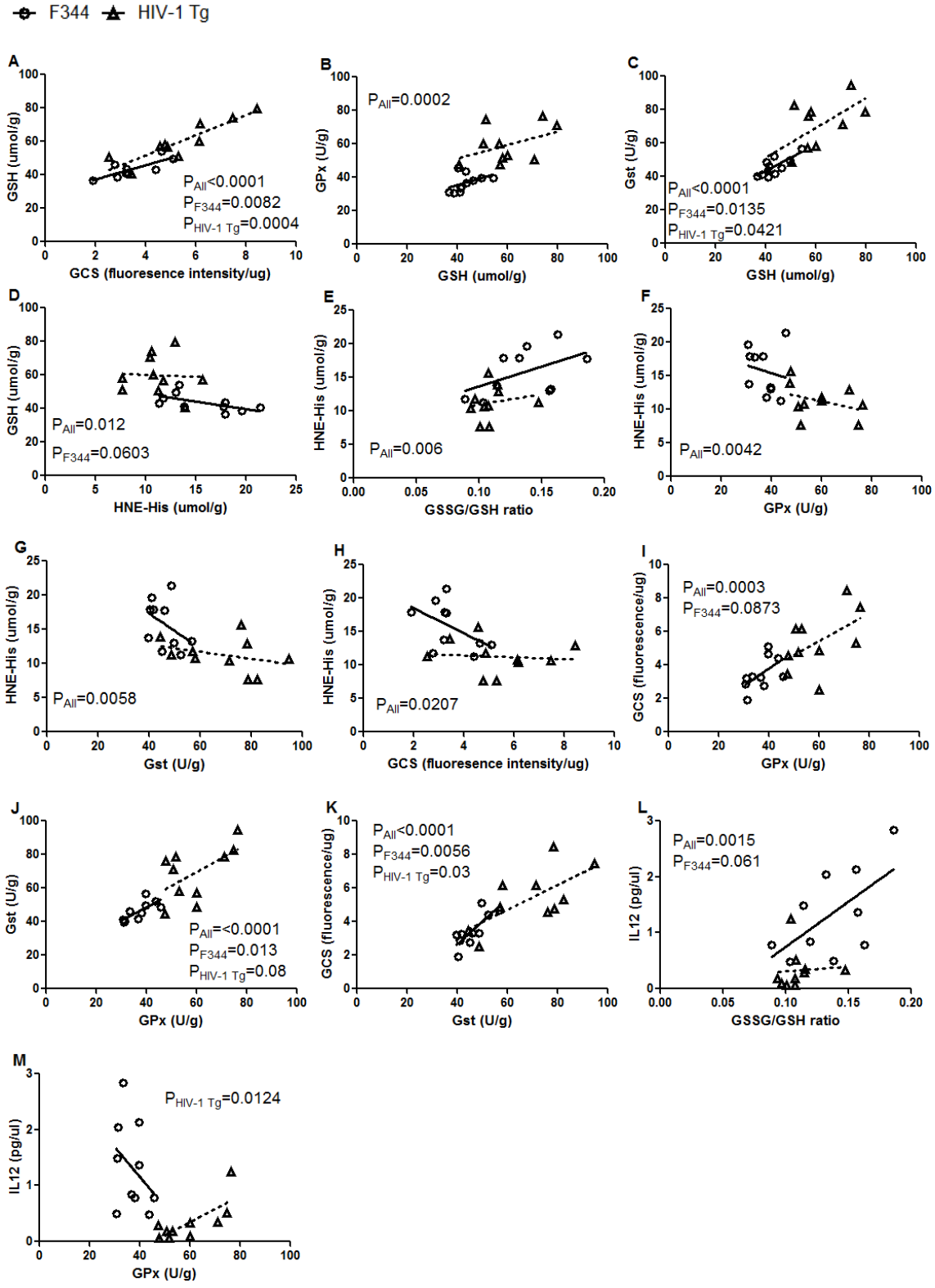

**Appendix B. Levels and correlations of GSH-centered enzymes, neuronal proteins and inflammatory marker IL12 in the hippocampus.**

**Appendix B1. GSH, GSH-centered proteins and IL12 level in the hippocampus.**

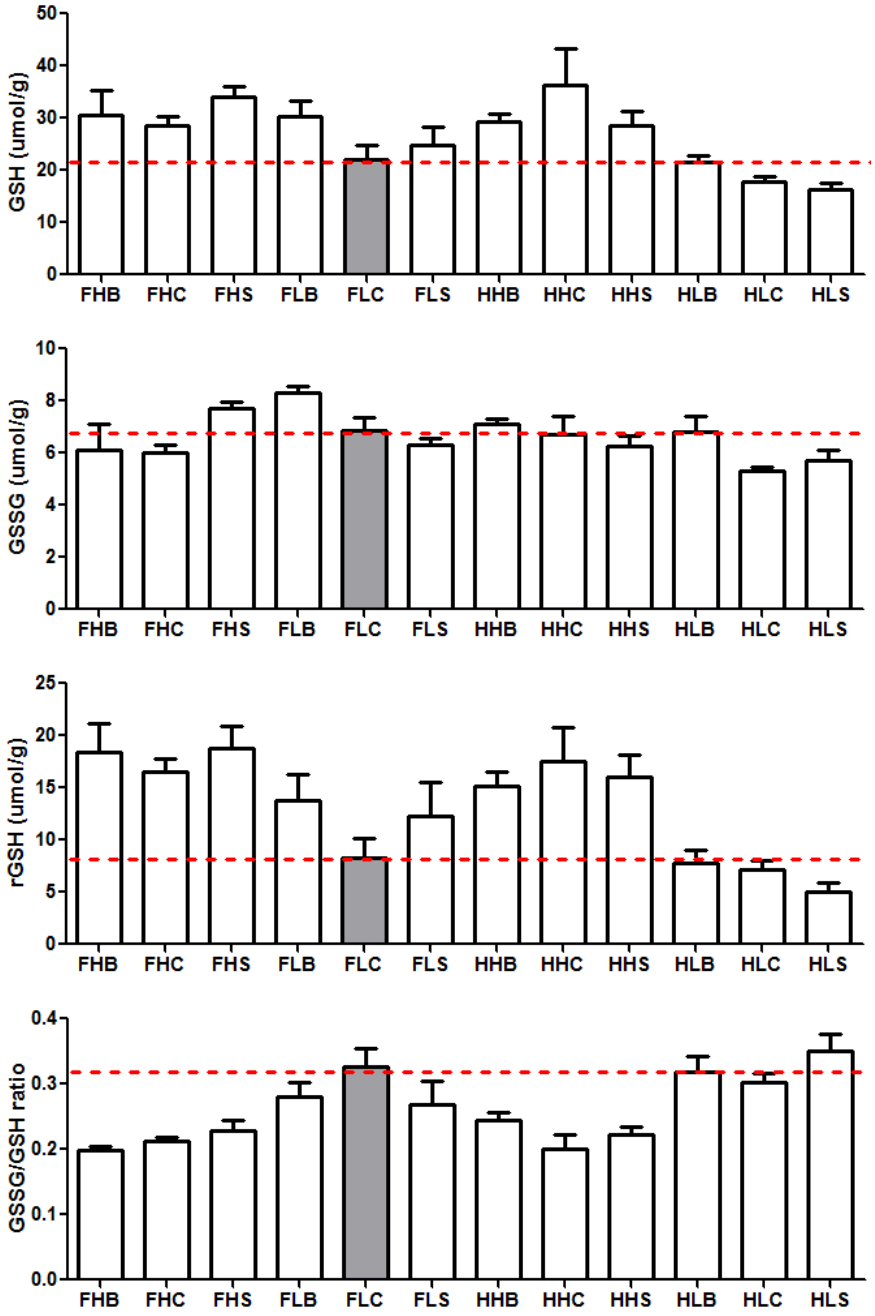

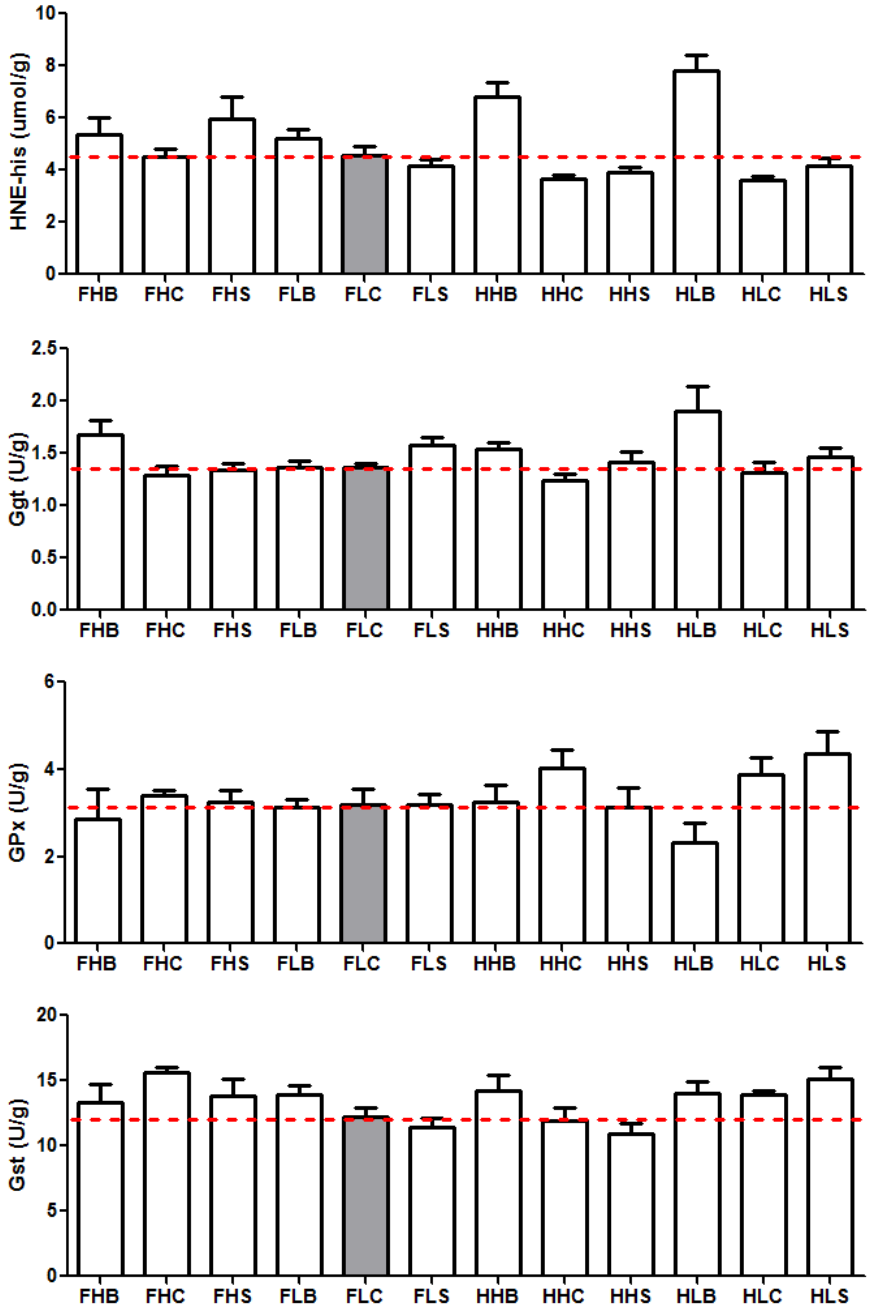
HNE-his (umol/g)
10
8
6
4
2
0
FHB FHC FHS FLB FLC FLS HHB HHC HHS HLB HLC HLS
Ggt (U/g)
2.5
2.0
1.5
1.0
0.5
0.0
FHB FHC FHS FLB FLC FLS HHB HHC HHS HLB HLC HLS
GPx (U/g)
6
4
2
0
FHB FHC FHS FLB FLC FLS HHB HHC HHS HLB HLC HLS
Gst (U/g)
20
15
10
5
0
FHB FHC FHS FLB FLC FLS HHB HHC HHS HLB HLC HLS

**Appendix B2. Status of GSH, GSH-centered enzymes and lipid peroxidation in hippocampus of F344 rats and HIV-1Tg rats fed low or high fat diet**. T-test: *, P<0.05. Two-way ANOVA: $P_{HIV}$ and $P_{Fat}$. Bonferroni post-hoc: #, P<0.05. F344 HIV-1 Tg

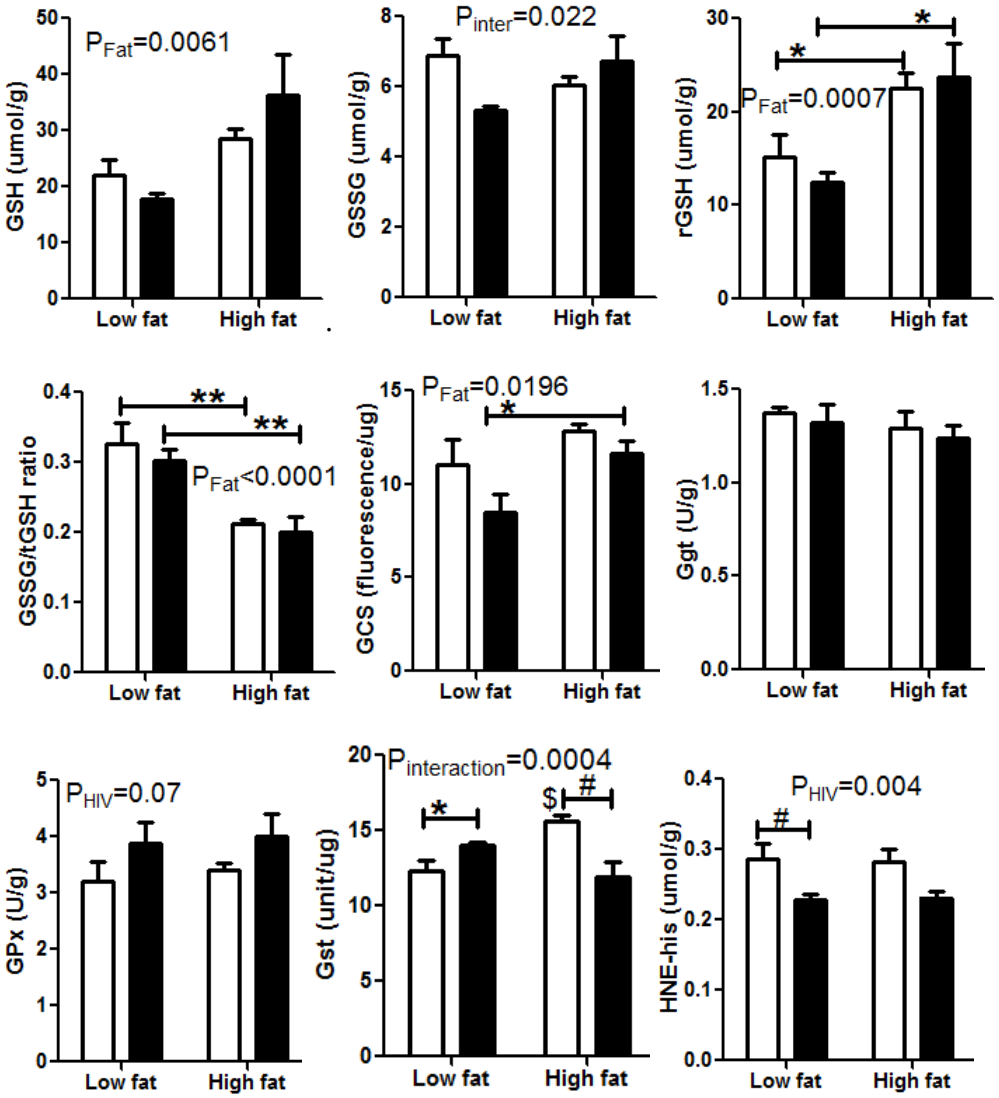

**Appendix B3. Western blot results of GCS-HC, Ggt7, MRP1, GFAP, NeuN, and MAP2 in the hippocampus of F344 rats and HIV-1Tg rats fed low or high fat diet.** FLC, F344 rats fed low fat; FHC, F344 rats fed high fat; HLC, HIV-1 Tg rats fed low fat; HHC, HIV-1 Tg rats fed high fat. T-test: *, P<0.05. Two-way ANOVA: $P_{HIV}$ and $P_{Fat}$. Bonferroni post-hoc: #, P<0.05.

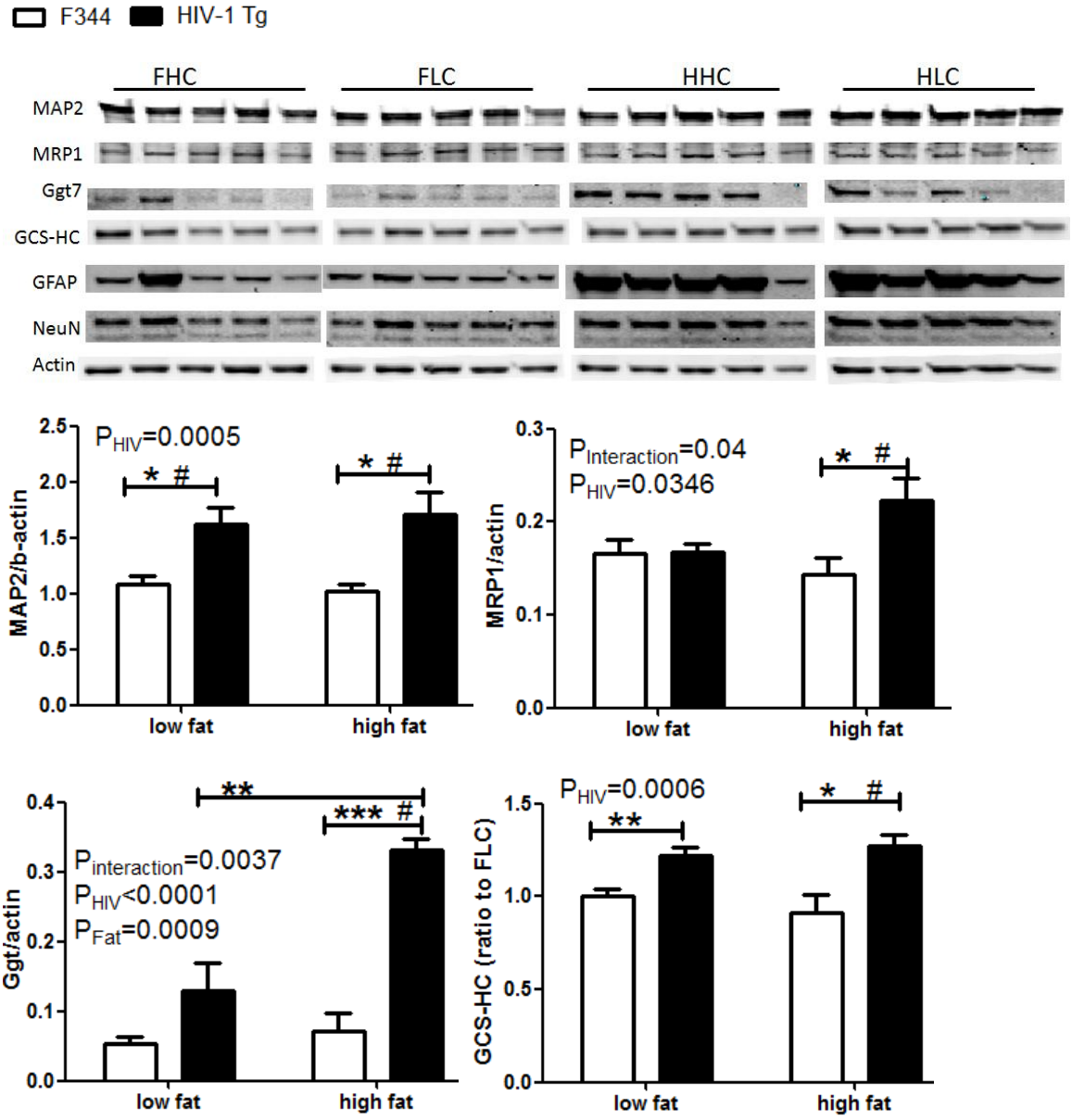

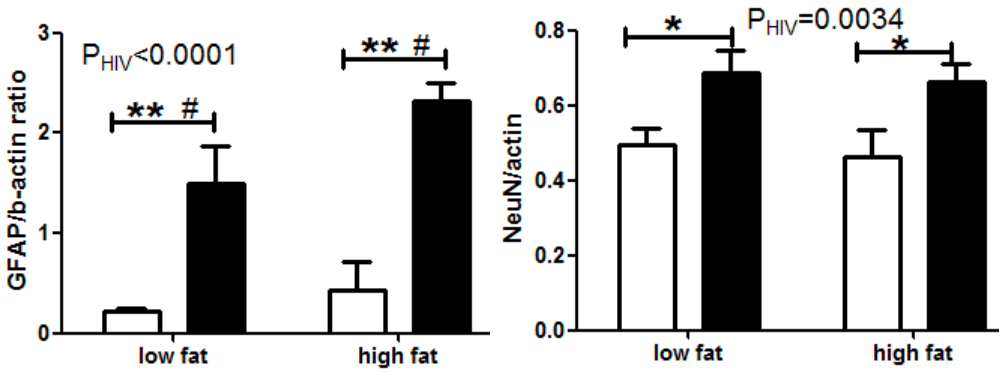
GFAP/b-actin ratio
3
2
1
0
P_HIV<0.0001
** #
** #
low fat
high fat
NeuN/actin
0.8
0.6
0.4
0.2
0.0
*
P_HIV=0.0034
*
low fat
high fat

**Appendix C. Western blot results of GCS-HC, Ggt7, MRP1, GFAP, NeuN, and MAP2 in the frontal cortex of F344 rats and HIV-1Tg rats fed low or high fat diet.** FLC, F344 rats fed low fat; FHC, F344 rats fed high fat; HLC, HIV-1 Tg rats fed low fat; HHC, HIV-1 Tg rats fed high fat. T-test: *, P<0.05. Two-way ANOVA: $P_{HIV}$ and $P_{Fat}$. Bonferroni post-hoc: #, P<0.05.

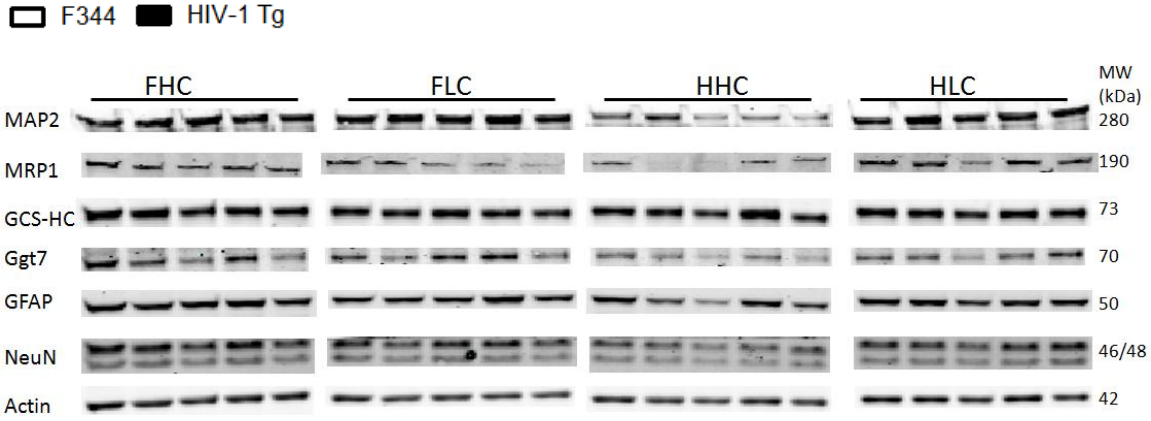


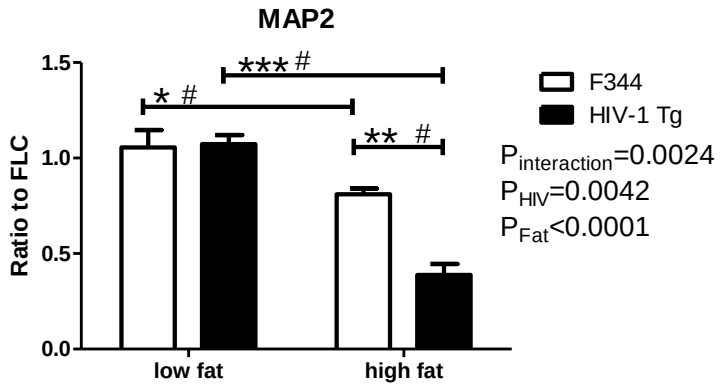


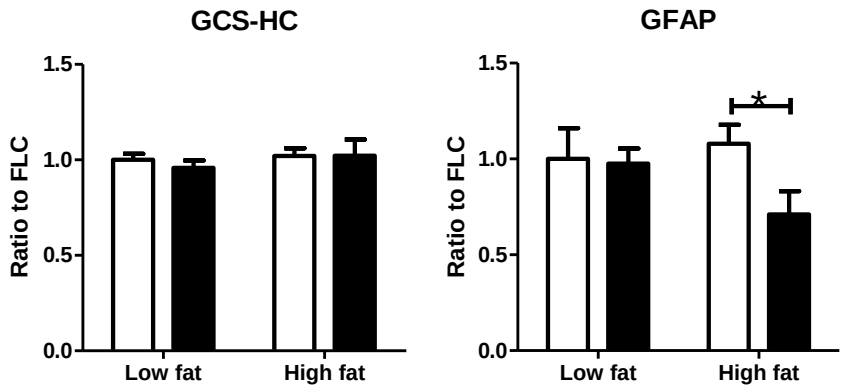

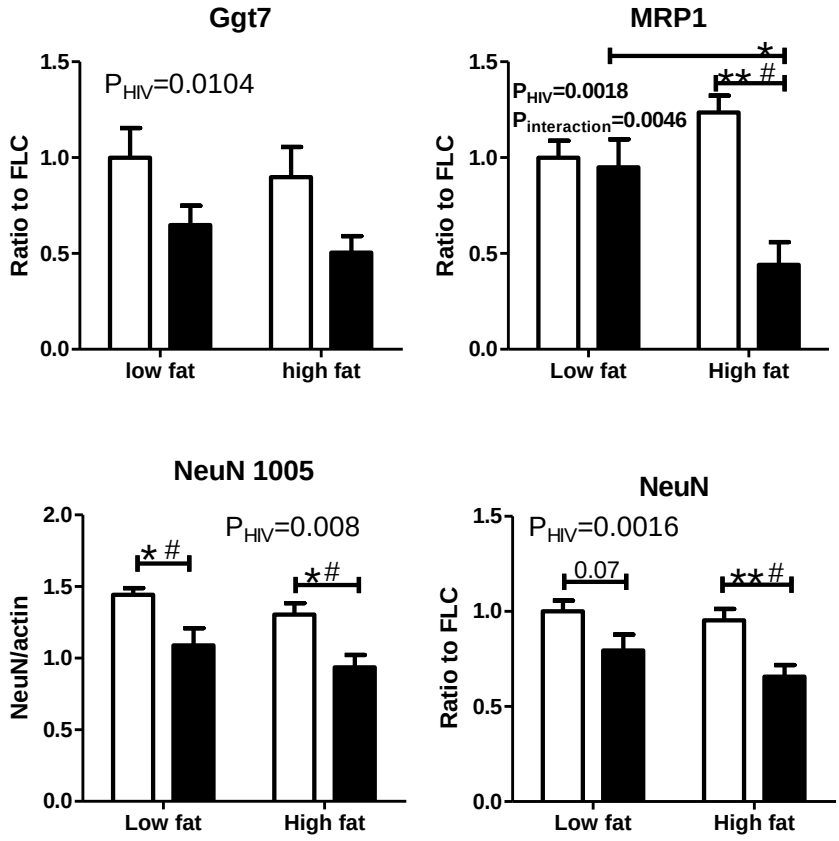
Ggt7
P_HIV=0.0104
Ratio to FLC
1.5
1.0
0.5
0.0
low fat
high fat
MRP1
P_HIV=0.0018
P_interaction=0.0046
*
** #
Ratio to FLC
Low fat
High fat
NeuN 1005
P_HIV=0.008
* #
*#
NeuN/actin
2.0
Low fat
High fat
NeuN
P_HIV=0.0016
0.07
** #
Ratio to FLC
Low fat
High fat

**Appendix D. The endpoint body, organ and fat weights of rats with different dietary treatments.**

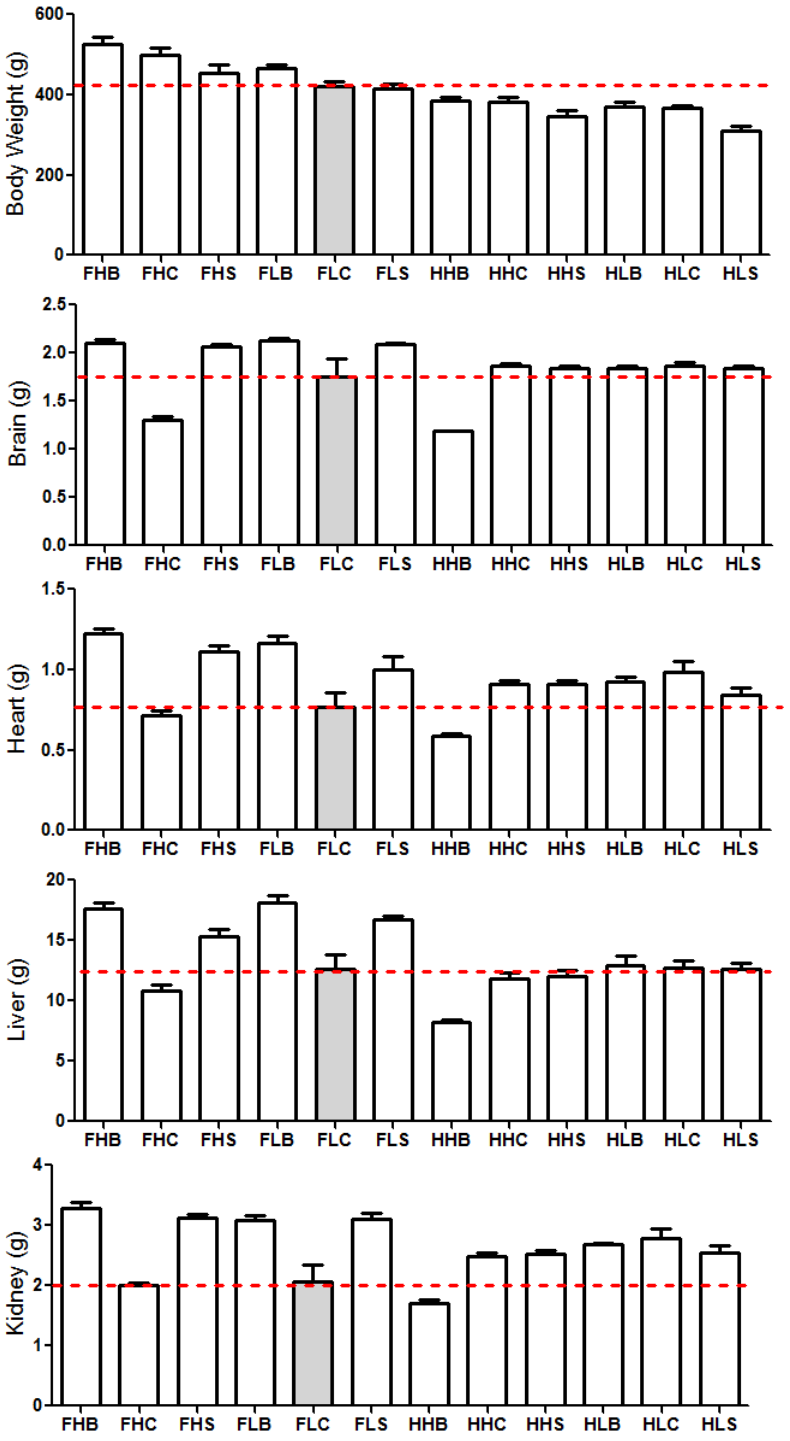

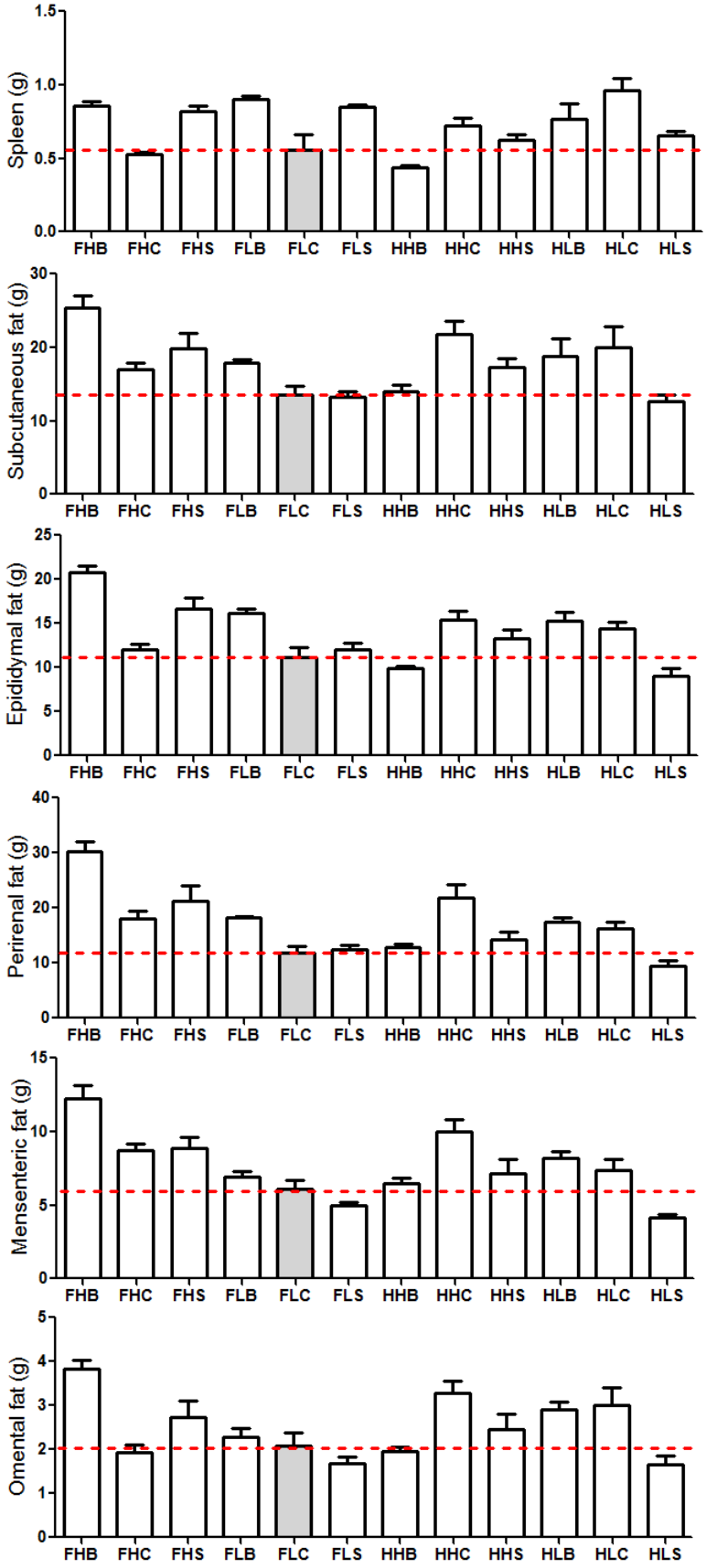
Spleen (g)
1.5
1.0
0.5
0.0
FHB FHC FHS FLB FLC FLS HHB HHC HHS HLB HLC HLS
Subcutaneous fat (g)
30
20
10
0
FHB FHC FHS FLB FLC FLS HHB HHC HHS HLB HLC HLS
Epididymal fat (g)
25
20
15
10
5
0
FHB FHC FHS FLB FLC FLS HHB HHC HHS HLB HLC HLS
Perirenal fat (g)
40
30
20
10
0
FHB FHC FHS FLB FLC FLS HHB HHC HHS HLB HLC HLS
Mensenteric fat (g)
15
10
5
0
FHB FHC FHS FLB FLC FLS HHB HHC HHS HLB HLC HLS
Omental fat (g)
5
4
3
2
1
0
FHB FHC FHS FLB FLC FLS HHB HHC HHS HLB HLC HLS

## References


1. Centers for Disease Control and Prevention C (2013) HIV Mortality (through 2009).
2. NorKin LC (2010) Virology: Molecular Biology and Pathogenesis. Washington, DC: ASM Press. 751 p.
3. Adamson CS (2012) Protease-Mediated Maturation of HIV: Inhibitors of Protease and the Maturation Process. Mol Biol Int 2012: 604261.
4. McArthur JC, Steiner J, Sacktor N, Nath A (2010) Human immunodeficiency virus-associated neurocognitive disorders: Mind the gap. Ann Neurol 67: 699-714.
5. Norkin LC (2010) Virolog: Molecular Biology and pathogenesis. Washington, DC: ASM Press.
6. Kramer-Hammerle S, Rothenaigner I, Wolff H, Bell JE, Brack-Werner R (2005) Cells of the central nervous system as targets and reservoirs of the human immunodeficiency virus. Virus Res 111: 194-213.
7. Kaul M, Garden GA, Lipton SA (2001) Pathways to neuronal injury and apoptosis in HIV-associated dementia. Nature 410: 988-994.
8. Jaeger LB, Nath A (2012) Modeling HIV-associated neurocognitive disorders in mice: new approaches in the changing face of HIV neuropathogenesis. Dis Model Mech 5: 313-322.
9. Thompson KA, McArthur JC, Wesselingh SL (2001) Correlation between neurological progression and astrocyte apoptosis in HIV-associated dementia. Ann Neurol 49: 745-752.
10. Masliah E, Heaton RK, Marcotte TD, Ellis RJ, Wiley CA, et al. (1997) Dendritic injury is a pathological substrate for human immunodeficiency virus-related cognitive disorders. HNRC Group. The HIV Neurobehavioral Research Center. Ann Neurol 42: 963-972.
11. Antinori A, Arendt G, Becker JT, Brew BJ, Byrd DA, et al. (2007) Updated research nosology for HIV-associated neurocognitive disorders. Neurology 69: 1789-1799.
12. Boisse L, Gill MJ, Power C (2008) HIV infection of the central nervous system: clinical features and neuropathogenesis. Neurol Clin 26: 799-819, x.
13. Berger JR, Kumar M, Kumar A, Fernandez JB, Levin B (1994) Cerebrospinal fluid dopamine in HIV-1 infection. AIDS 8: 67-71.
14. Asare E, Dunn G, Glass J, McArthur J, Luthert P, et al. (1996) Neuronal pattern correlates with the severity of human immunodeficiency virus-associated dementia complex. Usefulness of spatial pattern analysis in clinicopathological studies. Am J Pathol 148: 31-38.
15. Glass JD, Johnson RT (1996) Human immunodeficiency virus and the brain. Annu Rev Neurosci 19: 1-26.
16. Kure K, Llena JF, Lyman WD, Soeiro R, Weidenheim KM, et al. (1991) Human immunodeficiency virus-1 infection of the nervous system: an autopsy study of 268 adult, pediatric, and fetal brains. Hum Pathol 22: 700-710.
17. Brew BJ, Rosenblum M, Cronin K, Price RW (1995) AIDS dementia complex and HIV-1 brain infection: clinical-virological correlations. Ann Neurol 38: 563-570.
18. Yadav A, Collman RG (2009) CNS inflammation and macrophage/microglial biology associated with HIV-1 infection. J Neuroimmune Pharmacol 4: 430-447.
19. Wynn HE, Brundage RC, Fletcher CV (2002) Clinical implications of CNS penetration of antiretroviral drugs. CNS Drugs 16: 595-609.

20. Croteau D, Best BM, Letendre S, Rossi SS, Ellis RJ, et al. (2012) Lower than expected maraviroc concentrations in cerebrospinal fluid exceed the wild-type CC chemokine receptor 5-tropic HIV-1 50% inhibitory concentration. AIDS 26: 890-893.
21. Best BM, Letendre SL, Koopmans P, Rossi SS, Clifford DB, et al. (2012) Low cerebrospinal fluid concentrations of the nucleotide HIV reverse transcriptase inhibitor, tenofovir. J Acquir Immune Defic Syndr 59: 376-381.
22. Lanier ER, Sturge G, McClernon D, Brown S, Halman M, et al. (2001) HIV-1 reverse transcriptase sequence in plasma and cerebrospinal fluid of patients with AIDS dementia complex treated with Abacavir. AIDS 15: 747-751.
23. Tozzi V, Balestra P, Bellagamba R, Corpolongo A, Salvatori MF, et al. (2007) Persistence of neuropsychologic deficits despite long-term highly active antiretroviral therapy in patients with HIV-related neurocognitive impairment: prevalence and risk factors. J Acquir Immune Defic Syndr 45: 174-182.
24. Goodkin KS, Paul Verma, Ashok (2009) The Spectrum of Neuro-AIDS Disorders : Pathophysiology, Diagnosis, and Treatment: ASM Press 568 p.
25. Harezlak J, Buchthal S, Taylor M, Schifitto G, Zhong J, et al. (2011) Persistence of HIV-associated cognitive impairment, inflammation, and neuronal injury in era of highly active antiretroviral treatment. AIDS 25: 625-633.
26. Riddle DR (2007) Brain Aging: Models, Methods, and Mechanisms; Riddle DR, editor.
27. Kruman, II, Nath A, Mattson MP (1998) HIV-1 protein Tat induces apoptosis of hippocampal neurons by a mechanism involving caspase activation, calcium overload, and oxidative stress. Exp Neurol 154: 276-288.
28. Mattson MP, Haughey NJ, Nath A (2005) Cell death in HIV dementia. Cell Death Differ 12 Suppl 1: 893-904.
29. Castagna A, Le Grazie C, Accordini A, Giulidori P, Cavalli G, et al. (1995) Cerebrospinal fluid S-adenosylmethionine (SAMe) and glutathione concentrations in HIV infection: effect of parenteral treatment with SAMe. Neurology 45: 1678-1683.
30. Velazquez I, Plaud M, Wojna V, Skolasky R, Laspiur JP, et al. (2009) Antioxidant enzyme dysfunction in monocytes and CSF of Hispanic women with HIV-associated cognitive impairment. Journal of neuroimmunology 206: 106-111.
31. Everall IP, Hudson L, Kerwin RW (1997) Decreased absolute levels of ascorbic acid and unaltered vasoactive intestinal polypeptide receptor binding in the frontal cortex in acquired immunodeficiency syndrome. Neurosci Lett 224: 119-122.
32. Bandaru VV, McArthur JC, Sacktor N, Cutler RG, Knapp EL, et al. (2007) Associative and predictive biomarkers of dementia in HIV-1-infected patients. Neurology 68: 1481-1487.
33. Sacktor N, Haughey N, Cutler R, Tamara A, Turchan J, et al. (2004) Novel markers of oxidative stress in actively progressive HIV dementia. J Neuroimmunol 157: 176-184.
34. Turchan J, Pocernich CB, Gairola C, Chauhan A, Schifitto G, et al. (2003) Oxidative stress in HIV demented patients and protection ex vivo with novel antioxidants. Neurology 60: 307-314.
35. Tang H, Lu D, Pan R, Qin X, Xiong H, et al. (2009) Curcumin improves spatial memory impairment induced by human immunodeficiency virus type 1 glycoprotein 120 V3 loop peptide in rats. Life Sci 85: 1-10.
36. Desrosiers RC, Daniel MD, Li Y (1989) HIV-related lentiviruses of nonhuman primates. AIDS Res Hum Retroviruses 5: 465-473.
37. Hatziioannou T, Evans DT (2012) Animal models for HIV/AIDS research. Nat Rev Microbiol 10: 852-867.

38. Gorantla S, Poluektova L, Gendelman HE (2012) Rodent models for HIV-associated neurocognitive disorders. Trends Neurosci 35: 197-208.
39. Poluektova L, Gorantla S, Faraci J, Birusingh K, Dou H, et al. (2004) Neuroregulatory events follow adaptive immune-mediated elimination of HIV-1-infected macrophages: studies in a murine model of viral encephalitis. J Immunol 172: 7610-7617.
40. Reid W, Sadowska M, Denaro F, Rao S, Foulke J, Jr., et al. (2001) An HIV-1 transgenic rat that develops HIV-related pathology and immunologic dysfunction. Proc Natl Acad Sci U S A 98: 9271-9276.
41. Basselin M, Ramadan E, Igarashi M, Chang L, Chen M, et al. (2011) Imaging upregulated brain arachidonic acid metabolism in HIV-1 transgenic rats. J Cereb Blood Flow Metab 31: 486-493.
42. Vikulina T, Fan X, Yamaguchi M, Roser-Page S, Zayzafoon M, et al. (2010) Alterations in the immuno-skeletal interface drive bone destruction in HIV-1 transgenic rats. Proc Natl Acad Sci U S A 107: 13848-13853.
43. Kass MD, Liu X, Vigorito M, Chang L, Chang SL (2010) Methamphetamine-induced behavioral and physiological effects in adolescent and adult HIV-1 transgenic rats. J Neuroimmune Pharmacol 5: 566-573.
44. Hag AM, Kristoffersen US, Pedersen SF, Gutte H, Lebech AM, et al. (2009) Regional gene expression of LOX-1, VCAM-1, and ICAM-1 in aorta of HIV-1 transgenic rats. PLoS One 4: e8170.
45. Vigorito M, LaShomb AL, Chang SL (2007) Spatial learning and memory in HIV-1 transgenic rats. J Neuroimmune Pharmacol 2: 319-328.
46. Bruce Alberts AJ, Julian Lewis, Martin Raff, Keith Roberts, and Peter Walter (2002) Molecular Biology of the Cell, 4th edition. New York: Garland Science.
47. Meister A (1983) Selective modification of glutathione metabolism. Science 220: 472-477.
48. Griffith OW (1999) Biologic and pharmacologic regulation of mammalian glutathione synthesis. Free Radic Biol Med 27: 922–935.
49. Lewerenz J, Maher P, Methner A (2012) Regulation of xCT expression and system x (c) (-) function in neuronal cells. Amino Acids 42: 171-179.
50. Bannai S, Tateishi N (1986) Role of membrane transport in metabolism and function of glutathione in mammals. J Membr Biol 89: 1-8.
51. Liu RM, Gao L, Choi J, Forman HJ (1998) gamma-glutamylcysteine synthetase: mRNA stabilization and independent subunit transcription by 4-hydroxy-2-nonenal. Am J Physiol 275: L861-869.
52. Iles KE, Liu RM (2005) Mechanisms of glutamate cysteine ligase (GCL) induction by 4-hydroxynonenal. Free Radic Biol Med 38: 547-556.
53. Franklin CC, Backos DS, Mohar I, White CC, Forman HJ, et al. (2009) Structure, function, and post-translational regulation of the catalytic and modifier subunits of glutamate cysteine ligase. Mol Aspects Med 30: 86-98.
54. Dickinson DA, Forman HJ (2002) Glutathione in defense and signaling: lessons from a small thiol. Ann N Y Acad Sci 973: 488-504.
55. Drozdz R, Parmentier C, Hachad H, Leroy P, Siest G, et al. (1998) gamma-Glutamyltransferase dependent generation of reactive oxygen species from a glutathione/transferrin system. Free Radic Biol Med 25: 786-792.
56. Zhang H, Forman HJ, Choi J (2005) Gamma-glutamyl transpeptidase in glutathione biosynthesis. Methods Enzymol 401: 468-483.

57. Zhang H, Dickinson DA, Liu RM, Forman HJ (2005) 4-Hydroxynonenal increases gamma-glutamyl transpeptidase gene expression through mitogen-activated protein kinase pathways. Free Radic Biol Med 38: 463-471.
58. Zhang H, Forman HJ (2009) Redox regulation of gamma-glutamyl transpeptidase. Am J Respir Cell Mol Biol 41: 509-515.
59. Dubinina EE, Dadali VA (2010) Role of 4-hydroxy-trans-2-nonenal in cell functions. Biochemistry (Mosc) 75: 1069-1087.
60. Dringen R, Pfeiffer B, Hamprecht B (1999) Synthesis of the antioxidant glutathione in neurons: supply by astrocytes of CysGly as precursor for neuronal glutathione. J Neurosci 19: 562-569.
61. Rice ME, Russo-Menna I (1998) Differential compartmentalization of brain ascorbate and glutathione between neurons and glia. Neuroscience 82: 1213-1223.
62. Yamaguchi T, Takei N, Araki K, Ishii K, Nagano T, et al. (2000) Molecular characterization of a novel gamma-glutamyl transpeptidase homologue found in rat brain. J Biochem 128: 101-106.
63. Dallas S, Miller DS, Bendayan R (2006) Multidrug resistance-associated proteins: expression and function in the central nervous system. Pharmacol Rev 58: 140-161.
64. Aoyama K, Watabe M, Nakaki T (2008) Regulation of neuronal glutathione synthesis. J Pharmacol Sci 108: 227-238.
65. Kranich O, Hamprecht B, Dringen R (1996) Different preferences in the utilization of amino acids for glutathione synthesis in cultured neurons and astroglial cells derived from rat brain. Neurosci Lett 219: 211-214.
66. Eck HP, Gmunder H, Hartmann M, Petzoldt D, Daniel V, et al. (1989) Low concentrations of acid-soluble thiol (cysteine) in the blood plasma of HIV-1-infected patients. Biol Chem Hoppe Seyler 370: 101-108.
67. Buhl R, Jaffe HA, Holroyd KJ, Wells FB, Mastrangeli A, et al. (1989) Systemic glutathione deficiency in symptom-free HIV-seropositive individuals. Lancet 2: 1294-1298.
68. Staal FJ, Roederer M, Israelski DM, Bubp J, Mole LA, et al. (1992) Intracellular glutathione levels in T cell subsets decrease in HIV-infected individuals. AIDS Res Hum Retroviruses 8: 305-311.
69. Price TO, Uras F, Banks WA, Ercal N (2006) A novel antioxidant N-acetylcysteine amide prevents gp120- and Tat-induced oxidative stress in brain endothelial cells. Exp Neurol 201: 193-202.
70. Brooke SM, McLaughlin JR, Cortopassi KM, Sapolsky RM (2002) Effect of GP120 on glutathione peroxidase activity in cortical cultures and the interaction with steroid hormones. J Neurochem 81: 277-284.
71. Price TO, Ercal N, Nakaoke R, Banks WA (2005) HIV-1 viral proteins gp120 and Tat induce oxidative stress in brain endothelial cells. Brain Res 1045: 57-63.
72. Sulzer D, Sonders MS, Poulsen NW, Galli A (2005) Mechanisms of neurotransmitter release by amphetamines: a review. Prog Neurobiol 75: 406-433.
73. (2005) The NSDUH report: methamphetamine use, abuse, and dependence: 2002, 2003, and 2004. Substance Abuse and Mental Health Services Administration, Office of Applied Studies.
74. Abuse NIoD (2006) What is the scope of methamphetamine abuse in the United States?
75. SAMHSA (2012) Results from the 2011, National Survey on Drug Use and Health: Summary of National Findings
76. Centers for Disease Control and Prevention C (2011) Diagnoses of HIV Infection in the United States and Dependent Areas, 2011. Atlanta.

77. Strathdee SA, Galai N, Safaiean M, Celentano DD, Vlahov D, et al. (2001) Sex differences in risk factors for HIV seroconversion among injection drug users: a 10-year perspective. Arch Intern Med 161: 1281–1288.
78. Wood E, Kerr T, Spittal PM, Li K, Small W, et al. (2003) The potential public health and community impacts of safer injecting facilities: evidence from a cohort of injection drug users. J Acquir Immune Defic Syndr 32: 2–8.
79. Des Jarlais DC, Marmor M, Paone D, Titus S, Shi Q, et al. (1996) HIV incidence among injecting drug users in New York City syringe-exchange programmes. Lancet 348: 987–991.
80. Wood E, Tyndall MW, Spittal PM, Li K, Kerr T, et al. (2001) Unsafe injection practices in a cohort of injection drug users in Vancouver: could safer injecting rooms help? CMAJ 165: 405–410.
81. Nemoto T, Operario D, Soma T (2002) Risk behaviors of Filipino methamphetamine users in San Francisco: implications for prevention and treatment of drug use and HIV. Public Health Rep 117: S30–S38.
82. Farabee D, Prendergast M, Cartier J (2002) Methamphetamine use and HIV risk among substance-abusing offenders in California. J Psychoactive Drugs 34: 295–300.
83. Gibson DR, Leamon MH, Flynn N (2002) Epidemiology and public health consequences of methamphetamine use in California's Central Valley. J Psychoactive Drugs 34: 313–319.
84. Semple SJ, Patterson TL, Grant I (2002) Motivations associated with methamphetamine use among HIV+ men who have sex with men. Journal of Substance Abuse Treatment 22: 149–156.
85. Marshall JF, O'Dell SJ (2012) Methamphetamine influences on brain and behavior: unsafe at any speed? Trends Neurosci 35: 536-545.
86. Yamamoto BK, Raudensky J (2008) The role of oxidative stress, metabolic compromise, and inflammation in neuronal injury produced by amphetamine-related drugs of abuse. J Neuroimmune Pharmacol 3: 203-217.
87. Imam SZ, el-Yazal J, Newport GD, Itzhak Y, Cadet JL, et al. (2001) Methamphetamine-induced dopaminergic neurotoxicity: role of peroxynitrite and neuroprotective role of antioxidants and peroxynitrite decomposition catalysts. Ann N Y Acad Sci 939: 366-380.
88. Wilson JM, Kalasinsky KS, Levey AI, Bergeron C, Reiber G, et al. (1996) Striatal dopamine nerve terminal markers in human, chronic methamphetamine users. Nat Med 2: 699-703.
89. Sulzer D, Pothos E, Sung HM, Maidment NT, Hoebel BG, et al. (1992) Weak base model of amphetamine action. Ann N Y Acad Sci 654: 525-528.
90. Sulzer D, Rayport S (1990) Amphetamine and other psychostimulants reduce pH gradients in midbrain dopaminergic neurons and chromaffin granules: a mechanism of action. Neuron 5: 797-808.
91. Sulzer D, Chen TK, Lau YY, Kristensen H, Rayport S, et al. (1995) Amphetamine redistributes dopamine from synaptic vesicles to the cytosol and promotes reverse transport. J Neurosci 15: 4102-4108.
92. Graham DG (1978) Oxidative pathways for catecholamines in the genesis of neuromelanin and cytotoxic quinones. Mol Pharmacol 14: 633-643.
93. LaVoie MJ, Hastings TG (1999) Dopamine quinone formation and protein modification associated with the striatal neurotoxicity of methamphetamine: evidence against a role for extracellular dopamine. J Neurosci 19: 1484-1491.

94. Graham DG, Tiffany SM, Bell WR, Gutknecht WF (1978) Autoxidation versus covalent binding of quinones as the mechanism of toxicity of dopamine, 6-hydroxydopamine, and related compounds toward C1300 neuroblastoma cells in vitro. Mol Pharmacol 14: 644-653.
95. Spina MB, Cohen G (1989) Dopamine turnover and glutathione oxidation: implications for Parkinson disease. Proc Natl Acad Sci U S A 86: 1398-1400.
96. Olanow CF (1992) An introduction to the free radical hypothesis in Parkinson's disease. Ann Neurol 32: S2-S9.
97. Nash JF, Yamamoto BK (1992) Methamphetamine neurotoxicity and striatal glutamate release: Comparison to 3,4-methylenedioxymethamphetamine. Brain Res 581: 237-243.
98. Dawson TM, Dawson VL, Snyder SH (1992) A novel neuronal messenger molecule in the brain: The free radical, nitric oxide. Annals Neurol 32: 297-311.
99. Bolaños JP, Almeida A, Stewart V, Peuchen S, Land JM, et al. (1997) Nitric oxide-mediated mitochondrial damage in the brain: mechanisms and implications for neurodegenerative diseases. J Neurochem 68: 2227-2240.
100. Moncada S, Bolaños JP (2006) Nitric oxide, cell bioenergetics and neurodegeneration. J Neurochem 97: 1676-1689.
101. Brown JM, Quinton MS, Yamamoto BK (2005) Methamphetamine-induced inhibition of mitochondrial complex II : roles of glutamate and peroxynitrite. Journal of neurochemistr 95: 429-436.
102. Brown JM, Yamamoto BK (2003) Effects of amphetamines on mitochondrial function: role of free radicals and oxidative stress. Pharmacol Ther 99: 45-53.
103. Cubells JF, Rayport S, Rajendran G, Sulzer D (1994) Methamphetamine neurotoxicity involves vacuolation of endocytic organelles and dopamine-dependent intracellular oxidative stress. J Neurosci 14: 2260-2271.
104. Larsen KE, Fon EA, Hastings TG, Edwards RH, Sulzer D (2002) Methamphetamine-induced degeneration of dopaminergic neurons involves autophagy and upregulation of dopamine synthesis. J Neurosci 22: 8951-8960.
105. Yamamoto BK, Zhu W (1998) The effects of methamphetamine on the production of free radicals and oxidative stress. J Pharmacol Exp Ther 287: 107-114.
106. Flora G, Lee YW, Nath A, Maragos W, Hennig B, et al. (2002) Methamphetamine-induced TNF-alpha gene expression and activation of AP-1 in discrete regions of mouse brain: potential role of reactive oxygen intermediates and lipid peroxidation. Neuromolecular Med 2: 71-85.
107. Acikgoz O, Gonenc S, Kayatekin BM, Uysal N, Pekcetin C, et al. (1998) Methamphetamine causes lipid peroxidation and an increase in superoxide dismutase activity in the rat striatum. Brain Res 813: 200-202.
108. Harold C, Wallace T, Friedman R, Gudelsky G, Yamamoto B (2000) Methamphetamine selectively alters brain glutathione. Eur J Pharmacol 400: 99-102.
109. Aguirre N, Barrionuevo M, Ramírez MJ, Del Río J, Lasheras B (1999) Alpha-lipoic acid prevents 3,4-methylenedioxy-methamphetamine (MDMA)-induced neurotoxicity. Neuroreport 10: 3675-3680.
110. Ali SF, Imam SZ, Itzhak Y (2005) Role of peroxynitrite in methamphetamine-induced dopaminergic neurodegeneration and neuroprotection by antioxidants and selective NOS inhibitors. Ann N Y Acad Sci 1053: 97-98.
111. Hashimoto K, Tsukada H, Nishiyama S, Fukumoto D, Kakiuchi T, et al. (2004) Effects of N-acetyl-L-cysteine on the reduction of brain dopamine transporters in monkey treated with methamphetamine. Ann N Y Acad Sci 1025: 231-235.

112. Imam SZ, Ali SF (2000) Selenium, an antioxidant, attenuates methamphetamine-induced dopaminergic toxicity and peroxynitrite generation. Brain Res 855: 186-191.
113. Virmani A, Gaetani F, Imam S, Binienda Z, Ali S (2003) Possible mechanism for the neuroprotective effects of L-carnitine on methamphetamine-evoked neurotoxicity. Ann N Y Acad Sci 993: 197-207.
114. Bell JE, Brettle RP, Chiswick A, Simmonds P (1998) HIV encephalitis, proviral load and dementia in drug users and homosexuals with AIDS. Effect of neocortical involvement. Brain 121: 2043–2052.
115. Bouwman FH, Skolasky RL, Hes D, Selnes OA, Glass JD, et al. (1998) Variable progression of HIV-associated dementia. Neurology 50: 1814-1820.
116. Nath A, Maragos WF, Avison MJ, Schmitt FA, Berger JR (2001) Acceleration of HIV dementia with methamphetamine and cocaine. J Neurovirol 7: 66–71.
117. Toussi SS, Joseph A, Zheng JH, Dutta M, Santambrogio L, et al. (2009) Short communication: Methamphetamine treatment increases in vitro and in vivo HIV replication. AIDS Res Hum Retroviruses 25: 1117-1121.
118. Krasnova IN, Cadet JL (2009) Methamphetamine toxicity and messengers of death. Brain Res Rev 60: 379-407.
119. Theodore S, Cass WA, Nath A, Maragos WF (2007) Progress in understanding basal ganglia dysfunction as a common target for methamphetamine abuse and HIV-1 neurodegeneration. Curr HIV Res 5: 301-313.
120. Chang L, Ernst T, Speck O, Grob CS (2005) Additive effects of HIV and chronic methamphetamine use on brain metabolite abnormalities. Am J Psychiatry 162: 361-369.
121. Langford D, Adame A, Grigorian A, Grant I, McCutchan JA, et al. (2003) Patterns of selective neuronal damage in methamphetamine-user AIDS patients. J Acquir Immune Defic Syndr 34: 467-474.
122. Cass WA, Harned ME, Peters LE, Nath A, Maragos WF (2003) HIV-1 protein Tat potentiation of methamphetamine-induced decreases in evoked overflow of dopamine in the striatum of the rat. Brain Res 984: 133-142.
123. Maragos WF, Young KL, Turchan JT, Guseva M, Pauly JR, et al. (2002) Human immunodeficiency virus-1 Tat protein and methamphetamine interact synergistically to impair striatal dopaminergic function. J Neurochem 83: 955-963.
124. Langford D, Grigorian A, Hurford R, Adame A, Crews L, et al. (2004) The role of mitochondrial alterations in the combined toxic effects of human immunodeficiency virus Tat protein and methamphetamine on calbindin positive-neurons. J Neurovirol 10: 327-337.
125. Gavrilin MA, Mathes LE, Podell M (2002) Methamphetamine enhances cell-associated feline immunodeficiency virus replication in astrocytes. J Neurovirol 8: 240-249.
126. Phillips TR, Billaud JN, Henriksen SJ (2000) Methamphetamine and HIV-1: potential interactions and the use of the FIV/cat model. J Psychopharmacol 14: 244-250.
127. Nahin RL, Barnes PM, Stussman BJ, Bloom B (2009) Costs of complementary and alternative medicine (CAM) and frequency of visits to CAM practitioners: United States, 2007. Natl Health Stat Report: 1-14.
128. Debas HT, Laxminarayan R, Straus SE (2006) Complementary and Alternative Medicine. In: Jamison DT, Breman JG, Measham AR, Alleyne G, Claeson M et al., editors. Disease Control Priorities in Developing Countries. 2nd ed. Washington (DC).
129. Little SJ, Holte S, Routy JP, Daar ES, Markowitz M, et al. (2002) Antiretroviral-drug resistance among patients recently infected with HIV. N Engl J Med 347: 385-394.

130. Metzner KJ, Rauch P, Walter H, Boesecke C, Zollner B, et al. (2005) Detection of minor populations of drug-resistant HIV-1 in acute seroconverters. AIDS 19: 1819-1825.
131. Toni T, Masquelier B, Minga A, Anglaret X, Danel C, et al. (2007) HIV-1 antiretroviral drug resistance in recently infected patients in Abidjan, Cote d'Ivoire: A 4-year survey, 2002-2006. AIDS Res Hum Retroviruses 23: 1155-1160.
132. Melchior JC, Niyongabo T, Henzel D, Durack-Bown I, Henri SC, et al. (1999) Malnutrition and wasting, immunodepression, and chronic inflammation as independent predictors of survival in HIV-infected patients. Nutrition 15: 865-869.
133. Hori K, Hatfield D, Maldarelli F, Lee BJ, Clouse KA (1997) Selenium supplementation suppresses tumor necrosis factor alpha-induced human immunodeficiency virus type 1 replication in vitro. AIDS Res Hum Retroviruses 13: 1325-1332.
134. Wiysonge CS, Shey M, Kongnyuy EJ, Sterne JA, Brocklehurst P (2011) Vitamin A supplementation for reducing the risk of mother-to-child transmission of HIV infection. Cochrane Database Syst Rev: CD003648.
135. Allard JP, Aghdassi E, Chau J, Tam C, Kovacs CM, et al. (1998) Effects of vitamin E and C supplementation on oxidative stress and viral load in HIV-infected subjects. AIDS 12: 1653-1659.
136. Lee DY, Lin X, Paskaleva EE, Liu Y, Puttamadappa SS, et al. (2009) Palmitic Acid Is a Novel CD4 Fusion Inhibitor That Blocks HIV Entry and Infection. AIDS Res Hum Retroviruses 25: 1231-1241.
137. Olszewski A, Sato K, Aron ZD, Cohen F, Harris A, et al. (2004) Guanidine alkaloid analogs as inhibitors of HIV-1 Nef interactions with p53, actin, and p56lck. Proc Natl Acad Sci U S A 101: 14079-14084.
138. Nath S, Bachani M, Harshavardhana D, Steiner JP (2012) Catechins protect neurons against mitochondrial toxins and HIV proteins via activation of the BDNF pathway. J Neurovirol 18: 445-455.
139. Heaton RK, Clifford DB, Franklin DR, Jr., Woods SP, Ake C, et al. (2010) HIV-associated neurocognitive disorders persist in the era of potent antiretroviral therapy: CHARTER Study. Neurology 75: 2087-2096.
140. Wu CW, Ping YH, Yen JC, Chang CY, Wang SF, et al. (2007) Enhanced oxidative stress and aberrant mitochondrial biogenesis in human neuroblastoma SH-SY5Y cells during methamphetamine induced apoptosis. Toxicol Appl Pharmacol 220: 243-251.
141. Zhang X, Banerjee A, Banks WA, Ercal N (2009) N-Acetylcysteine amide protects against methamphetamine-induced oxidative stress and neurotoxicity in immortalized human brain endothelial cells. Brain Res 1275: 87-95.
142. Banerjee A, Zhang X, Manda KR, Banks WA, Ercal N (2010) HIV proteins (gp120 and Tat) and methamphetamine in oxidative stress-induced damage in the brain: potential role of the thiol antioxidant N-acetylcysteine amide. Free Radic Biol Med 48: 1388-1398.
143. Aukrust P, Muller F, Svardal AM, Ueland T, Berge RK, et al. (2003) Disturbed glutathione metabolism and decreased antioxidant levels in human immunodeficiency virus-infected patients during highly active antiretroviral therapy--potential immunomodulatory effects of antioxidants. J Infect Dis 188: 232-238.
144. Awodele O, Olayemi SO, Nwite JA, Adeyemo TA (2012) Investigation of the levels of oxidative stress parameters in HIV and HIV-TB co-infected patients. J Infect Dev Ctries 6: 79-85.
145. de la Asuncion JG, del Olmo ML, Sastre J, Millan A, Pellin A, et al. (1998) AZT treatment induces molecular and ultrastructural oxidative damage to muscle mitochondria. Prevention by antioxidant vitamins. J Clin Invest 102: 4-9.

146. Manda KR, Banerjee A, Banks WA, Ercal N (2011) Highly active antiretroviral therapy drug combination induces oxidative stress and mitochondrial dysfunction in immortalized human blood-brain barrier endothelial cells. Free Radic Biol Med 50: 801-810.
147. Brandmann M, Tulpule K, Schmidt MM, Dringen R (2012) The antiretroviral protease inhibitors indinavir and nelfinavir stimulate Mrp1-mediated GSH export from cultured brain astrocytes. J Neurochem 120: 78-92.
148. Tietze F (1970) Disulfide reduction in rat liver. I. Evidence for the presence of nonspecific nucleotide-dependent disulfide reductase and GSH-disulfide transhydrogenase activities in the high-speed supernatant fraction. Arch Biochem Biophys 138: 177-188.
149. Meister A, Tate SS, Griffith OW (1981) Gamma-glutamyl transpeptidase. Methods Enzymol 77: 237-253.
150. Panee J, Stoytcheva ZR, Liu W, Berry MJ (2007) Selenoprotein H is a redox-sensing high mobility group family DNA-binding protein that up-regulates genes involved in glutathione synthesis and phase II detoxification. J Biol Chem 282: 23759-23765.
151. Meister A (1973) On the enzymology of amino acid transport. Science 180: 33-39.
152. Lieberman MW, Wiseman AL, Shi ZZ, Carter BZ, Barrios R, et al. (1996) Growth retardation and cysteine deficiency in gamma-glutamyl transpeptidase-deficient mice. Proc Natl Acad Sci U S A 93: 7923-7926.
153. Niemela O, Alatalo P (2010) Biomarkers of alcohol consumption and related liver disease. Scand J Clin Lab Invest 70: 305-312.
154. Mason JE, Starke RD, Van Kirk JE (2010) Gamma-glutamyl transferase: a novel cardiovascular risk biomarker. Prev Cardiol 13: 36-41.
155. Corti A, Franzini M, Paolicchi A, Pompella A (2010) Gamma-glutamyltransferase of cancer cells at the crossroads of tumor progression, drug resistance and drug targeting. Anticancer Res 30: 1169-1181.
156. Targher G (2010) Elevated serum gamma-glutamyltransferase activity is associated with increased risk of mortality, incident type 2 diabetes, cardiovascular events, chronic kidney disease and cancer - a narrative review. Clin Chem Lab Med 48: 147-157.
157. Yavuz BB, Yavuz B, Halil M, Cankurtaran M, Ulger Z, et al. (2008) Serum elevated gamma glutamyltransferase levels may be a marker for oxidative stress in Alzheimer's disease. Int Psychogeriatr 20: 815-823.
158. Nand N, Sharma M, Saini DS, Khosla SN (1992) Gamma glutamyl transpeptidase in meningitis. J Assoc Physicians India 40: 167-169.
159. VayÃƒ A, De la Fuente J, Montero M, Perez R, Ricart J (2012) Erythrocyte deformability in naÃ¯ve HIV-infected patients. Clinical hemorheology and microcirculation 51: 235-241.
160. Li H, Zheng YH, Shen Z, Liu M, Liu C, et al. (2007) [Evaluation for two-year highly active antiretroviral therapy in Chinese HIV-1 infection patients]. Zhonghua Yi Xue Za Zhi 87: 2973-2976.
161. Almond LM, Boffito M, Hoggard PG, Bonora S, Raiteri R, et al. (2004) The relationship between nevirapine plasma concentrations and abnormal liver function tests. AIDS Res Hum Retroviruses 20: 716-722.
162. Jean JC, Liu Y, Joyce-Brady M (2003) The importance of gamma-glutamyl transferase in lung glutathione homeostasis and antioxidant defense. Biofactors 17: 161-173.
163. Jean JC, Liu Y, Brown LA, Marc RE, Klings E, et al. (2002) Gamma-glutamyl transferase deficiency results in lung oxidant stress in normoxia. Am J Physiol Lung Cell Mol Physiol 283: L766-776.

164. Zhang H, Liu H, Dickinson DA, Liu RM, Postlethwait EM, et al. (2006) gamma-Glutamyl transpeptidase is induced by 4-hydroxynonenal via EpRE/Nrf2 signaling in rat epithelial type II cells. Free Radic Biol Med 40: 1281-1292.
165. Helbling B, von Overbeck J, Lauterburg BH (1996) Decreased release of glutathione into the systemic circulation of patients with HIV infection. Eur J Clin Invest 26: 38-44.
166. Ronaldson PT, Bendayan R (2008) HIV-1 viral envelope glycoprotein gp120 produces oxidative stress and regulates the functional expression of multidrug resistance protein-1 (Mrp1) in glial cells. J Neurochem 106: 1298-1313.
167. Gross A, Hack V, Stahl-Hennig C, Droge W (1996) Elevated hepatic gamma-glutamylcysteine synthetase activity and abnormal sulfate levels in liver and muscle tissue may explain abnormal cysteine and glutathione levels in SIV-infected rhesus macaques. AIDS Res Hum Retroviruses 12: 1639-1641.
168. Choi J, Liu RM, Kundu RK, Sangiorgi F, Wu W, et al. (2000) Molecular mechanism of decreased glutathione content in human immunodeficiency virus type 1 Tat-transgenic mice. J Biol Chem 275: 3693-3698.
169. Koriem KM, Abdelhamid AZ, Younes HF (2012) Caffeic acid Protects Tissue Antioxidants and DNA Content in Methamphetamine Induced Tissue Toxicity in SD Rats. Toxicol Mech Methods.
170. Cadet JL, McCoy MT, Cai NS, Krasnova IN, Ladenheim B, et al. (2009) Methamphetamine preconditioning alters midbrain transcriptional responses to methamphetamine-induced injury in the rat striatum. PLoS One 4: e7812.
171. Liu X, Chang L, Vigorito M, Kass M, Li H, et al. (2009) Methamphetamine-induced behavioral sensitization is enhanced in the HIV-1 transgenic rat. Journal of neuroimmune pharmacology : the official journal of the Society on NeuroImmune Pharmacology 4: 309-316.
172. Chen J, Lindmark-Mansson H, Gorton L, Akesson B (2003) Total antioxidant capacity of bovine milk as assayed by spectrophotometric and amperometric methods. International Dairy Journal 13: 927-935.
173. White CC, Viernes H, Krejsa CM, Botta D, Kavanagh TJ (2003) Fluorescence-based microtiter plate assay for glutamate-cysteine ligase activity. Anal Biochem 318: 175-180.
174. Diotte NM, Xiong Y, Gao J, Chua BH, Ho YS (2009) Attenuation of doxorubicin-induced cardiac injury by mitochondrial glutaredoxin 2. Biochim Biophys Acta 1793: 427-438.
175. Gonzalez P, Tunon MJ, Manrique V, Garcia-Pardo LA, Gonzalez J (1989) Changes in hepatic cytosolic glutathione S-transferase enzymes induced by clotrimazole treatment in rats. Clin Exp Pharmacol Physiol 16: 867-871.
176. Doorn JA, Petersen DR (2002) Covalent modification of amino acid nucleophiles by the lipid peroxidation products 4-hydroxy-2-nonenal and 4-oxo-2-nonenal. Chem Res Toxicol 15: 1445-1450.
177. Bronowicka-Adamska P, Zagajewski J, Czubak J, Wróbel M (2011) RP-HPLC method for quantitative determination of cystathionine, cysteine and glutathione: An application for the study of the metabolism of cysteine in human brain. J Chromatogr B Analyt Technol Biomed Life Sci Epub May 23.
178. Lee DW, Kim SY, Lee T, Nam YK, Ju A, et al. (2012) Ex vivo detection for chronic ethanol consumption-induced neurochemical changes in rats. Brain Res 1429: 134-144.
179. Banerjee A, Zhang X, Manda KR, Banks WA, Ercal N (2010) HIV proteins (gp120 and Tat) and methamphetamine in oxidative stress-induced damage in the brain: potential role of the thiol antioxidant N-acetylcysteine amide. Free radical biology & medicine 48: 1388-1398.

180. Morris D, Guerra C, Donohue C, Oh H, Khurasany M, et al. (2012) Unveiling the mechanisms for decreased glutathione in individuals with HIV infection. Clin Dev Immunol 2012: 734125.
181. Peng J, Vigorito M, Liu X, Zhou D, Wu X, et al. (2010) The HIV-1 transgenic rat as a model for HIV-1 infected individuals on HAART. J Neuroimmunol 218: 94-101.
182. Kenchappa RS, Ravindranath V (2003) Glutaredoxin is essential for maintenance of brain mitochondrial complex I: studies with MPTP. FASEB journal : official publication of the Federation of American Societies for Experimental Biology 17: 717-719.
183. Daily D, Vlamis-Gardikas A, Offen D, Mittelman L, Melamed E, et al. (2001) Glutaredoxin protects cerebellar granule neurons from dopamine-induced apoptosis by activating NF-kappa B via Ref-1. The Journal of biological chemistry 276: 1335-1344.
184. Saeed U, Durgadoss L, Valli RK, Joshi DC, Joshi PG, et al. (2008) Knockdown of cytosolic glutaredoxin 1 leads to loss of mitochondrial membrane potential: implication in neurodegenerative diseases. PLoS One 3: e2459.
185. Moszczynska A, Yamamoto BK (2011) Methamphetamine oxidatively damages parkin and decreases the activity of 26S proteasome in vivo. J Neurochem 116: 1005-1017.
186. Conrad M, Sato H (2011) The oxidative stress-inducible cystine/glutamate antiporter, system x (c) (-) : cystine supplier and beyond. Amino Acids Epub ahead of print.
187. Albrecht P, Lewerenz J, Dittmer S, Noack R, Maher P, et al. (2010) Mechanisms of oxidative glutamate toxicity: the glutamate/cystine antiporter system xc- as a neuroprotective drug target. CNS Neurol Disord Drug Targets 9: 373-382.
188. Watabe M, Aoyama K, Nakaki T (2008) A dominant role of GTRAP3-18 in neuronal glutathione synthesis. J Neurosci 28: 9404-9413.
189. Ernst T, Jiang CS, Nakama H, Buchthal S, Chang L (2010) Lower brain glutamate is associated with cognitive deficits in HIV patients: a new mechanism for HIV-associated neurocognitive disorder. J Magn Reson Imaging 32: 1045-1053.
190. Pendyala G, Trauger SA, Siuzdak G, Fox HS (2011) Short communication: quantitative proteomic plasma profiling reveals activation of host defense to oxidative stress in chronic SIV and methamphetamine comorbidity. AIDS research and human retroviruses 27: 179-182.
191. Minagar A, Barnett MH, Benedict RH, Pelletier D, Pirko I, et al. (2013) The thalamus and multiple sclerosis: modern views on pathologic, imaging, and clinical aspects. Neurology 80: 210-219.
192. Pfefferbaum A, Rosenbloom MJ, Sassoon SA, Kemper CA, Deresinski S, et al. (2012) Regional brain structural dysmorphology in human immunodeficiency virus infection: effects of acquired immune deficiency syndrome, alcoholism, and age. Biol Psychiatry 72: 361-370.
193. Heaps JM, Joska J, Hoare J, Ortega M, Agrawal A, et al. (2012) Neuroimaging markers of human immunodeficiency virus infection in South Africa. J Neurovirol 18: 151-156.
194. Ances BM, Ortega M, Vaida F, Heaps J, Paul R (2012) Independent effects of HIV, aging, and HAART on brain volumetric measures. J Acquir Immune Defic Syndr 59: 469-477.
195. Heyes MP, Ellis RJ, Ryan L, Childers ME, Grant I, et al. (2001) Elevated cerebrospinal fluid quinolinic acid levels are associated with region-specific cerebral volume loss in HIV infection. Brain 124: 1033-1042.
196. Toborek M, Lee YW, Pu H, Malecki A, Flora G, et al. (2003) HIV-Tat protein induces oxidative and inflammatory pathways in brain endothelium. J Neurochem 84: 169-179.

197. Singh S, Vrishni S, Singh BK, Rahman I, Kakkar P (2010) Nrf2-ARE stress response mechanism: a control point in oxidative stress-mediated dysfunctions and chronic inflammatory diseases. Free Radic Res 44: 1267-1288.
198. Balogh LM, Atkins WM (2011) Interactions of glutathione transferases with 4-hydroxynonenal. Drug Metab Rev 43: 165-178.
199. Martinez-Lara E, Siles E, Hernandez R, Canuelo AR, Luisa del Moral M, et al. (2003) Glutathione S-transferase isoenzymatic response to aging in rat cerebral cortex and cerebellum. Neurobiol Aging 24: 501-509.
200. Cheng JZ, Yang Y, Singh SP, Singhal SS, Awasthi S, et al. (2001) Two distinct 4-hydroxynonenal metabolizing glutathione S-transferase isozymes are differentially expressed in human tissues. Biochem Biophys Res Commun 282: 1268-1274.
201. Raza H (2011) Dual localization of glutathione S-transferase in the cytosol and mitochondria: implications in oxidative stress, toxicity and disease. FEBS J 278: 4243-4251.
202. Franklin CC, Backos DS, Mohar I, White CC, Forman HJ, et al. (2009) Structure, function, and post-translational regulation of the catalytic and modifier subunits of glutamate cysteine ligase. Mol Aspects Med 30: 86-98.
203. Sian J, Dexter DT, Lees AJ, Daniel S, Jenner P, et al. (1994) Glutathione-related enzymes in brain in Parkinson's disease. Ann Neurol 36: 356-361.
204. Hirrlinger J, Schulz JB, Dringen R (2002) Glutathione release from cultured brain cells: multidrug resistance protein 1 mediates the release of GSH from rat astroglial cells. J Neurosci Res 69: 318-326.
205. Takahashi K, Tatsunami R, Sato K, Tampo Y (2012) Multidrug resistance associated protein 1 together with glutathione plays a protective role against 4-hydroxy-2-nonenal-induced oxidative stress in bovine aortic endothelial cells. Biol Pharm Bull 35: 1269-1274.
206. Aoyama K, Suh SW, Hamby AM, Liu J, Chan WY, et al. (2006) Neuronal glutathione deficiency and age-dependent neurodegeneration in the EAAC1 deficient mouse. Nat Neurosci 9: 119-126.
207. Velazquez I, Plaud M, Wojna V, Skolasky R, Laspiur JP, et al. (2009) Antioxidant enzyme dysfunction in monocytes and CSF of Hispanic women with HIV-associated cognitive impairment. J Neuroimmunol 206: 106-111.
208. Look MP, Rockstroh JK, Rao GS, Kreuzer KA, Barton S, et al. (1997) Serum selenium, plasma glutathione (GSH) and erythrocyte glutathione peroxidase (GSH-Px)-levels in asymptomatic versus symptomatic human immunodeficiency virus-1 (HIV-1)-infection. Eur J Clin Nutr 51: 266-272.
209. Ogunro PS, Ogungbamigbe TO, Elemie PO, Egbewale BE, Adewole TA (2006) Plasma selenium concentration and glutathione peroxidase activity in HIV-1/AIDS infected patients: a correlation with the disease progression. Niger Postgrad Med J 13: 1-5.
210. Stephensen CB, Marquis GS, Douglas SD, Kruzich LA, Wilson CM (2007) Glutathione, glutathione peroxidase, and selenium status in HIV-positive and HIV-negative adolescents and young adults. Am J Clin Nutr 85: 173-181.
211. Deresz LF, Sprinz E, Kramer AS, Cunha G, de Oliveira AR, et al. (2010) Regulation of oxidative stress in response to acute aerobic and resistance exercise in HIV-infected subjects: a case-control study. AIDS Care 22: 1410-1417.
212. Lovell MA, Xie C, Markesbery WR (1998) Decreased glutathione transferase activity in brain and ventricular fluid in Alzheimer's disease. Neurology 51: 1562-1566.
213. Whitworth AJ, Theodore DA, Greene JC, Benes H, Wes PD, et al. (2005) Increased glutathione S-transferase activity rescues dopaminergic neuron loss in a Drosophila model of Parkinson's disease. Proc Natl Acad Sci U S A 102: 8024-8029.

214. Miller EA, Spadaccia MR, O'Brien MP, Rolnitzky L, Sabado R, et al. (2012) Plasma factors during chronic HIV-1 infection impair IL-12 secretion by myeloid dendritic cells via a virus-independent pathway. J Acquir Immune Defic Syndr 61: 535-544.
215. Chougnet C, Clerici M, Shearer GM (1995) Role of IL12 in HIV disease/AIDS. Res Immunol 146: 615-622.
216. Chougnet C, Wynn TA, Clerici M, Landay AL, Kessler HA, et al. (1996) Molecular analysis of decreased interleukin-12 production in persons infected with human immunodeficiency virus. J Infect Dis 174: 46-53.
217. Guerra C, Morris D, Sipin A, Kung S, Franklin M, et al. (2011) Glutathione and adaptive immune responses against Mycobacterium tuberculosis infection in healthy and HIV infected individuals. PLoS One 6: e28378.
218. Fraternale A, Paoletti MF, Dominici S, Buondelmonte C, Caputo A, et al. (2011) Modulation of Th1/Th2 immune responses to HIV-1 Tat by new pro-GSH molecules. Vaccine 29: 6823-6829.
219. Alam K, Ghousunnissa S, Nair S, Valluri VL, Mukhopadhyay S (2010) Glutathione-redox balance regulates c-rel-driven IL-12 production in macrophages: possible implications in antituberculosis immunotherapy. J Immunol 184: 2918-2929.
220. Gutierrez JG, Valdez SR, Di Genaro S, Gomez NN (2008) Interleukin-12p40 contributes to protection against lung injury after oral Yersinia enterocolitica infection. Inflamm Res 57: 504-511.
221. Shah D, Kiran R, Wanchu A, Bhatnagar A (2010) Oxidative stress in systemic lupus erythematosus: relationship to Th1 cytokine and disease activity. Immunol Lett 129: 7-12.
222. Sa MJ, Madeira MD, Ruela C, Volk B, Mota-Miranda A, et al. (2004) Dendritic changes in the hippocampal formation of AIDS patients: a quantitative Golgi study. Acta Neuropathol 107: 97-110.
223. Everall IP, Heaton RK, Marcotte TD, Ellis RJ, McCutchan JA, et al. (1999) Cortical synaptic density is reduced in mild to moderate human immunodeficiency virus neurocognitive disorder. HNRC Group. HIV Neurobehavioral Research Center. Brain Pathol 9: 209-217.
224. Panee J (2013) Potential Medicinal Application and Toxicity Evaluation of Extracts from Bamboo Plants. Journal of Ethnopharmacology submitted.
225. Higa JK, Panee J (2011) Bamboo extract reduces interleukin 6 (IL-6) overproduction under lipotoxic conditions through inhibiting the activation of NF-kappaB and AP-1 pathways. Cytokine 55: 18-23.
226. Higa JK, Liu W, Berry MJ, Panee J (2011) Supplement of bamboo extract lowers serum monocyte chemoattractant protein-1 concentration in mice fed a diet containing a high level of saturated fat. Br J Nutr: 1-4.
227. Del Rosario A MM, Panee J. (2011) Bamboo extract alters anxiety- and depression-like neurobehaviors in mice fed a high fat diet. British Journal of Nutrition. British Journal of Nutrition.
228. Lee MJ, Park WH, Song YS, Lee YW, Song YO, et al. (2008) Effect of bamboo culm extract on oxidative stress and genetic expression: bamboo culm extract ameliorates cell adhesion molecule expression and NFkappaB activity through the suppression of the oxidative stress. Clin Nutr 27: 755-763.
229. Son YH, Jeong YT, Lee KA, Choi KH, Kim SM, et al. (2008) Roles of MAPK and NF-kappaB in interleukin-6 induction by lipopolysaccharide in vascular smooth muscle cells. J Cardiovasc Pharmacol 51: 71-77.

230. Wickremasinghe MI, Thomas LH, O'Kane CM, Uddin J, Friedland JS (2004) Transcriptional mechanisms regulating alveolar epithelial cell-specific CCL5 secretion in pulmonary tuberculosis. J Biol Chem 279: 27199-27210.
231. Lee JS, Lee JY, Son JW, Oh JH, Shin DM, et al. (2008) Expression and regulation of the CC-chemokine ligand 20 during human tuberculosis. Scand J Immunol 67: 77-85.
232. Liu R, Zhao X, Gurney TA, Landau NR (1998) Functional analysis of the proximal CCR5 promoter. AIDS Res Hum Retroviruses 14: 1509-1519.
233. Huang Y, Krein PM, Muruve DA, Winston BW (2002) Complement factor B gene regulation: synergistic effects of TNF-alpha and IFN-gamma in macrophages. J Immunol 169: 2627-2635.
234. Bunting K, Rao S, Hardy K, Woltring D, Denyer GS, et al. (2007) Genome-wide analysis of gene expression in T cells to identify targets of the NF-kappa B transcription factor c-Rel. J Immunol 178: 7097-7109.
235. Peng Z, Geh E, Chen L, Meng Q, Fan Y, et al. (2010) Inhibitor of kappaB kinase beta regulates redox homeostasis by controlling the constitutive levels of glutathione. Mol Pharmacol 77: 784-792.
236. Gerbod-Giannone MC, Li Y, Holleboom A, Han S, Hsu LC, et al. (2006) TNFalpha induces ABCA1 through NF-kappaB in macrophages and in phagocytes ingesting apoptotic cells. Proc Natl Acad Sci U S A 103: 3112-3117.
237. Gilmore TD (1999) The Rel/NF-kappaB signal transduction pathway: introduction. Oncogene 18: 6842-6844.
238. Batra S, Balamayooran G, Sahoo MK (2011) Nuclear factor-kappaB: a key regulator in health and disease of lungs. Arch Immunol Ther Exp (Warsz) 59: 335-351.
239. Brabers NA, Nottet HS (2006) Role of the pro-inflammatory cytokines TNF-alpha and IL-1beta in HIV-associated dementia. Eur J Clin Invest 36: 447-458.
240. Xu C, Bailly-Maitre B, Reed JC (2005) Endoplasmic reticulum stress: cell life and death decisions. J Clin Invest 115: 2656-2664.
241. Lindl KA, Akay C, Wang Y, White MG, Jordan-Sciutto KL (2007) Expression of the endoplasmic reticulum stress response marker, BiP, in the central nervous system of HIV-positive individuals. Neuropathol Appl Neurobiol 33: 658-669.
242. Roussel BD, Kruppa AJ, Miranda E, Crowther DC, Lomas DA, et al. (2013) Endoplasmic reticulum dysfunction in neurological disease. Lancet Neurol 12: 105-118.
243. Huang CY, Chiang SF, Lin TY, Chiou SH, Chow KC (2012) HIV-1 Vpr triggers mitochondrial destruction by impairing Mfn2-mediated ER-mitochondria interaction. PLoS One 7: e33657.
244. Bruning A (2011) Analysis of nelfinavir-induced endoplasmic reticulum stress. Methods Enzymol 491: 127-142.
245. Del Rosario A, McDermott MM, Panee J (2012) Effects of a high-fat diet and bamboo extract supplement on anxiety- and depression-like neurobehaviours in mice. Br J Nutr 108: 1143-1149.
246. Anthony IC, Bell JE (2008) The Neuropathology of HIV/AIDS. Int Rev Psychiatry 20: 15-24.
247. Anthony IC, Ramage SN, Carnie FW, Simmonds P, Bell JE (2005) Influence of HAART on HIV-related CNS disease and neuroinflammation. J Neuropathol Exp Neurol 64: 529-536.
248. Kweon MH, In Park Y, Sung HC, Mukhtar H (2006) The novel antioxidant 3-O-caffeoyl-1-methylquinic acid induces Nrf2-dependent phase II detoxifying genes and alters intracellular glutathione redox. Free Radic Biol Med 40: 1349-1361.

249. Higa JK, Liang Z, Williams PG, Panee J (2012) Phyllostachys edulis compounds inhibit palmitic acid-induced monocyte chemoattractant protein 1 (MCP-1) production. PLoS One 7: e45082.
250. Eng LF, Ghirnikar RS (1994) GFAP and astrogliosis. Brain Pathol 4: 229-237.